

**Alexandra Dorothee Hofmann**

**An Approach to 3D Building Model Reconstruction  
from Airborne Laser Scanner Data  
Using Parameter Space Analysis and Fusion of Primitives**

**München 2007**

---

**Verlag der Bayerischen Akademie der Wissenschaften  
in Kommission beim Verlag C. H. Beck**



An Approach to 3D Building Model Reconstruction  
from Airborne Laser Scanner Data  
Using Parameter Space Analysis and Fusion of Primitives

Von der Fakultät Forst-, Geo- und Hydrowissenschaften  
der Technischen Universität Berlin  
zur Erlangung des akademischen Grades  
Doktor der Ingenieurwissenschaften (Dr.-Ing.)  
genehmigte Dissertation

vorgelegt von

Diplom-Ingenieur Alexandra Dorothee Hofmann

München 2007

---

Verlag der Bayerischen Akademie der Wissenschaften  
in Kommission beim Verlag C. H. Beck

Adresse der Deutschen Geodätischen Kommission:

**Deutsche Geodätische Kommission**

Marstallplatz 8 • D – 80 539 München

Telefon +49 - (0)89 - 23 031 -0 / -1113 • Telefax +49 - (0)89 - 23 031 -1283 / -1100

E-mail [hornik@dgfi.badw.de](mailto:hornik@dgfi.badw.de) • <http://dgk.badw.de>

Gutachter: Prof. Dr. sc.techn. habil. Hans-Gerd Maas  
Prof.Dr.-Ing.habil Siegfried Fuchs  
Prof. O.Univ.Prof. Dr.-Ing. Dr.h.c. Karl Kraus

Tag der Einreichung: 19. Januar 2005

---

© 2007 Deutsche Geodätische Kommission, München

Alle Rechte vorbehalten. Ohne Genehmigung der Herausgeber ist es auch nicht gestattet,  
die Veröffentlichung oder Teile daraus auf photomechanischem Wege (Photokopie, Mikrokopie) zu vervielfältigen

## Selbständigkeitserklärung

Hiermit versichere ich, dass ich die vorliegende Arbeit ohne unzulässige Hilfe Dritter und ohne Benutzung anderer als der angegebenen Hilfsmittel angefertigt habe; die aus fremden Quellen direkt oder indirekt übernommenen Gedanken sind als diese kenntlich gemacht worden. Bei der Auswahl und Auswertung des Materials sowie bei der Herstellung des Manuskriptes habe ich Unterstützungsleistungen von folgenden Personen erhalten:

Prof. Dr. habil. Hans-Gerd Maas, Institute of Photogrammetry and Remote Sensing,  
Technische Universität Dresden

Dipl.-Ing. (FH) Gudrun Kraut, Institute of Photogrammetry and Remote Sensing,  
Technische Universität Dresden

Msc. Avril Behan, Department of Geomatics, Faculty of the Built Environment,  
Dublin Institute of Technology DIT

Msc. Dorothy Stewart, Futures Academy, Faculty of the Built Environment, Dublin  
Institute of Technology DIT

Dr. Audrey Martin, Department of Geomatics, Faculty of the Built Environment,  
Dublin Institute of Technology DIT

Weitere Personen waren an der geistigen Herstellung der vorliegenden Arbeit nicht beteiligt. Insbesondere habe ich nicht die Hilfe eines Promotionsberaters in Anspruch genommen. Dritte haben von mir weder unmittelbar noch mittelbar geldwerte Leistungen für Arbeiten erhalten, die im Zusammenhang mit dem Inhalt der vorgelegten Dissertation stehen.

Die Arbeit wurde bisher weder im Inland noch im Ausland in gleicher oder ähnlicher Form einer anderen Prüfungsbehörde zum Zwecke der Promotion vorgelegt und ist auch noch nicht veröffentlicht worden.

Ich bestätige, dass ich die Promotionsordnung der Fakultät Forst-, Geo- und Hydrowissenschaften der TU Dresden anerkenne.

Ort, Datum,

Unterschrift

---

## Abstract

Within this work an approach was developed, which utilises airborne laser scanner data in order to generate 3D building models. These 3D building models may be used for technical and environmental planning. The approach has to follow certain requirements such as working automatically and robust and being flexible in use but still practicable.

The approach starts with small point clouds containing one building at the time extracted from laser scanner data set by applying a pre-segmentation scheme. The laser scanner point cloud of each building is analysed separately. A 2.5D-Delaunay triangle mesh structure (TIN) is calculated into the laser scanner point cloud. For each triangle the orientation parameters in space (orientation, slope and perpendicular distance to the barycentre of the laser scanner point cloud) are determined and mapped into a parameter space. As buildings are composed of planar features, primitives, triangles representing these features should group in parameter space. A cluster analysis technique is utilised to find and outline these groups/clusters. The clusters found in parameter space represent plane objects in object space. Grouping adjacent triangles in object space – which represent points in parameter space – enables the interpolation of planes in the ALS points that form the triangles. In each cluster point group a plane in object space is interpolated. All planes derived from the data set are intersected with their appropriate neighbours. From this, a roof topology is established, which describes the shape of the roof. This ensures that each plane has knowledge on its direct adjacent neighbours. Walls are added to the intersected roof planes and the virtual 3D building model is presented in a file written in VRML (Virtual Reality Macro Language).

Besides developing the 3D building model reconstruction scheme, this research focuses on the geometric reconstruction and the derivation of attributes of 3D building models. The developed method was tested on different data sets obtained from different laser scanner systems. This study will also show, which potential and limits the developed method has when applied to these different data sets.

---

## Kurzfassung

In der vorliegenden Arbeit wird eine neue Methode zur automatischen Rekonstruktion von 3D Gebäudemodellen aus Flugzeuglaserscannerdaten vorgestellt. Diese 3D Gebäudemodelle können in technischer und landschaftsplanerischer Hinsicht genutzt werden. Bezüglich der zu entwickelnden Methode wurden Regelungen und Bedingungen erstellt, die eine voll automatische und robuste Arbeitsweise sowie eine flexible und praktikable Nutzung gewährleisten sollten.

Die entwickelte Methode verwendet Punktwolken, welche mittels einer Vorsegmentierung aus dem gesamten Laserscannerdatensatz extrahiert wurden und jeweils nur ein Gebäude beinhalten. Diese Laserscannerdatenpunktwolken werden separat analysiert. Eine 2,5D-Delaunay-Dreiecksvermaschung (TIN) wird in jede Punktwolke gerechnet. Für jedes Dreieck dieser Vermaschung werden die Lageparameter im Raum (Ausrichtung, Neigungsgrad und senkrechter Abstand der Ebene des Dreiecks zum Schwerpunkt der Punktwolke) bestimmt und in einen Parameterraum aufgetragen. Im Parameterraum bilden diejenigen Dreiecke Gruppen, welche sich im Objektraum auf ebenen Flächen befinden. Mit der Annahme, dass sich ein Gebäude aus ebenen Flächen zusammensetzt, dient die Identifizierung von Clustern im Parameterraum der Detektierung dieser Flächen. Um diese Gruppen/Cluster aufzufinden wurde eine Clusteranalysetechnik genutzt. Über die detektierten Cluster können jene Laserscannerpunkte im Objektraum bestimmt werden, die eine Dachfläche formen. In die Laserscannerpunkte der somit gefundenen Dachflächen werden Ebenen interpoliert. Alle abgeleiteten Ebenen gehen in den entwickelten Rekonstruktionsalgorithmus ein, der eine Topologie zwischen den einzelnen Ebenen aufbaut. Anhand dieser Topologie erhalten die Ebenen „Kenntnis“ über ihre jeweiligen Nachbarn und können miteinander verschnitten werden. Der fertigen Dachgestalt werden Wände zugefügt und das komplette 3D Gebäudemodell wird mittels VRML (Virtual Reality Macro Language) visualisiert.

Diese Studie bezieht sich neben der Entwicklung eines Schemas zu automatischen Gebäuderekonstruktion auch auf die Ableitung von Attributen der 3D Gebäudemodellen. Die entwickelte Methode wurde an verschiedenen Flugzeuglaserscannerdatensätzen getestet. Es wird gezeigt, welche Potentiale und Grenzen die entwickelte Methode bei der Bearbeitung dieser verschiedenen Laserscannerdatensätze hat.



---

# Table of Contents

<b>1</b>	<b>INTRODUCTION .....</b>	<b>9</b>
1.1	MOTIVATION.....	9
1.2	AIRBORNE LASER SCANNER SYSTEMS .....	10
1.3	TERMS OF 3D BUILDING MODEL RECONSTRUCTION.....	11
1.3.1	Terms .....	11
1.3.2	3D Building Reconstruction Tools Available at the Market .....	13
1.4	OVERVIEW OF THE METHOD .....	14
1.5	OUTLINE OF THE THESIS .....	14
<b>2</b>	<b>BUILDING DETECTION AND EXTRACTION .....</b>	<b>15</b>
<b>3</b>	<b>3D BUILDING MODEL RECONSTRUCTION.....</b>	<b>18</b>
3.1	KNOWN APPROACHES TO THE EXTRACTION OF BUILDING INFORMATION.....	18
3.2	DERIVING BUILDING PARAMETERS.....	22
3.2.1	Parameter Space Approach Using Cluster Analysis.....	23
3.2.1.1	Parameter Space of Laser Scanner Data.....	24
3.2.1.2	General Terms of Cluster Analysis .....	30
3.2.1.3	The Applied Cluster Algorithm.....	31
3.2.1.4	Collection of Laser Scanner Points of Roof Faces .....	36
3.2.2	Segmentation Approach.....	38
3.2.3	Discussion of the Approaches.....	38
3.3	PLANE INTERPOLATION.....	40
3.4	ISSUES TO THE GROUPING OF PLANAR FACES TO BUILD UP A ROOF TOPOLOGY .....	41
3.4.1	Previously Published Grouping Strategies.....	42
3.4.2	Analysis of Available Information.....	43
3.4.3	A Grouping Strategy by Means of Couples.....	46
3.4.4	Intersection Strategy Using Couples and Pairs.....	47
3.5	RECONSTRUCTION OF BUILDING MODELS .....	48
3.5.1	Roof Plane Bounding Box .....	50
3.5.2	Detect Dormers and Remove Doubled Planes.....	50
3.5.3	Intersect Ridges.....	52
3.5.4	Adjust Gable Ends of Roof Faces.....	53
3.5.5	Grouping of Planes and Intersecting Sides .....	55
3.5.6	Linearization of Gable Ends .....	58
3.5.7	Adjustment of Gutters.....	58
3.5.8	Adjustment of Dormers.....	59
3.5.9	Determining the Outline of the Roof .....	60
3.5.10	Discussion of the Intersection Algorithm .....	60
<b>4</b>	<b>LASER SCANNER DATA SETS USED FOR PRACTICAL TESTING.....</b>	<b>64</b>
4.1	AIRBORNE LASER SCANNER SENSOR SYSTEMS .....	64

---

4.2	CHARACTERISTICS OF THE DATA SETS .....	68
<b>5</b>	<b>VERIFICATION OF RECONSTRUCTED BUILDING MODELS .....</b>	<b>73</b>
5.1	QUALITY VERIFICATION OF RECONSTRUCTED BUILDING MODELS.....	73
5.1.1	Statistics on Study Areas .....	76
5.1.2	Discussion of the Results.....	87
5.2	ACCURACY VERIFICATION OF RECONSTRUCTED BUILDING MODELS .....	92
5.2.1	The Fit of Reconstructed Building Models into the LiDAR Data.....	92
5.2.2	Comparison with Photogrammetric Measurements .....	94
5.2.3	Comparison with Terrestrial Measurements.....	95
5.3	AUTOMATIC LABELLING OF CORRECT RESULTS.....	97
5.4	APPLICABILITY OF THE OVERALL PROCESS .....	99
<b>6</b>	<b>SUMMARY, CONCLUSIONS AND OUTLOOK.....</b>	<b>101</b>
6.1	SUMMARY AND CONCLUSIONS .....	101
6.2	FUTURE WORK .....	102
<b>7</b>	<b>REFERENCES.....</b>	<b>104</b>
7.1	ARTICLES .....	104
7.2	MONOGRAPHS .....	107
7.3	WEB PAGES .....	107
7.4	THESIS .....	108
7.5	PERSONS .....	108

---

## Symbols, Names, and Units

<i>Symbol</i>	<i>physical Name</i>	<i>Unit</i>
$\varphi$	Slope	degree
$\omega$	Orientation	degree
$\delta$ Orientation	Difference in Orientation	
$\delta$ Slope	Difference in Slope	
$\lambda$	Eigenvalue	scalar
a	Precision of single laser scanner points	m
a, b, c, d	Parameters of plane equation	
A	Matrix of barycentric reduced coordinates	
Acc	Accuracy parameter of reconstruction scheme	m
B	Matrix	
$b_i$	Variables of the characteristic polynomial	
$d$	Perpendicular distance of a plane to barycentre	m
D	Determinant	
d	Distance	m
dist	Orthogonal distance of an ALS point to its plane	m
h	Height	m
I	Unit matrix	
$l, l_l, l_u$	Point spacing	m
meandi	Mean distance	m
meanPtdist	Mean point spacing	m
MergeAcc	Relative height parameter of reconstruction scheme	m
Mergedist	Distance parameter of reconstruction scheme	m
MinNr	Minimal number	#
MinSlope	Angle parameter of reconstruction scheme	degree
npts	Number of points	#
nv	Normal vector	
O	Origin/barycenter of a point cloud	
$P_i$	Point	
ROV	Roof orientation variation	degree
stdev	Standard deviation	m
x, y, z	coordinates	

---

---

## Abbreviations

ALS	Airborne Laser Scanner
ALTMS	Airborne Laser Topographic Mapping System
DEM	Digital Elevation Model
DTM	Digital Terrain Model
GIS	Geographic Information System
GPS	Global Positioning System
INS	Inertial Navigation System
InSAR	Interferometric Synthetic Aperture Radar
LiDAR	Light Detection and Range
LL	Lower Left
LR	Lower Right
LTOP	Swiss Federal Office of Topography
UL	Upper Left
UR	Upper Right
VRML	Virtual Reality Macro Language

# 1 Introduction

## 1.1 Motivation

There appears to be a gap in the market that needs to be filled for inexpensive reliable and up-to-date 3D models for technical and environmental planning. The information, which 3D building models provide, is required in many applications such as architecture, city planning, environmental planning, telecommunication as well as tourism. Throughout the years, there has been research in the field of automated 3D building model reconstruction, but none of the developed systems has made it into industrial production yet. Nonetheless, systems that work automatically in specific tasks or under specific requirements have been introduced to the scientific community.

It follows that, the ideal system, which reconstructs any 3D building models automatically and which does not require additional information sources, has still to be developed. The aim of this research has been to develop such a system. The following ideas and criteria are necessary and include:

- **Robustness:** Ideally, each building in a chosen scene should be reconstructed. This is a formidable task to achieve as the data source, the laser scanner data, is not perfect and the objects, the buildings, exist in vast diversity. It is still envisaged to reconstruct as many buildings as possible. The system should thus indicate any failure in reconstruction to the operator. This may be accomplished in a “traffic light” manner whereby each building is assigned a colour code:
  - Green: correctly reconstructed building model
  - Yellow: probably a partially correct reconstructed building model
  - Red: not usable building model
- **Flexibility:** An ideal system is able process any airborne laser scanner point data, regardless of the point spacing or point pattern. Ideally, it should be able to process any surface information that is given with discrete x,y,z-points. It can also take already existing map information into account and is able to transfer the new information to the former information at a later stage.
- **Resolution:** The resolution refers to the feature detail that is achieved by the reconstruction and it is mainly dependent on the point density of the airborne laser scanner data. At the very least the level of detail of the reconstruction should match those of large-scale maps. In general, the main building and larger covers have to be reconstructed, but smaller features such as dorms may be omitted.
- **Reliability and Precision:** The precision of reconstructed information is extremely important, but may be only as good as the accuracy of airborne laser scanner data in correlation with its point spacing.
- **Computation time:** Preferably, it should not take longer than a few seconds to reconstruct a building model, since information is usually requested for a larger area.

These five criteria are fundamental to a practical system, which is not limited to certain roof styles and does not require interactive processes. The system should be able to produce suitable results with LiDAR only, but if additional information is available it should be able to avail of this information also.

In order to build up such a system certain information must be known about roof structures and features. The next sections will introduce them.

## 1.2 Airborne Laser Scanner Systems

Airborne laser scanning (ALS), also referred to as LiDAR (Light Detection and Ranging), was used initially for photogrammetric applications approximately a decade ago. The system, which bases on an active remote sensing technique, measures the running time of an emitted laser beam to an object on the earth's surface and back. The laser beam is directed across the flight direction using, for instance, an oscillating mirror. The coordinates of the point on earth, which is hit by the laser beam, is calculated taking the time measurement, the mirror position as well as Global Positioning System (GPS) and Inertial Navigation System (INS) information into account. Figure 1-1 outlines the relationship of these components. A detailed description of the system can be found in [Wehr1999] and [Baltsavias1999a]. In [Ackermann1999] a first summary of laser scanning's capabilities are given and a well defined outlook is provided.

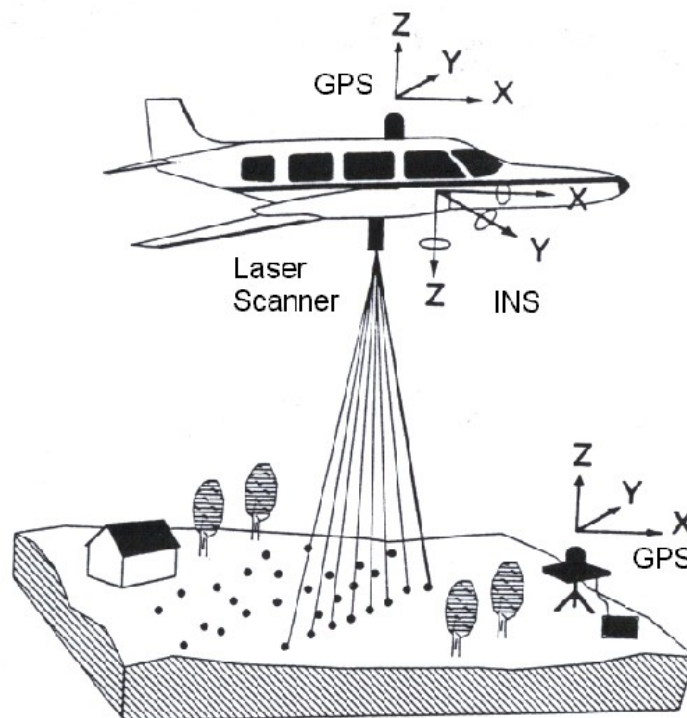


Figure 1-1: Principle of airborne laser scanning (Modified from illustration in Flood, 1997)

A high sampling frequency can be achieved and thus a high information density when using this technique. The main application of airborne laser scanning is the generation of detailed terrain models (DTMs). The origins and purpose of these ideas can be traced back

to the 1990s and the published works of [Kraus1997] and [Kraus1999]. This field has been extended to breakline detection [Kraus00] in order to represent the actual surface more precisely. Momentarily, the trend is also to extract 3D-GIS information from ALS data. Besides terrain, this GIS information may be buildings or vegetation areas. To extract vegetation information from LiDAR data is a fairly new application, which is discussed in [Anderson02] or [Pyysalo2002] for example. Known approaches to building extraction and reconstruction from ALS data are introduced in the sections 2.1 and 3.1.

### 1.3 Terms of 3D Building Model Reconstruction

The following section outlines the terms and definitions which will be used within this work. The naming and defining is necessary since there is no unique use or idea connected with certain words, such as extraction or model.

#### 1.3.1 Terms

The terms building extraction and building model reconstruction are neither defined nor uniformly used in literature. Nonetheless, it is necessary for this work to settle on unambiguous meanings. Building extraction is understood here as the act of deriving building parameters such as roof inclination or the outline of the building, but not creating a virtual 3D building object. A (3D) building model is used here as a term for a virtual 3D building object with a full roof topology. Roof topology means that each surface of a building model has a label to it, whether it is a wall or a roof plane and it “knows” its neighbours and its relationship to its neighbours. Part of that information can be called semantic as well.

A 3D building model is a generalised or rather abstract and scaled virtual representation of the real building. It is a compromise between which generalisation is due to resolution and which information is actually given by the data and further on which semantic information can be used without being at odds with the generalisation. [Förstner1999] classifies and defines building models in different levels of complexity, as shown in Figure 1-2. Parametric and prismatic building models have the highest degree of generalisation. They reduce buildings to either predefined shapes or to blocks of one height.

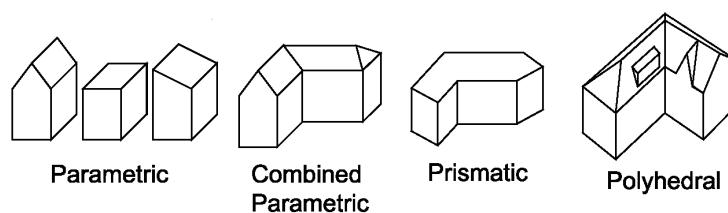


Figure 1-2: Classes of building models [Brenner2000]

Polyhedral building models are more complex but still generalised descriptions of roof structures, which are closely related to the original. The main properties of the roof are observable; however, they ignore parts of the roof that are unimportant, such as chimneys. All of these building models have the following simplifications/assumptions in common concerning their appearance:

- Roofs and walls are planar surfaces,

- The gutter as well as the ridge is a horizontal edge line.
- The roof inclination does not exceed 75 degrees,

A building model can be constructed out of vertices, lines and/or planes. Using lines and vertices a skeleton of the building, also called a wire-frame model, is created. The lines and vertices may be grouped into polygons. A building model that is represented by planes and vertices is a planar model, which is the preferred model representation for this study.

Individual buildings have different roof structures. The most frequently occurring roof structures are the pent, gable and hipped roof. Figure 1-3 illustrates these basic styles. A complex is any roof structure that arises when combining at least two of the basic styles.

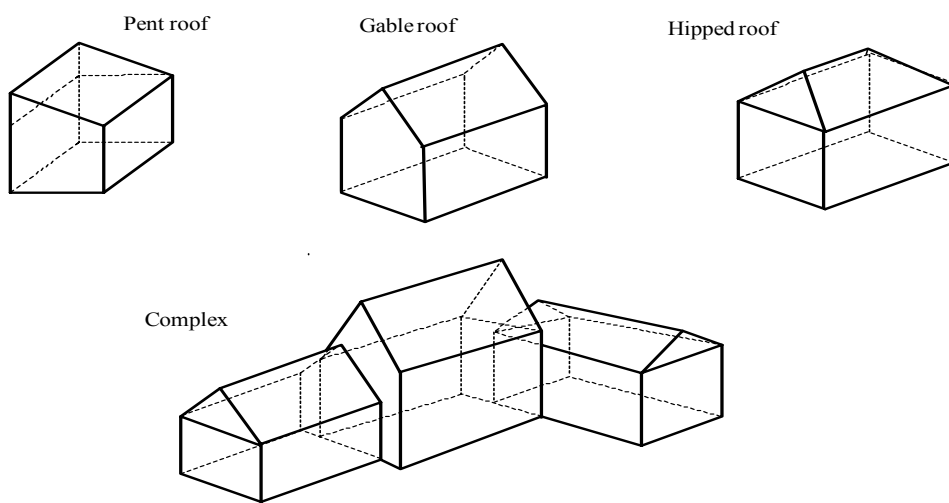


Figure 1-3: Roof types

The basic styles have special cases. A flat roof is a special case of a pent roof that has a roof inclination of less than four degrees. A gambrel roof is a roof that looks like a gable roof, but that has two different inclinations as exemplified in Figure 1-4. A mansard roof is the equivalent to the gambrel roof. A roof called a tent roof is a special case of a hipped roof if its four roof faces meet at one point at the top.

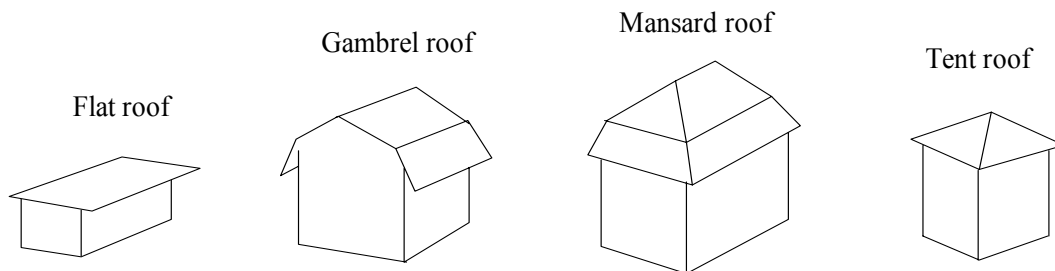


Figure 1-4: Special cases of roof types

Almost all roof faces that occur on a building can be described by four corner coordinates and thus by four sides. In some cases, corner coordinates of a roof face are identical in certain situations such as when giving the roof faces a triangular shape. Roof faces, which have to be represented by more than four corner points, can be composed of triangle and rectangle shapes.

In order to simplify the definition of roof edges, they are assigned logical names. The lower edge, for example, is called the gutter, although this should not be taken literally, as there may not be a gutter in the scene. Figure 1-5 shows a named graphic of a building explaining the ridge, the eaves, the gable and the dormer – a pitched dormer in that case.

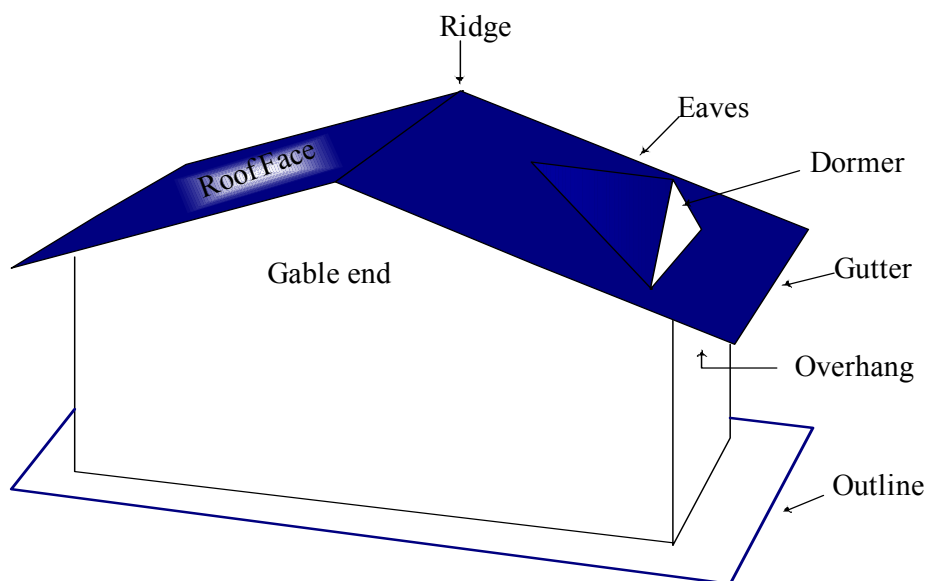


Figure 1-5: Features of a roof

A dormer is a feature attached to the roof. It can have any number of roof faces, but the feature in its entity must not exceed the borders of the roof face it is attached to. Any object exceeding the borders of a roof face is identified as part of the roof itself. Dormers may have two main shapes: They can look like the example in Figure 1-5 and are then called pitched dormer. They may also be flat, represented by only one roof face that has the same orientation as the main roof face. These types are usually referred to as flat dormers.

### 1.3.2 3D Building Reconstruction Tools Available at the Market

At this moment in time, there is no software tool on the market, which reconstructs 3D building models automatically. Software tools that are currently available require user interaction. Examples of user interaction software include the CyberCity-Modeller [CyberCity] and the INPHO inJECT software [Inpho], which allow a semi-automatic reconstruction of 3D building models in aerial imagery. 3D building model reconstruction in LiDAR data can be performed with TerraScan in TerraSolid [TerraSolid] semi-automatically as well.

Research groups in Universities, such as Delft, Vienna, Aalborg and Ohio are currently developing systems that work almost automatically using LiDAR alone.

## 1.4 Overview of the Method

Building model reconstruction can be divided into the different phases: detection, geometric reconstruction and eventually derivation of additional attributes. This research focuses on the geometric reconstruction and the derivation of additional attributes of 3D building models.

The method represented here is a data-driven method – it analyses and derives information directly from the airborne laser scanner data.

The laser scanner point cloud of each building is analysed separately. A 2.5D-Delaunay triangle mesh structure (TIN) is calculated into the laser scanner point cloud. For each triangle the orientation parameters in space (orientation, slope and perpendicular distance to the barycentre of the laser scanner point cloud) are determined and mapped into a parameter space. As buildings are composed of planar features, triangles representing these features should group in parameter space. A cluster analysis technique is utilised to find and outline these groups/clusters. This approach can be understood as a modified 3D-Hough-Transformation.

The clusters found in parameter space represent plane objects in object space. Grouping adjacent triangles in object space – which represent points in parameter space – enables the interpolation of planes in the ALS points that form the triangles. In each cluster point group a plane in object space is interpolated. All planes derived from the data set are intersected with their appropriate neighbours. From this, a roof topology is established, which describes the shape of the roof. This ensures that each plane has knowledge on its direct adjacent neighbours. Walls are added to the intersected roof planes and the virtual 3D building model is presented in a file written in VRML (Virtual Reality Macro Language).

## 1.5 Outline of the Thesis

This thesis' work is presented in the following six chapters as described now: Chapter 2 briefly describes a fast solution of building detection and extraction in airborne laser scanner data. This preliminary work is necessary in order to derive 3D building model objects from ALS data. Chapter 3 represents the crux of the thesis. It contains the explanations of the parameter space algorithm as well as the 3D building reconstruction algorithm. The developed approach is tested on a variety of ALS data, which are introduced in chapter 4. Chapter 5 discusses the results of the tested data sets. In chapter 6 the main points of the presented work are summarised and future work is suggested. Any used literature is listed in chapter 7.

## 2 Building Detection and Extraction

The simplest way to retrieve building information, such as a 3D building model, from airborne laser scanner data is to process smaller laser scanner point clouds, which only contain one building at a time. For this, the position of a building must be known. If that is the case, the laser scanner point cloud can be extracted by selecting those laser scanner points that are in the specified area. If the information regarding the building's position is not known, a challenging task arises. This chapter refers to published methods of building detection and suggests an approach.

Presently, ALS data are filtered and classified in order to obtain information on object locations. These objects may be bridges, buildings or trees. In [Sithole2003], actually developed filtering techniques are compared and discussed. Other described procedures, which specialised on detecting buildings only in LiDAR data, segment and classify rasterised laser scanner data as it was done by [Nardinocchi2001] or [Hofmann2002] for example. Other methods such as published by [Axelson1999] classify LiDAR points in profiles and then group the line segments in order to get areas delineating buildings. Since there still has to be developed a method, which works reliably, for the time being a fast approach on building detection is suggest in the following. In general, it is suggests that using segmentation and understanding of the context of the landscape being filtered and data fusion, object detection may be completed in future.

### *Suggestion of a Building Detection Approach*

In [Hofmann2002] a relatively simple approach is explained that is flexible with respect to additional information other than LiDAR data. The procedure is not a solution of the whole process, but describes an approach that quickly provides information on building locations. The data sets "Freiberg", "Dresden" and "Brienz" introduced in section 4.2 have been processed as described. In order to acquaint the reader with this procedure, it shall be explained briefly in the following.

The commercially available region-based segmentation software eCognition 3.0 was utilised. Image analysis with eCognition is based upon contiguous, homogeneous image regions, which are generated by initial image segmentation. The image content is represented as a network of image objects. The segmentation algorithm of eCognition is based on the so-called "bottom up region-merging" technique. Thus, starting with the pixel level, each pixel is joined with its most similar neighbouring pixel. In a number of steps, these two-pixel-objects are enlarged to bigger pixel groups until a certain heterogeneity value (scale parameter) is reached. These pixel groups (segments) are optimised considering the homogeneity criterions colour and shape. With these three parameters (scale, colour and shape) the user can influence the segmentation process. [Definiens]

Referring to laser scanner data, it is supposed that objects, having a different height in comparison to their surroundings, are assigned into one segment and the surroundings into another. The experience shows that segmenting laser scanner data (Figure 2-1) does not always produce the desired result. The reason is that there are smooth transitions between the objects and their neighbours such as between houses and nearby trees. Attempts were

made to modify the laser scanner data to improve the segmentation result, but none showed better results.



Figure 2-1: Segmentation result (blue polygons) of LiDAR data using eCognition with overlaid aerial imagery and map information (red polygons)

The following classification rules were applied to the data sets, although the exact values did vary between the data sets:

- Buildings are not to be found within forest or water areas, if a map is available
- Building segments are smaller than 6000m<sup>2</sup>
- Buildings do not have higher neighbour objects than other buildings, except if they are situated on a slope – thus the relative border to higher neighbours in the laser scanner data segments should not exceed a certain value, if the area has flat terrain
- The length/width ratio is smaller than a user-set value
- The standard deviation of laplacian values for buildings are within a certain range

Segments exceeding 6000m<sup>2</sup> usually represent field or branched street areas. The length/width criterion excludes long narrow segments, as they are to be found on grassland and streets. The standard deviation of the laplacian values of the segments is small for flat areas and high for undulating regions. To apply the laplacian value of a segment as a classification criterion works only with a good segmentation result. The building has to be entirely within a segment and the segment should not be too long-ranged around the building. Figure 2-2 shows an example of a classified segmentation result.

For each polygon the likelihood is given for whether there is a building or not. [Hofmann2002] contains the analysis of the procedure in respect to its efficiency and applicability.



Figure 2-2: Classification result (yellow areas) of “building-polygons” with overlaid aerial imagery and map information (red polygons)

### *Building Extraction*

It follows that the as “building-polygons” classified areas are laid over the laser scanner point data. A smaller point cloud, which contains all points that are within a certain area of a “building-polygon”, is extracted from the LiDAR data for each “building-polygon”. These smaller point clouds are then used to derive building information in the form of a 3D building model.

### 3 3D Building Model Reconstruction

This chapter discusses the developed building model reconstruction approach in detail. It starts in section 3.1 with an introduction to already published methods which extract building information not only from LiDAR data, but also from aerial imagery or InSAR data. The ideas behind those methods, which use LiDAR only, are examined and information for a new approach is collected. The newly suggested approach that derives primer building information and the collection of ALS points is described in section 3.2. This chapter also gives an overview about the theory of cluster analysis itself. In section 3.3 the used plane interpolation technique is explained which is utilised in order to get plane parameters from collected ALS point groups. The grouping of the interpolated planes is reviewed in section 3.4. Section 3.5 finally explains the reconstruction algorithm that was developed in order to obtain 3D building models.

#### 3.1 Known Approaches to the Extraction of Building Information

Efficient extraction of features, particularly man-made features, from airborne data has been a topic of intense research for many years. In this research, aerial photography has been the preferred way to obtain 3D information of buildings. Although very well understood and delivering accurate results, the major difficulty is that automation of the measurement process, which is closely related to image understanding, is a hard task to solve. This research suggests that LiDAR seems to have advantages with regard to image interpretation, as the provided geometry of objects is more capacious. However, the problem shifts from image understanding to geometry recognition, and this is confirmed by the results of many other researchers. To substantiate this, published key approaches to automatic building extraction and reconstruction will be introduced. From the many articles available on the whole procedure of building object extraction and building model reconstruction the articles deemed most relevant to this research have been selected for critical evaluation. To date, a large number of 3D building object reconstruction methods using aerial imagery were developed, but only a few come close to an automatic building model reconstruction. These methods are based on different ideas; some of them have been copied in order to work with airborne laser scanner data and vice versa. Traditionally, breakline detection in a stereo pair is the primer task, which is performed in order to get basic information which is necessary for 3D building model reconstruction. These breaklines are then grouped to planes using probabilistic [Heuel2000], semantic [Baillard1999] or model [Gerke2001] approaches or combinations [Brunn1998] of them. The planes are grouped and intersected then to form a reconstructed building model.

In 1995 Weidner made the first attempt at using LiDAR data as the information source for 3D building object reconstruction and as soon as the scientific community became receptive to LiDAR systems, a number of building extraction approaches followed.

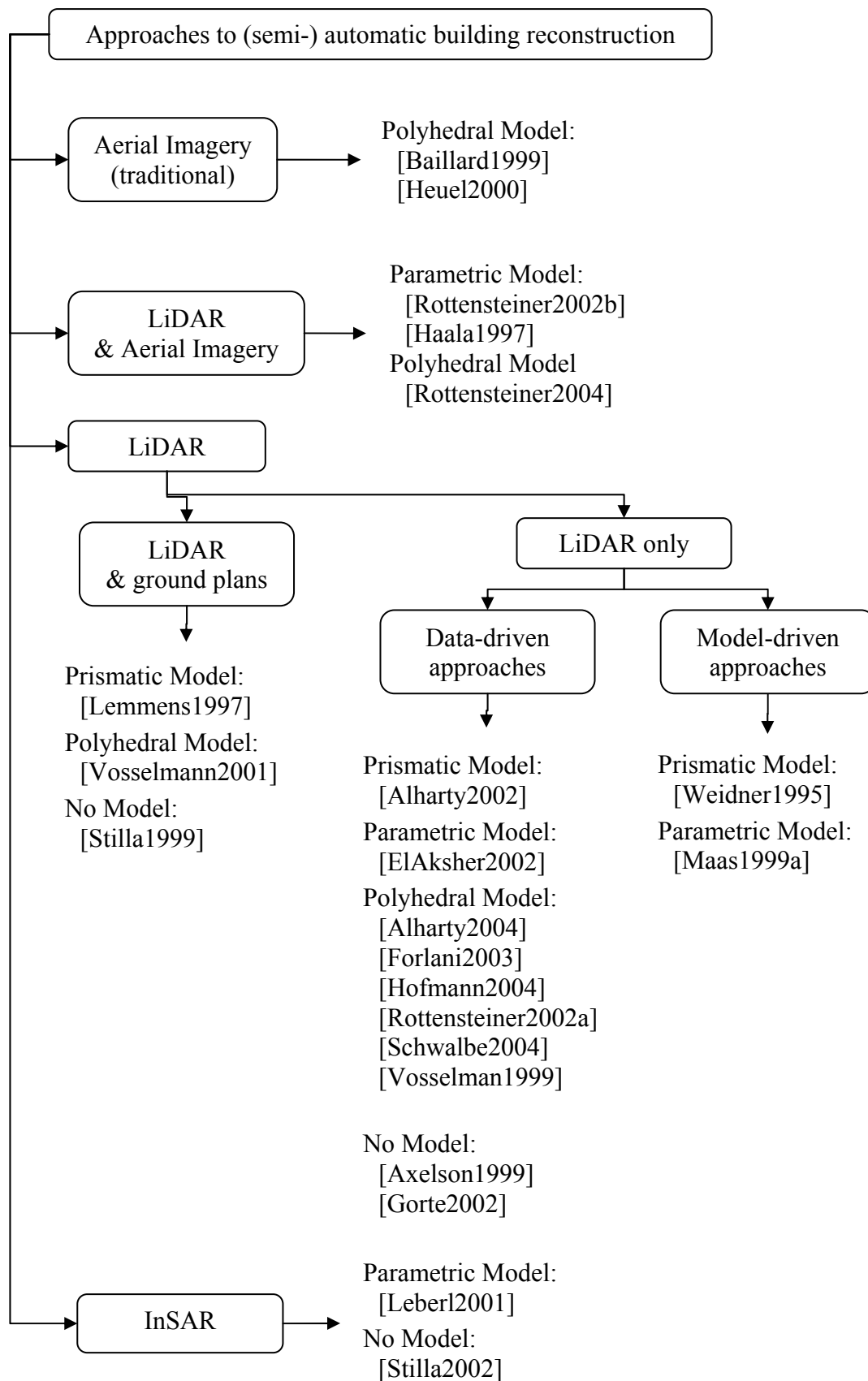


Figure 3-1: Methodised diagram of approaches to (semi-)automatic building extraction

Starting with approaches that work in the context of traditionally derived 3D building objects, some use LiDAR in co-existence with aerial imagery. The LiDAR is used here for the derivation of plane segments and the aerial imagery aids the edge detection of the plane segments. Of the many examples of this procedure, this research examined [Haala1997] and [Rottensteiner2002b] and his later work [Rottensteiner2004]. Both build up a roof topology of the 3D building objects using line-based intersection algorithms.

Furthermore, strategies using LiDAR as the main data source to derive building parameters as well as building models have become more complex. [Lemmens1997], [Stilla1999], and [Vosselman2001] are examples of methods, which have been developed to obtain the height or geometry information from the LiDAR but which utilise ground plan information. Vosselman represents an example of a more intricate method that uses the ground plan information to delimit plane features in the object space.

During the last years four key strategies have been developed that use only laser scanner data. These four strategies can be divided into model-driven and data-driven approaches. From the outset, there are two model-driven approaches: [Maas1999a] and [Weidner1995]. Both use pre-segmented point clouds of laser scanner data sets. They presume that the building in the point cloud has a certain roof structure, such as a gable roof. By using statistical measures, they identify the parameter set of a prismatic building model which best fits the point cloud. According to the published statistics, the methods work well for single standing buildings. Complexes have to be split up and the single modelled parts have to be united later on.

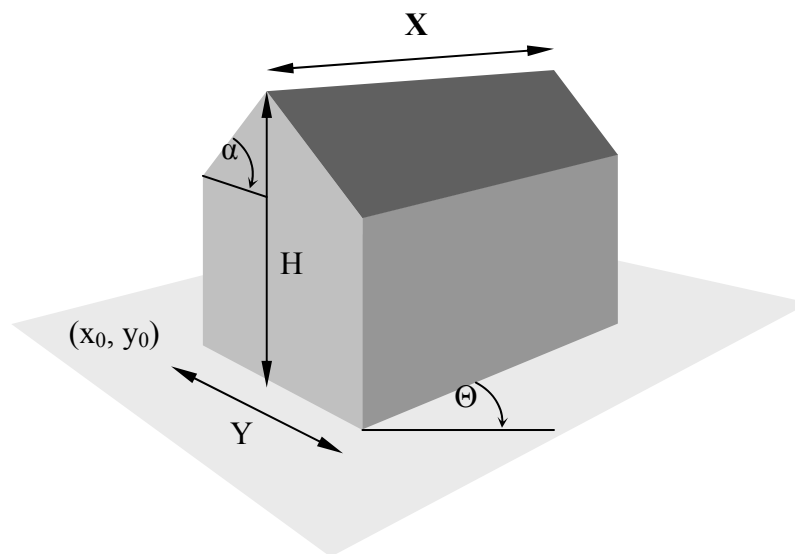


Figure 3-2: Parameter definition of a building primitive [Maas1999a]

The developed data-driven approaches can generate different levels of 3D building objects as indicated in Figure 3-1. They use points, edges, lines, TIN-structures or rasterised LiDAR data to accomplish this.

A fast and simple approach is introduced by [Alharty2002], who extracts prismatic building objects from rasterised LiDAR data by applying an edge detection scheme to the LiDAR raster image.

The segmentation procedures within rasterised LiDAR data is presented by [Forlani2003], [Rottensteiner2002a] and [ElAksher2002]. The approach of ElAksher is improved and extended by [Alharty2004]. Both approaches collect three parameters (slope, orientation and height intercept) of pixels within a kernel. Parameter pixels with the same parameters are grouped and the plane parameters of this group are known. In contrast to this, [Forlani2003] and [Alharty2004] generate wire-frame building objects out of the collected pixel groups. In [Rottensteiner2002a] a segmentation approach is described wherein homogeneous pixels within a slope image are collected and the segments are connected to form a polyhedral building model (see Figure 3-3).



Figure 3-3: Segmentation results as seen in [Rottensteiner2002a] for plane interpolation

When using the raw laser scanner point data, as in [Axelson1999], it is possible to extract building features by detecting large height differences while checking the height values of laser scanner points within one profile. The result is that LiDAR points belonging to a building are grouped. Unfortunately, the method was not completed in terms of getting a 3D building model.

Other approaches such as that outlined in [Gorte2002] apply a segmentation algorithm to a TIN-structure that was calculated in the raw laser scanner point cloud. Gorte describes the approach as working well but being time-consuming. He also identified that the success of the approach depends on the data and thus the orientation of the triangles in space. It follows that only a very complex segmentation procedure could perform an optimal segmentation [Gorte2002].

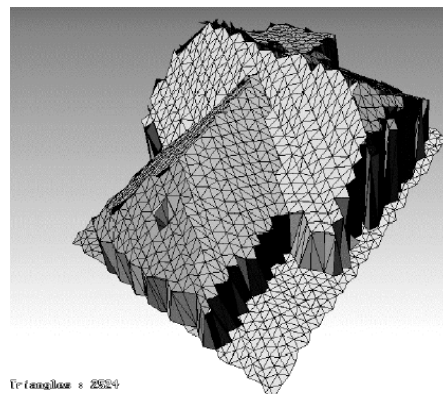


Figure 3-4: Segmentation result of [Gorte2002]

Vosselman presents in [Vosselman1999] a method that applies a 3D Hough transform to pre-segmented raw laser scanner point clouds. The clusters found in the Hough space represent LiDAR points that belong to planar surfaces. These points are collected via a TIN-structure, and a plane interpolation and intersection procedure takes place. The method

shows good results with 43 buildings reconstructed out of 51, but is denoted in the paper as less robust than the approach presented in [Maas1999a]. The given reason for this result is that the outlines of buildings were not used.

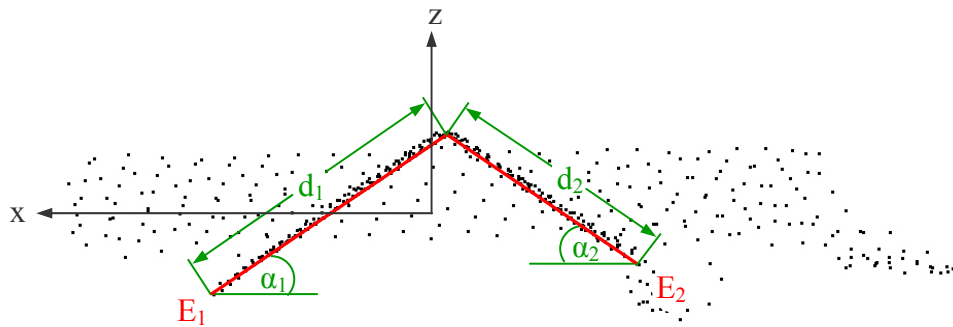


Figure 3-5: Illustration of the building reconstruction technique from [Schwalbe2004]

[Schwalbe2004] presents an entirely different strategy of deriving building parameters whereby she reduces a pre-segmented 2.5D laser scanner point cloud, as shown in Figure 3-5, into 2D space by projecting it onto a plane that is parallel to the gable end side of a house. In this projection the roof's inclination and length can be obtained by detecting the roof planes representing lines. Further roof information is collected by rotating and projecting the 2.5D point cloud in main directions. The generated building models are of polyhedral style with roof topology.

Seeing that geometric information shows promising results for 3D building model reconstruction, researchers also approach InSAR data in order to retrieve 3D building models from this data source. In [Leberl2001] and [Stilla2002] InSAR data are discussed and tested for their information content. Both methods show that reconstruction is possible and conclude that this data may be used for building model reconstruction in rural areas, since urban areas are structured too densely in comparison to the resolution of InSAR data.

### 3.2 Deriving Building Parameters

Section 3.1 introduced published methods of 3D building reconstruction. It made clear that using a model-driven approach with limited number of parameters the reconstruction is somewhat limited to roof structures with one ridge. To apply a model driven approach, such as the one proposed in [Maas1999a], to building complexes, would require the splitting of the roof structure into single elements such as a gable or hipped roof part. Even with supplied ground plan information, this is an extremely challenging task as proven by [Brenner2000].

Similar to the model-driven approaches, the data-driven methods discussed above each have their own advantages and disadvantages. The approach presented by Schwalbe requires ground plan information in order to reconstruct building complexes, though it is a robust and fast approach. The suggested segmentation algorithms are reported to require high computation times and are sensitive to errors in the LiDAR data.

An improved approach would try to unite the advantageous parts of the data-driven approaches. In addition, the goal of this work is to create a system that is flexible to use and that gives results in accordance with the provided point information. As said in section 1.1, the motivation is to be able to reconstruct those features of any roof structure, which are

represented by a suitable number of points. This means that with large point spacing small dormers may not be recognised. However, dormers will be found if the point density allows it. The following paragraphs will introduce the methodology thus developed.

### 3.2.1 Parameter Space Approach Using Cluster Analysis

Using a parameter space that points out planar features of the point cloud – the object space – is reasonable, as it gives an overview of the existing features. It may decrease computation time by reducing the search area to parts of the parameter space that are most likely occupied by planar surfaces. The parameter space should directly indicate the parameters of the planar features and it should be undemanding in its creation.

Beside the demands on the parameter space, the point cloud must not be altered in order to derive the parameters. Interpolation of the laser scanner data, for instance, is not approved. The parameter space should work for any point density that comes with the LiDAR data, without any changes being made to both of them. To suit the regulations on using these “truth” data, a mesh by means of a TIN-structure, such as seen in Figure 3-6, can be calculated in the LiDAR points. This provides further information without changing the LiDAR data. Via the triangles parameters of planar surfaces, which are formed by the LiDAR points, can be obtained.

However, the error of the LiDAR points may influence the triangles directly. The position error of a LiDAR point has components in all three directions ( $x$ ,  $y$ ,  $z$ ). The error model of LiDAR points originating from one flight strip can be simplified under the presumption that the error in  $x$  and  $y$  are highly correlated for points within a smaller area. [Maas2002] Hence, only the error in height remains to be taken care of and is considered in detail in the following section.

In accordance to the error of the laser scanner data in  $z$ , the triangles in object space of a planar surface have slightly different parameters of their orientation in object space. It ought to be possible to handle these variations in parameter space. To collect all the parameter points that belong to a roof face, a cluster analysis technique may be applied.

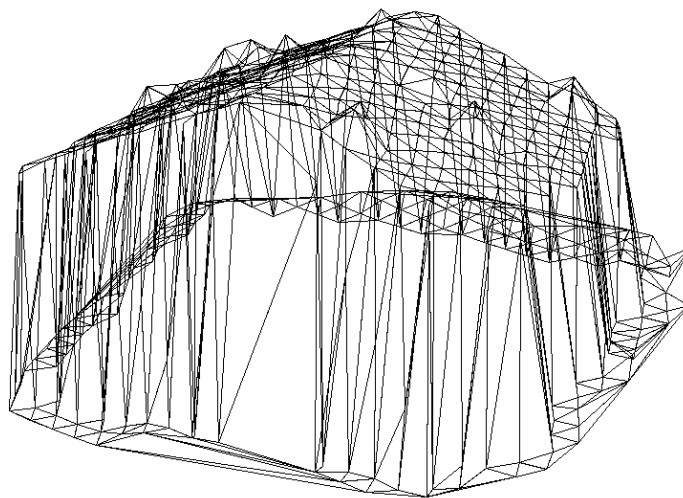


Figure 3-6: Point cloud of a building with a Delauney-triangle-mesh structure

The next pages will introduce the mentioned parameter space in more detail. The following section discusses then clustering approaches and gives reasons for the applied algorithm

that is described in the section thereafter (section 3.2.1.3). The third and last section of this part explains the collection of triangles in object space through the collected clusters.

### 3.2.1.1 Parameter Space of Laser Scanner Data

As mentioned, by calculating a TIN-structure in the LiDAR points parameters can be derived that would indicate planar features in the LiDAR point cloud. A suitable TIN-structure for this purpose is a Delauney triangulation that is calculated in the  $x$  and  $y$  coordinates of the points. The  $z$ -value of the LiDAR points is then an attribute of the corner points of the triangles. The structure can therefore be called a 2.5D TIN-structure whereof an example is visualised with Figure 3-7. The mesh generator that was used to realise the TIN-structure is explained in detail in [Shewchuk1996].

In order to use the position parameters of the triangles, they have to be carefully chosen and they have to fulfil certain requirements. There should only be as few parameters as necessary, i.e. three, but they have to define the triangles position in space uniquely. Figure 3-7 visualises the chosen parameters, which fulfil these requirements. These parameters are: The slope,  $\varphi$ , is the angle that the triangle's normal vector encloses with  $x,y$ -plane; the orientation,  $\omega$ , is the angle that the triangle's normal vector encloses with the northing ( $y$ -axis); and the perpendicular distance,  $d$ , between the triangle's plane and the origin of the point cloud. The shape information of the triangles was not taken into account, as it can be irregular and cannot be defined for a specific object. Still, larger triangles are less sensitive to errors in the laser scanner data as the following section will show. Thus, assigning a weight to each triangle would be an option to increase the information taken from each triangle. The weight should then be increased with the size of the triangle as long as the triangle is equilateral. Failing that, the triangle may represent parts of a wall.

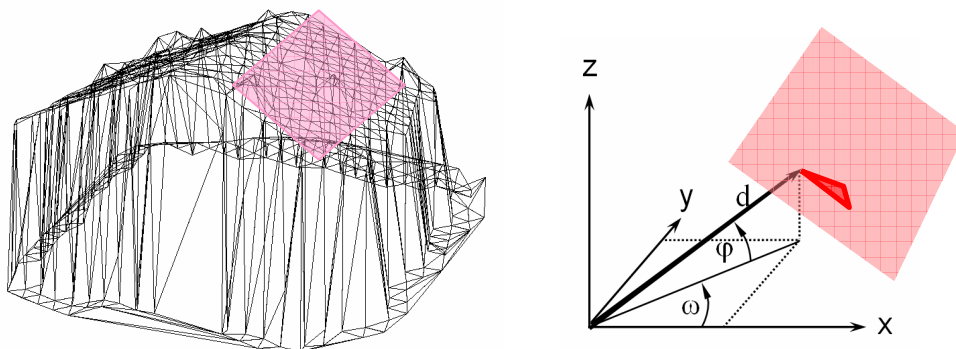


Figure 3-7: 2.5D TIN-structure and definition of the triangle parameters  $\varphi$  for slope,  $\omega$  for orientation and  $d$  for the perpendicular distance of the triangle's plane to the origin  $O$

Displaying then the position parameters of the triangles of such a point cloud in a parameter space should show an accumulation of parameter points in certain areas. Each parameter point group would then represent a planar feature such as a roof face. Figure 3-8 shows the parameter space of the triangle structure from Figure 3-7. The upper image displays parameter points in the  $\varphi,\omega$ -plane and the lower image displays them in the  $d,\omega$ -plane. Two clusters of considerable extent in the lower part in the  $\varphi,\omega$ -plane can be recognised at first glance. Four other smaller clusters are visible at the top of the  $\varphi,\omega$ -plane.

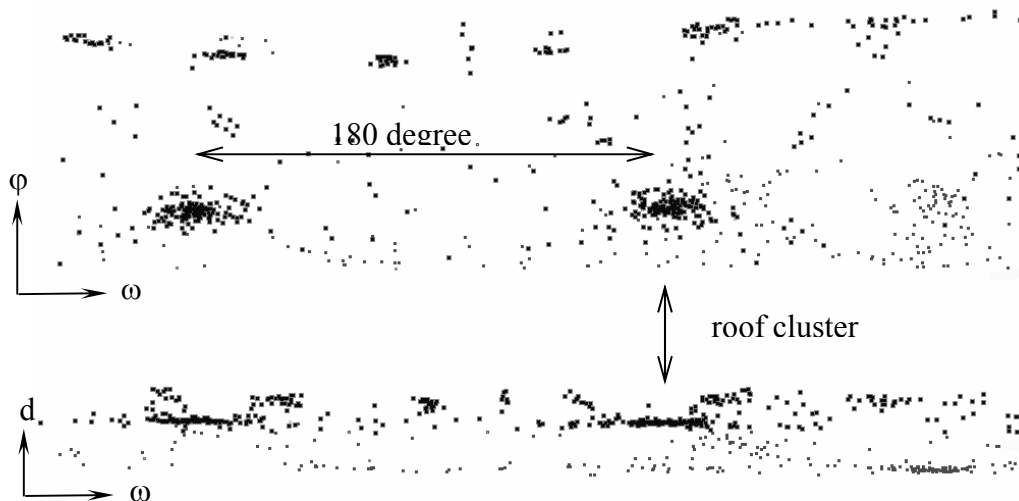


Figure 3-8: Example of a building's 3D parameter space

The hypothesis made previously was that for ideal data and roof types, the parameters of the triangles of a roof face should be the same. In Figure 3-8 it is obvious that this is not the case. Roofs possess a certain structure because of cover material and features such as dorms or chimneys, which provides an additional error to that normally present in the laser scanner data. Roof features, such as chimneys, are mainly a random disturbance and are expressed as outliers. The impact of height variation caused by tiles on the roof is of a more homogeneous nature causing a maximum error in  $z$  of 3cm – in the case of curved tiles. The main influence on the clusters' shape is presumed to be caused by the laser scanner data itself. The next paragraphs will discuss this influence.

#### *Variation and characteristics of the parameters caused by errors of the laser scanner data in height*

Since planimetric as well as height errors of laser scanner data are mainly caused by the GPS system on board, laser points within an object of little extent can be understood as correlated. Only the accuracy in  $z$  must be taken into account than, which is mainly caused by the laser scanner system and the method alone. This presumption can be made since the mean size of the analysed objects in this study is small and  $x$  and  $y$  coordinates of laser points are correlated to each other. Thus, the relative planimetric accuracy of neighbouring laser points is in range of few centimetres, whereas the relative accuracy in height may be a decimetre.

For the slope parameter, Figure 3-9 exemplifies the effect that the error  $a$  in the laser scanner data in  $z$  has on the triangle meshes.  $\delta\text{Slope}$  in Figure 3-9 describes the angle by which a triangle can vary around its actual inclination. Of course, as well as the variation in slope  $\phi$ , a variation in orientation  $\omega$  and distance  $d$  occur. Each of the three parameters is discussed and analysed in the following:

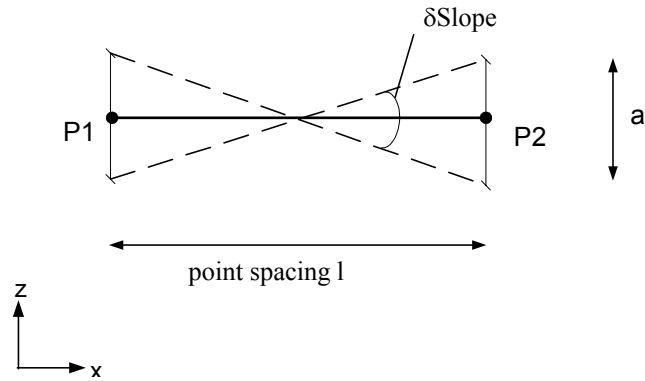


Figure 3-9: Demonstration of parameter variation  $\delta$  caused by the error  $a$  in the laser scanner data in relation to a given point spacing

First to be discussed is the slope parameter. As shown in Figure 3-10 the amount of variation decreases with increasing slope.<sup>1</sup> The angle  $\delta\text{Slope P3}$  is obviously smaller than  $\delta\text{Slope P2}$ .

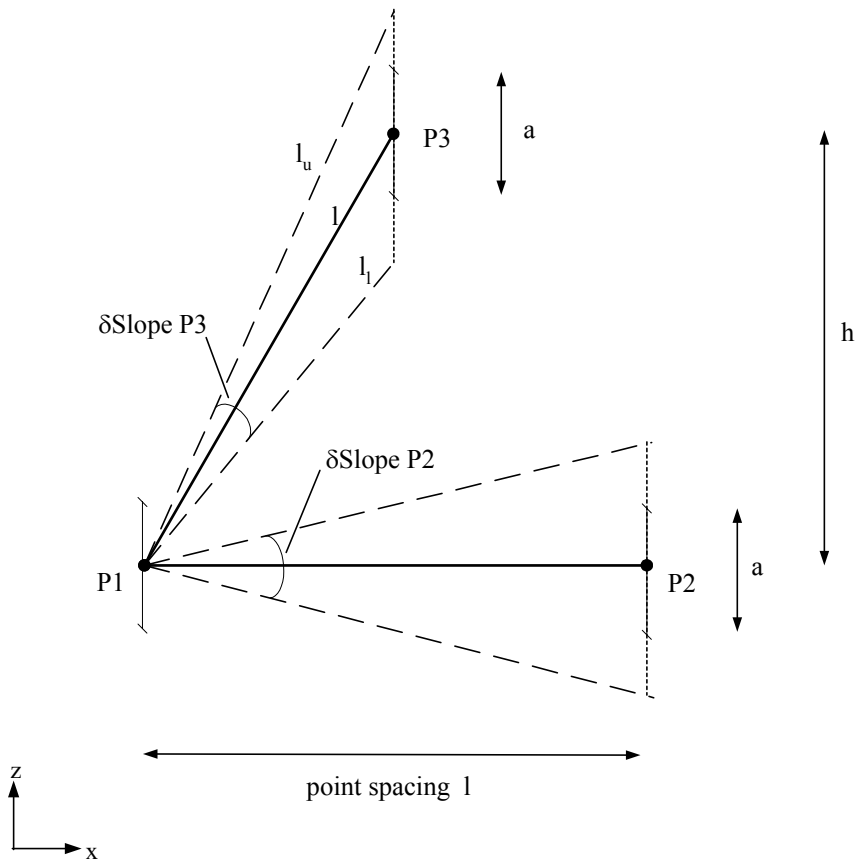


Figure 3-10: Relation between variation in slope and the inclination of a triangle

The function of the variation in slope as a function of the triangle's inclination can be described by equation 3-1:

<sup>1</sup> This theory may be applied if the same accuracy is assumed for roof faces with different slopes. It is known, though, through theoretical thoughts and empirical derived accuracies that the accuracy may depend on the slope of the object's surface. Still, it has to be analysed, if this is also the case for roof faces, which have an homogenous morphology.

$$\delta Slope = \arccos\left(\frac{h-a}{l_l}\right) - \arccos\left(\frac{h+a}{l_u}\right) = \arccos\left(\frac{l_l^2 + l_u^2 - 4a^2}{2l_l l_u}\right) \quad \text{Eq. 3-1}$$

Figure 3-11 shows the graphs of different point spacings. The graphs have been obtained using equation 3-1. The relation visualised in Figure 3-10 can be seen in Figure 3-11: With increasing slope the variation in slope decreases. The dark brown graph in Figure 3-11 represents a point spacing that is smaller than the full amount of the standard deviation of the laser scanner data in z. It is obvious that this point spacing with the presumed data accuracy cannot be analysed. It can also be suspected that it will be difficult to achieve proper results with the method, if the data accuracy comes close to the point spacing. To be able to process high density data the data accuracy has to be sufficiently high then. In interpreting Figure 3-11 it becomes clear that with decreasing point spacing to data accuracy ratio the cluster will increase in size.

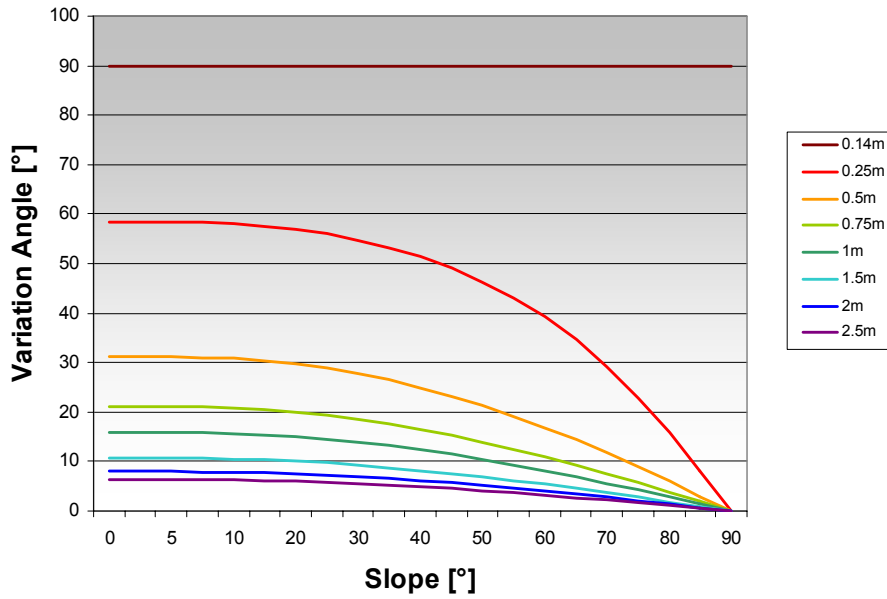


Figure 3-11: Variation in triangle slope  $\phi$  in relation to point density and as a function of slope for a laser scanner data accuracy in height of  $\pm 0.07\text{m}$

The variation in orientation can be best described with Figure 3-12. The triangles are tilted by the height error of the laser scanner points. The difference in the normal vector  $nv$  and thus the variation in orientation is given in equation 3-2.



Figure 3-12: Demonstration of the triangle's variation in Orientation

$$\delta Orientation = \tan^{-1}\left(\frac{nv_{\Delta x}}{nv_{\Delta y}}\right) \quad \text{Eq. 3-2}$$

In Figure 3-13 the graphs can be seen that describe the variation in orientation for laser scanner points with a standard deviation in height of 0.07m for various point spacings. Again, the rule applies that the lower the point spacing to data accuracy ratio the more variation in orientation. The graphs also demonstrate that for slopes lower than seven degree the clusters with these characteristics will scatter too widely to be recognizable.

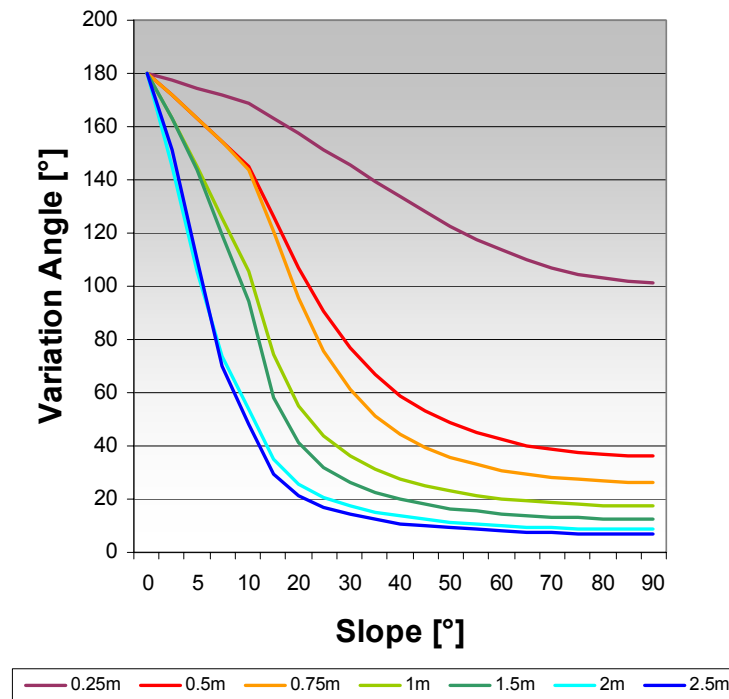


Figure 3-13 Variation in triangle orientation  $\omega$  in relation to point density and as a function of slope for a laser scanner data accuracy of  $\pm 0.07\text{m}$

The third parameter, the perpendicular distance  $d$  (see Figure 3-14) of the triangle's plane to the origin  $O$  is mainly a function of the point spacing and accuracy in relation to the distance from the triangle centre  $P_M$  to that point  $P$  of the plane that is closest to the origin  $O$ . Of course, the amount of variation changes with the triangle's inclination as described above and cannot be scaled in this parameter space without falsifying the distance of the actual plane to the origin  $O$ . Including the triangles actual distance to the origin cannot be suggested as problems may occur for long and large roof faces. Another parameter, which could be used to discriminate between two parallel roof faces, is described further on.

According to Figure 3-14, the range of  $d$ -values varies with the extension of the point cloud in object space and with the position of triangles in the local coordinate system. To visualise the variation in  $d$ , Figure 3-15 shows the graphs for a triangle of laser scanner data with 1m point spacing and 7cm standard deviation for multiple distances to the origin. It can be seen that the variation in  $d$  increases exponentially with the planes perpendicular distance to the origin. This variation is extremely large for flat surfaces, which have a large planimetric distance to the origin. Besides this variation, also the variation in orientation causes those surfaces to scatter in parameter space. The scattering may prevent clusters to be detected. Steep roof faces are less affected by this, even if they have a large distance to the origin. In general, there may be difficulties when detecting extremely long roof faces while using the described parameters. In praxis, these problems did not occur.

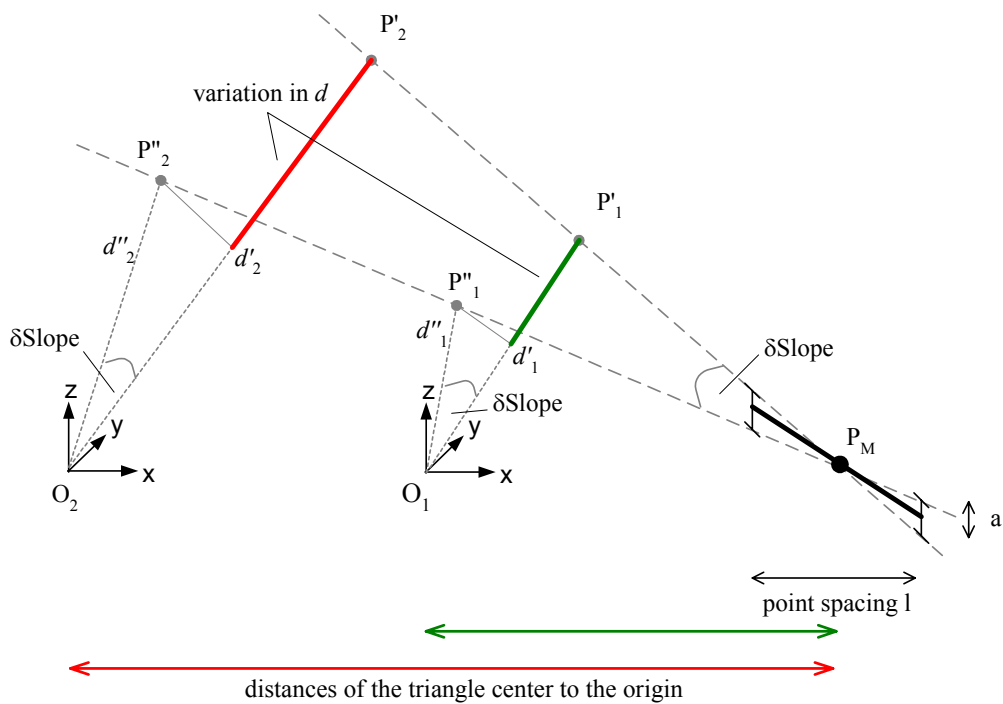


Figure 3-14: Relation between variation in parameter  $d$  to distance from the centre point  $P_M$  of the triangle to origin  $O$

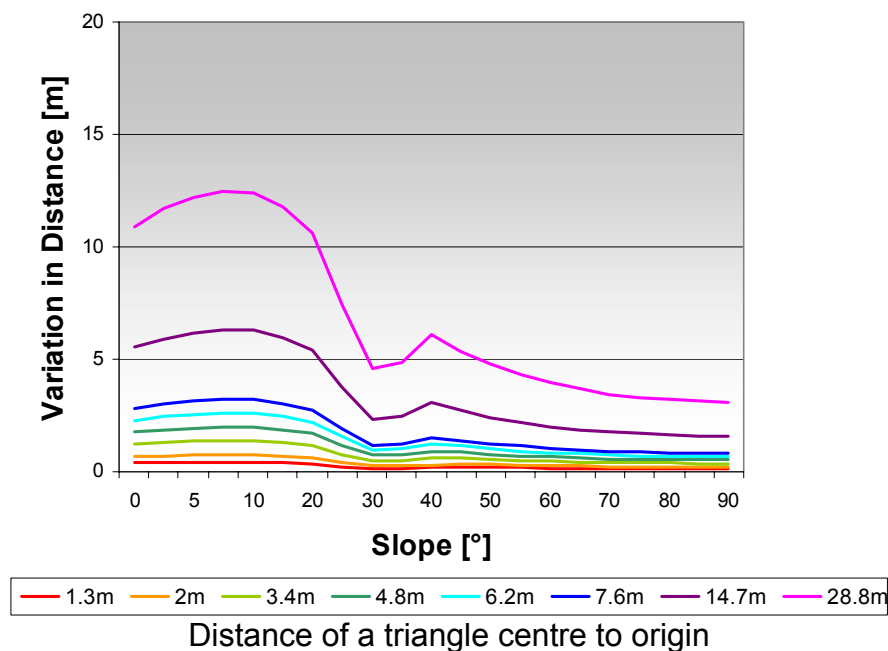


Figure 3-15: Variation in Distance  $d$  in relation to point density and as a function of slope for an example of a laser scanner data accuracy of  $\pm 0.07m$

Instead of using the described parameter  $d$  another version of this parameter could have been used. It would require cluster analysis in a parameter space given by the orientation and slope parameters of the triangles of an ALS point cloud. The cluster analysis would have the task of identifying clusters representing roof faces. For each found cluster the cluster centre is calculated. A plane representing these characteristics is generated and the

minimal perpendicular distance from the plane to each triangle originating from the cluster is calculated. Triangles with similar distance values belong most likely to one roof face. If the cluster mean was determined correctly, this parameter should also indicate surfaces, which have a large distance to the origin and a small inclination. In [Hofmann2003a] it was shown that by using only two parameters roof faces may be detected inadequately. In addition to that, practice showed that the previously described parameter  $d$  is sufficient to collect all parameter points of a roof face in one cluster – see section 3.2.1.3. For these reasons, the parameter  $d$  was utilised.

### 3.2.1.2 General Terms of Cluster Analysis

This section explains the very basic methodologies and approaches of cluster analysis that could be of interest for the parameter space shown in Figure 3-8 on page 25. These basics may be combined to customised approaches.

In principal, there are two basic approaches in cluster analysis: hierarchical and partitioning. Partitioning approaches, such as k-means, require that the number of clusters is known. The data is then subdivided into the according number of parts by optimising user defined criteria. As the number of clusters will not be known for the parameter space of a given ALS point cloud, such an approach is not practicable here.

Hierarchical approaches are either organised in an agglomerative (“bottom up”) or a divisive (“top down”) course [Anderberg73], [Kaufman90]. For both, the number of clusters may not be known. The agglomerative approach first presumes that each data point belongs to an individual cluster. The single data points are grouped taking user-defined thresholds and parameters into account. The grouping is finished if no cluster or data point is left that meets the requirements. A divisive approach has a converse proceeding: All data points are suspected to be in one group. The group is then iteratively split into single clusters in order to fulfil certain requirements. These requirements by means of thresholds and parameters are correlated to the data itself and the user’s application.

A threshold is a distance in parameter space, which can be a maximal or minimal distance, a data point has to have to a group to be accumulated or to be divided from it. The parameter space that can be n-dimensional defines the space, clusters are collected in. The type of distance between two points in a parameter space can be user-defined as well. Commonly used distances are the Euclidean, Mahalanobis or block distance. The reader can find a detailed description of them in common books about cluster analysis, such as [Nagel94]. Parameter settings specify the size of the clusters in terms of shape or number of data points. There are multiple methodologies in practice concerning the assignment of a point to a cluster, but the most frequent ones are: single-linkage, complete-linkage and centre-linkage. Single-linkage means that the shortest distance between the tested point and the cluster is taken as distance criteria. Complete-linkage refers to the largest distance and centre-linkage refers to the mean distance of the tested point to the cluster. Figure 3-16 illustrates them. Using linkages such as complete-linkage or centre-linkage delimits the clusters in size. In opposition to that, a single-linkage approach tolerates clusters of any size.

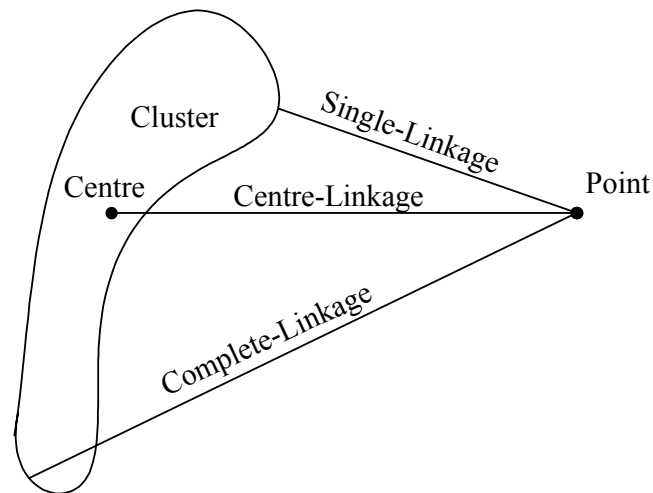


Figure 3-16: Possible assignments of a data point to a cluster

As the cluster analysis is a statistical approach of handling data, the data points can either be assigned straight to the best fitting cluster or a fuzzy description is applied. The latter one is advantageous, if multiple possible assignments for one data point occur repeatedly. Using fuzzy logic, a likelihood value is assigned to each point for each cluster.

### 3.2.1.3 The Applied Cluster Algorithm

The main characteristics of the cluster analysis to be applied in parameter space are ruled by certain pre-conditions of the data. The following information on the chosen parameter space and the clusters can be formulated:

- The number of clusters, by means of surfaces, is unknown
- The size of the clusters can only be estimated for planes, if the accuracy and point spacing of the laser scanner data is given. Higher order parametric surfaces cannot be identified at all.
- The maximal point spacing between parameter points of a cluster is given by the accuracy and the point spacing of the laser scanner data.

As said before, a partitioning approach is not suitable since the number of clusters is not known; remains a hierarchical approach. Figure 3-17 shows an example of a typical parameter space. Only those parameter points are of interest that group with other parameter points. Single standing points can be left out of further analysis. An agglomerative approach would be faster in collecting close parameter points, whereby a divisive approach would rather be recommended for collecting points that are different from their neighbours. From that perspective an agglomerative approach was chosen.

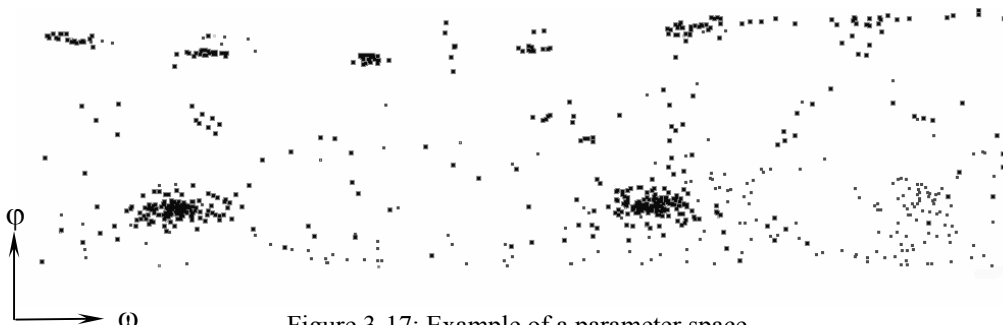


Figure 3-17: Example of a parameter space

Since the size of the clusters is not known and clusters may have any size, the approach should use single-linkage distance criteria to collect cluster points. In applying single-linkage distance criteria also ruled surfaces could be identified. The maximal single linkage distance, which would assign a parameter point to a cluster, is defined by the third pre-condition. Section 3.2.1.1 discussed the relation between the point spacing of parameter points in parameter space and the laser scanner data accuracy. It was concluded that for each of the three parameters different variations occur, and thus, the thresholds have been set at different levels for the three parameters.

To apply a fuzzy approach is not recommended, since the clusters should have a specific size due to the accuracy and point spacing of the laser scanner data. In addition, a parameter point at the periphery of a cluster, must not necessarily be at the outskirts of a roof face, but can be right in the middle of it. If it would be in the middle of the roof face, it would be added to it later on.

#### *Strategy*

In reference to the above given reasons, a suitable cluster analysis approach is agglomerative using single-linkage distances. The first task of the clustering approach is then to identify neighbouring parameter points. A point-by-point search would then have to take place. In order to make the procedure more efficient, coarse clusters are detected by counting the number of parameter points within 3D grid boxes in the parameter space. The clusters thus found are refined by collecting points in neighbouring boxes that fit the requirements. The mean of each cluster is calculated using a weighted function that takes the number of points in the cluster into account that are close to each cluster point. Thereafter, an organisation of the clusters by means of merging very close clusters takes place. This is because each parameter point was assigned accordingly to the actual cluster's thresholds even in cases where it would have fit multiple clusters. As a result, the multiple clusters have to be merged to one large cluster. The clusters are later put into the modelling routine that selects the triangles of roof faces via the collected parameter points and interpolates planes into the laser scanner points of the gathered triangles. Figure 3-18 outlines the main steps of the cluster analysis. The following paragraphs will explain them in detail.

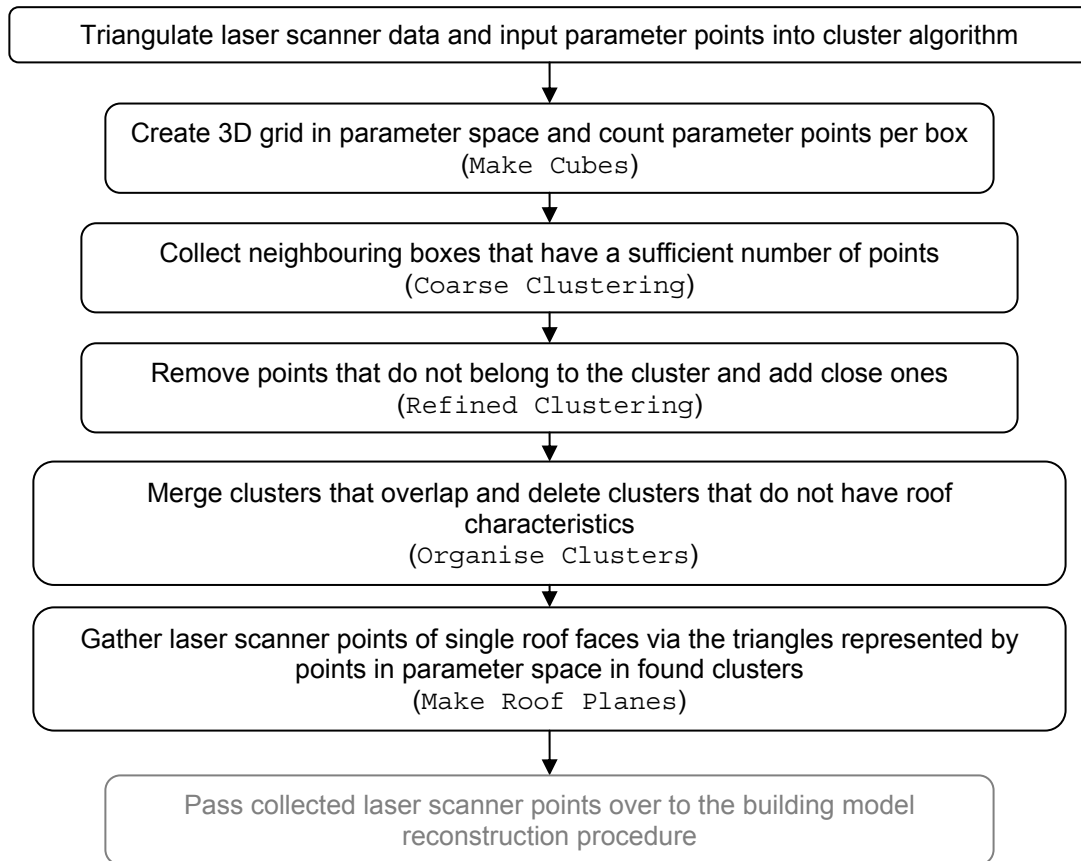


Figure 3-18: Flow chart of clustering process

### *Make Cubes*

For the coarse clustering a 3D grid, as visualised in Figure 3-19, is projected into the parameter space and the number of points per box is counted. The extent of the grid's boxes needs, of course, to be adapted to the properties of the clusters to be found. It was mentioned before that the variation in slope and orientation increases with decreasing inclination. The variation in the distance  $d$  mainly increases with the plane's position to the barycentre of the ALS points. Thus, the proportions of the boxes' edges should take these findings into consideration. The optimal size of the boxes must also take into account the fact that boxes that are too large could inherit two clusters that cannot be separated later. Boxes that are too small will increase the computation time cubically. In addition, too many clusters would be found. The size of the boxes was optimised for data of approximately 1.5m point spacing and 15cm accuracy with 7 degrees in slope, 10 degrees in orientation and 2m in distance  $d$ . The flatness of roof clusters in  $d$  made it also necessary to increase the search area by the standard deviation that a mean roof face cluster has. Thus, each point is assigned twice. Clusters that might have been split are later merged.

In favour of a better cluster analysis the box size could be varied with the slope and the amount of variation in slope and orientation. An easier approach is to vary the required minimal number of parameter points within a box, as explained below.

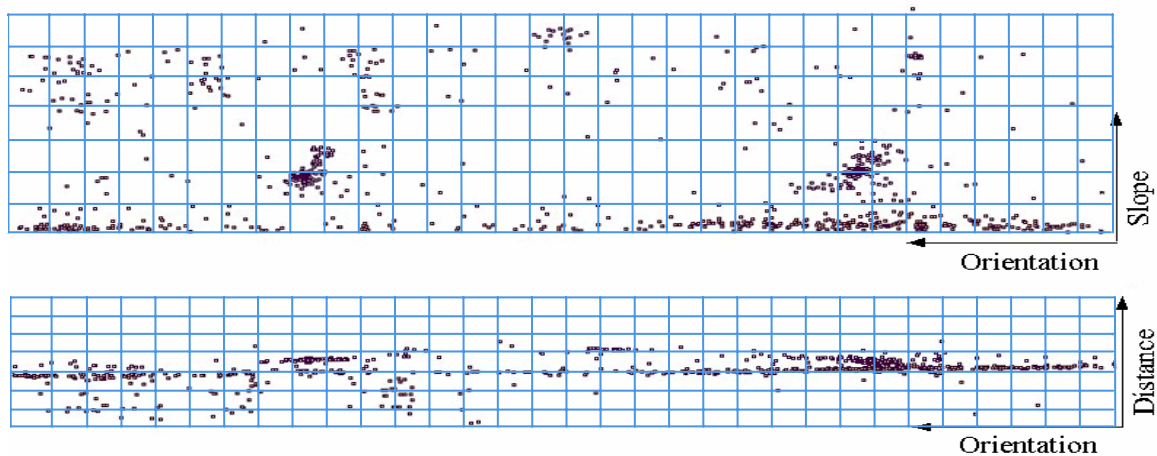


Figure 3-19: 3D grid box visualization in parameter space

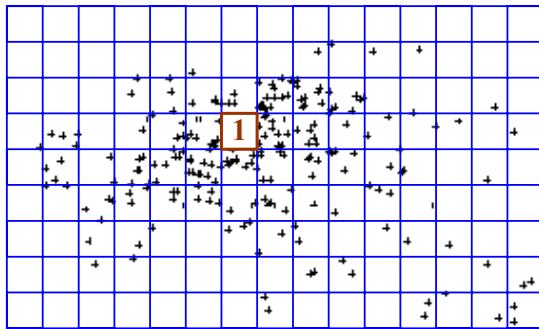
### *Coarse Clustering*

The number of points per box is counted. If the number of points exceeds a certain minimum number, the neighbouring boxes, where enough points are contained, are accumulated. The minimum number of points ( $MinNr$ ), which is necessary to start the clustering, depends on the point spacing and data accuracy and the slope. Since the cluster extent increases with decreasing slope, thus the clusters become less dense, fewer points are found within one box. Therefore,  $MinNr$  should be altered with the slope. Still, a generally set number must be defined, in order to avoid a random point concentration passing as a cluster. The optimal  $MinNr$  has empirically been found with five.

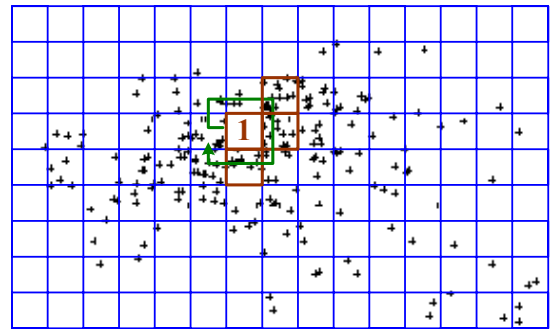
From neighbouring boxes only those that are direct neighbours in slope and orientation but not in distance are included. Figure 3-20 visualises the process. Those points that are in the neighbouring boxes in  $d$  have been assigned to two boxes (see previous paragraph). The grouping process is a simple region growing technique. Each box neighbouring to the boxes of a cluster is accumulated if it contains more than the required minimum number of parameter points. The position of the parameter points in the box is here not yet taken into account. This requires boxes that are smaller than the variation in Slope, Orientation and  $d$  caused by the laser scanner data and that will allow a distinction of two close clusters.

Single standing boxes with at least twice the minimal number of points are accepted as groups as well. This accumulation of triangles in object space indicates a plane surface that can be a roof face, in respect to its size.

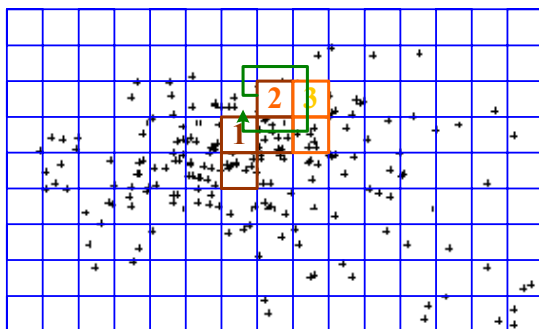
The thus formed groups of boxes represent coarse clusters.



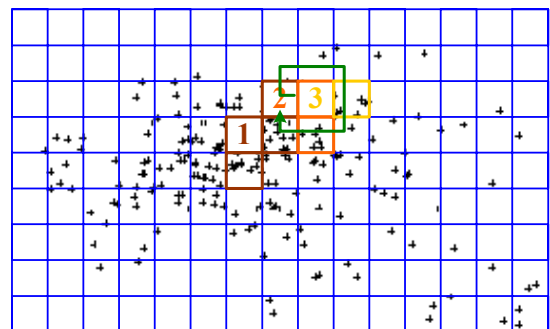
- Select an arbitrarily chosen box.



- Check neighbouring boxes for their content.  
- If number of points per box exceeds  $MinNr$ , select box.



- Choose one of the selected boxes.  
- Check its neighbouring boxes for their content.  
- If number of points per box exceeds  $MinNr$ , select new box.



- Continue as described until no new boxes are found.

Figure 3-20: Coarse clustering procedure

### *Refine Clusters*

The coarse clusters must be refined. First points that do not belong to the cluster, but are within the box should be removed. This is accomplished by counting the number of parameter points that are close to each of the points in the cluster. Whether a parameter point is close to another or not is determined by the variation in slope, orientation and distance  $d$  caused by the laser scanner data taking the slope parameter of the tested parameter point into account. The calculated number of parameter points that are close to a parameter point represents the weight for this point. The weight is later used to calculate the mean of the cluster. Thus, if there are no close points, the weight is 0 – the point is eliminated from the cluster.

### *Organise Clusters*

As not only clusters that indicate roof faces and that are represented by groups of boxes are found but also other, maybe randomly existing clusters, the clusters have to be analysed.

The graph of Figure 3-13 on page 28 (Variation in Orientation) visualises the fact that the amount of variation caused by the error in the laser scanner data is correlated to the inclination of the object. Clusters that have a mean slope value of less than set with the variable  $MinSlope$  and that have a negative distance value are deleted, as they are most

likely ground points. Also clusters that have a mean slope value that is higher than 75 degree are deleted, since they represent triangles connecting the ground with the roof, so-called wall triangles. Setting *MinSlope* is a responsibility of the user, but it is suggested, that the value is greater than three degree. Clusters with a slope close to zero cannot be controlled in their extent in orientation and as a consequence cannot be collected correctly.

The remaining clusters are checked to see whether they should be merged or not. If the mean points of multiple clusters are within the area defined by the data accuracy, the clusters are merged. As a pre-requisite for a good plane interpolation, the last test removes clusters that have fewer than three parameter points.

In case that only one possible cluster was left, the parameter space is checked whether there is a group of points 180 degree shifted in orientation at a slope that is valid for roof faces. All parameter points, which are within the search area, are collected. If there are points that group, they would then be taken as a roof cluster as well. At this point, the cluster algorithm is finished.

#### **3.2.1.4 Collection of Laser Scanner Points of Roof Faces**

Clusters, derived as described in section 3.2.1.3, contain parameter points that represent triangles of a plane in object space. Consequently, the link is provided to collect the laser scanner points of these triangles. Figure 3-21 illustrates this link. The next task is then to associate, for one roof face, the parameter points with the triangles in object space. As a cluster contains all “triangles” belonging to one plane in object space, there may be parameter points in the cluster that fit the plane, but do not belong to the roof face. It may also be possible that two roof faces are positioned in exactly one plane, although they are far apart from each other. To make sure, that only triangles, and so laser scanner points, of one roof face are collected in one region, a region growing technique is applied to each cluster’s data in object space. Another reason is that there may be points in neighbouring boxes, which were not collected, but still belong to the cluster. Their triangles in parameter space would than be associated as well.

A region is created by starting with the parameter point closest to the cluster centre. Taking this triangle, its neighbours are checked whether they occur in the cluster or not. If so, they are added to the region. Each neighbour of each triangle added to the region is assessed to ascertain if it is already in the region or if it belongs to the cluster. All parameter points that are added to a region are removed from the cluster. In doing so at least one region is created out of the cluster. If the point cloud is rather large there can be several regions. In Figure 3-21 it can be seen that each roof face represents one region. Laser scanner points, which are not on the roof face and that might have been caused by chimneys or antennas, are not included in these regions.

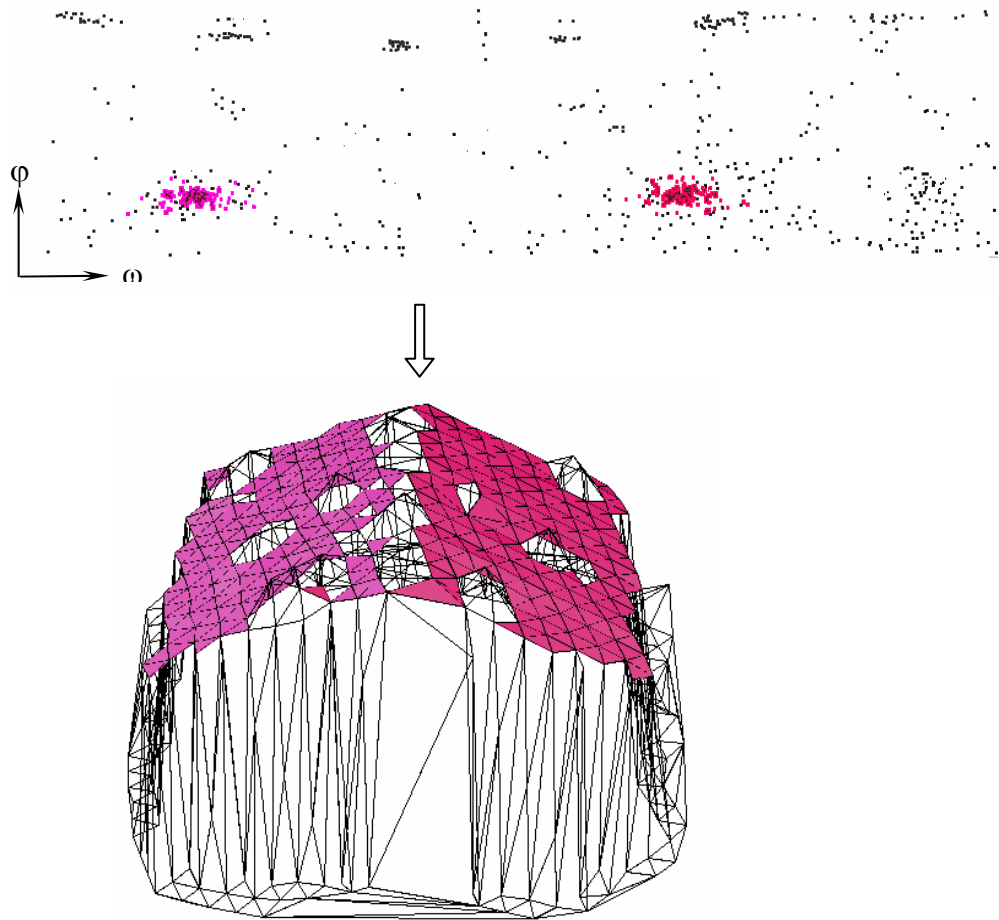


Figure 3-21: Association of parameter points of clusters and triangles between laser scanner points

Multiple regions can be created out of one cluster if there are:

- Ruled surfaces [Mathworld] that need to be split into smaller parts to be able to reconstruct them.
- Errors in the scan line registration
- Two individual roof faces

In cases where multiple regions are created, they are checked to ascertain if they can be merged. A single-linkage measuring between the regions in object space takes place. If the planimetric distance between two regions exceeds a certain threshold (*Mergedist*), they are not merged. *Mergedist* is set by the user. A value that is approximately 1.8 times the mean point spacing of the laser scanner data is suggested. If the distance is larger than two times the point spacing, it is quite likely that both regions represent neighbouring individual roof faces. As the point spacing gives no sufficient information for this detail, it is presumed that if there is no point close enough for connecting the regions, then the regions do not belong to each other. The maximum permitted height difference for merging regions is given with the parameter *MergeAcc* that is the accuracy of the laser scanner data.

In the single regions planes are interpolated as described in section 3.3. Thereafter, the building model reconstruction procedure takes place (see section 3.5).

### 3.2.2 Segmentation Approach

There are multiple approaches (e.g. [Rottensteiner2002a] and [Gorte2002]) and examples in literature, which prove that a segmentation procedure can be sufficient to collect ALS points in order to derive plane parameters of an ALS point cloud. The question is then: Why should a cluster analysis be preferred? In order to substantiate the 3D parameter space approach it is compared to a segmentation approach.

When comparing both approaches, the prerequisites to the segmentation as well as the building model reconstruction procedure have to be identical. To ensure this, the data, by means of a point cloud and its TIN-structure, given to the segmentation process is the same as for the 3D parameter space analysis. The segmentation process is the previously explained region-growing procedure of section 3.2.1.4, except that all parameter points are put into one cluster. Thus, the segmentation procedure is an agglomerative approach that starts with a randomly chosen triangle. In order to create segments all neighbours of this triangle are united with it, to one region that has a similar orientation in space by means of slope and orientation. All neighbours of the triangles that have been assigned to the region are analysed. A segmented group is finished if there are no further triangles that are direct neighbours of a region member. A new random triangle is chosen and a new region is started. This process is repeated until all triangles are assigned to a region. In doing so, all triangles that form a plane are collected in one region. The next section discusses both methods.

### 3.2.3 Discussion of the Approaches

In this section the advantages and disadvantages of the proposed cluster analysis method and the used segmentation approached are reviewed.

#### *Cluster Analysis*

The algorithm of the proposed cluster analysis is controlled mainly by two parameters: the accuracy parameter *Acc* and the mean point spacing *meanPtDist*. As described in section 3.2.1.1 the ratio of *Acc* to *meanPtDist* determines more or less the expansion of the roof clusters. As a consequence, both parameters must be set properly. The latter parameter is easy to find out, but the correct accuracy value may only be found empirically if it is not given with the laser scanner data.

If *Acc* is set too high (the number is too small), not all parameter points of a plane are detected and the roof face cannot be reconstructed completely. Vice versa, *Acc* set to low will result in merging planar faces which should not be merged.

On the other side there is the question, whether it would be appropriate or not to use complete linkage, if the ratio of the laser scanner point spacing to the laser scanner accuracy controls the cluster size. This would be true, if the roof faces were perfectly planar objects. Since this is not the case, the cluster's expansion is also a function of the roofs appearance.

Within cluster analysis membership assignments are applied often to all points put in the analysis. The proposed method has no membership assignment for points that were not included in clusters. These points usually originate from triangles belonging to walls or

other non-building objects and can be separated well from roof clusters using the parameters *Acc* and *meanPtdist*.

The cell size of the 3D grid and the minimal number of points (*MinNr*), which allows the collection of the cell, was optimised for a certain data density. In order to be able to process also different data densities on of these values may be varied with the data accuracy. As a fact, it is not relevant if the cell size or if the minimal number of points is varied. The easiest way would be to vary the minimal number of points. However, this number also represents the minimal roof face size that can be detected and reconstructed. Also, a *MinNr* that is too small would allow random clusters as roof clusters.

Relating to the laser scanner data, variations within a roof face suppress a successful cluster analysis. The variations may be caused by objects on the roof face or problems with the scan line registration or the strip adjustment if no strip information is given. In order to reduce these causes, an edge-preserving filtering could be applied to the laser scanner data on demand.

Although, it was presumed that the minimum roof inclination, which can be processed, is three degrees, experience also shows that roof inclinations of at least one degree can be recognised with this method.

#### *Segmentation*

The segmentation procedure does not require pre-analyses such as cluster analysis. However, each triangle in object space must be checked whether it belongs to a potential roof surface or not. Parameters and thresholds have to be set to steer the region growing. Similar to the parameter *Acc* in the cluster analysis, a threshold must be used which controls the assignment of triangles to groups on the basis of their orientations in object space. If the threshold is set too loose, too many triangles are collected and the group of triangles does not represent the planar surface correctly. Setting the threshold too low creates many small regions which have to be merged later. The difficulty is here to start and steer the segmentation algorithm in a way that all triangles of a planar surface are collected properly. Experiences [DAWach] show that a badly chosen seed triangle falsifies the whole segmentation result. Using the proposed parameter space this problem does not occur.

After the segmentation process is finished, the found regions must be inspected if they actually represent roof faces or if they should be merged. At this point cluster analysis and segmentation have following parameters in common: The slope criterion is used to tell wall and bottom triangles apart from roof triangles. *Mergedist* defines the maximal distance between two regions that is allowed in order to join the regions. *MergAcc* is the maximal difference in height the closest point of the one region has to have to the other region. Both parameters must be chosen in accordance to the laser scanner data set quality. Also, a minimal number of triangles for triangle groups representing planes must be set with the purpose of identifying triangle groups which do not indicate roof faces. Here, cluster analysis has the advantage that smaller regions, which often appear on roof faces of weak laser scanner data (see Figure 5-19 on page 90 for example), can be related to each other because they originate from the same cluster.

### 3.3 Plane Interpolation

This section will briefly introduce the method, which was used to interpolate a best-fitting plane into a group of points. This group of points may be ALS points representing roof faces of a house. There exist a number of methods on fitting a plane into a given group of points. Although previously made theories disregarded planimetric errors of the laser scanner data, it was decided on using singular value decomposition, as described in [Luhmann00], to derive the plane parameters. This takes the orthogonal distances of the points to the plane into account and is therefore the most exact method. Thus, the error in  $x$ ,  $y$  and  $z$  of the laser scanner data is considered. In order to make sure that the plane parameters were derived correctly, the mean distance of the points to the interpolated plane and the standard deviation of the orthogonal distances of the laser scanner points to the plane are calculated. If both values exceed a certain threshold a least-square adjustment is used to derive the plane parameters. The following paragraphs will explain the procedure.

First, the given coordinates of the laser scanner points are reduced to barycentric coordinates and put in the matrix  $A$  (Eq. 3-3). The eigenvalues of the point cloud can be derived using matrix  $B$  (Eq. 3-4), which is a symmetrical square matrix.

$$A = [x_i - x_0 \quad y_i - y_0 \quad z_i - z_0] \quad \text{Eq. 3-3}$$

$$B = A^T A \quad \text{Eq. 3-4}$$

The singular value decomposition of the matrix  $B$  into eigenvalues, as shown in [Mathworld], can be done using the characteristic equation (Eq. 3-5):

$$\det(B - \lambda I) = 0 \quad \text{Eq. 3-5}$$

The eigenvalues arise by the solution of the characteristic equation with the characteristic polynomial (Eq. 3-6), which is obtained by applying the “rule of Sarrus”.

$$b_0 \lambda^3 + b_1 \lambda^2 + b_2 \lambda + b_3 = 0 \quad \text{Eq. 3-6}$$

In order to find a solution of equation 3-6, by means of finding a root, an iterative approximation using the “Pegasus” method, which is described in [Engeln-Müllges96], was chosen. The root has to be calculated as accurate as possible, as its accuracy determines the adjustment of the interpolated plane. If this accuracy is not suitable, the plane parameters are adjusted.

Via the three sub-determinants  $D_i$  of the matrix  $B$  the normal vector elements  $a$ ,  $b$ , and  $c$  can be calculated (see Eq. 3-7 and Eq. 3-8).

$$D_i = \det B \quad \text{Eq. 3-7}$$

$$a = \frac{D_1}{D} \quad b = \frac{D_2}{D} \quad c = \frac{D_3}{D} \quad \text{Eq. 3-8}$$

Eq. 3-9 is the preferred version of the plane equation used, as it allows simple calculations for e.g. plane intersections.

$$ax + by + cz = d \quad \text{Eq. 3-9}$$

In order to verify the fit of the interpolated plane, the standard deviation as well as the mean distance *meandi* of the orthogonal distances *dist* of the laser scanner points to the interpolated plane is calculated using the equations 3-10 and 3-11.

$$meandi = \frac{1}{npts} \sum dist \quad \text{Eq. 3-10}$$

$$stdev = \sqrt{\frac{1}{npts - 1} \sum (dist - meandi)^2} \quad \text{Eq. 3-11}$$

When using singular value decomposition for estimating plane parameters certain circumstances will falsify the results. Those circumstances may be: the characteristic polynomial has no root or a very steep zero-crossing. Thus, the root cannot be determined or not very accurately. A very regular point pattern or all points exactly within a plane will result in a singular matrix B and a solution is not possible. In these cases the standard deviation or the mean distance may exceed the defined accuracy *Acc* or may even not be calculated, a second method is tested. Here, three randomly chosen laser scanner points are used to approximate plane parameters. These are then refined by applying a least-square adjustment. The least-square adjustment has the disadvantage of minimising the distance of the laser scanner points to the plane in z. Thus, the adjusted plane may not fit exactly for steep planes (see [Luhmann] for details). Again, the standard deviation and mean distance is calculated. The better fitting plane parameters are taken.

In principal, planes are only interpolated in laser scanner point groups with more than three points minding a good spatial arrangement. In case there are more than three points and all of them are aligned approximately along a line, the plane is not calculated. The reason is the low stability of the plane parameters perpendicular to the line.

### 3.4 Issues to the Grouping of Planar Faces to Build Up a Roof Topology

Previously, a 3D building model was defined as a virtual 3D building object with a full roof topology. Just a virtual representation of a 3D building object, without roof topology, could not be called an object since the single components are individuals and do not have knowledge of each other. In order to make use of a 3D building object the topology of all features must be known as well as the meaning of these features (semantic information).

Semantics is defined here as the study of meaning and topology as the study of the property of figures. Topology deals with those properties of geometric configurations, which are unaltered by elastic deformations (as a stretching or a twisting). An example is the relation between neighbours. [Bartelme00] Semantics may be used to help the grouping of planes. Via the analysis of the meaning of planes, it can be decided whether and which sides of two planes are intersected or not. If the outlines of planes are determined and all planes are intersected and thus grouped correctly and if this information is stored, the roof topology is known. Via the roof topology the roof style (e.g. a hipped or gable roof) can be derived and given to the map/outline information as additional information.

Section 3.1 already offered a summary of recently published works on building model extraction. Section 3.4.1 discusses their intersection approaches, which are mainly line-

based methods. This means that a roof plane is defined by a number of lines and the intersection itself is carried out by testing the relation of lines to each other. A method is plane-based, when the relation of planes to each other is of importance while grouping and intersecting them to an entire building model.

Section 3.4.2 - 3.4.4 explain the different strategies, which have been developed in order to find an algorithm that fulfils the criteria of proper roof face intersection. For all three strategies, the goal was to find one algorithm, which creates a 3D building model from an input plane constellation without knowledge of the building's size, shape and roof structure. A proper grouping allows the intersection of all planes, which are roof planes, with each other and gives these planes the correct, according to the ALS point cloud, extensions.

#### **3.4.1 Previously Published Grouping Strategies**

In literature on building model reconstruction there are only few that actually discuss the topic of grouping planes. Most of them only mention the fact that single planes must be grouped and intersected in order to create a model. Many articles speak about roof topology, which was built up during the intersection, but only few developed a system, which works automatically. This section will introduce these published grouping techniques.

In principal, two different approaches have been published. The first uses CSGs (Constructive Solid Geometry) and the second one, the more often used approach, uses line-based grouping methods. CSGs are used for instance by [PhDSüveg]. Although this work bases on aerial imagery, the grouping concept is related to lines, but not to their origin. These lines are the only information, which is fed into the grouping strategy. The general idea behind this method is that all buildings, also complexes, can be modelled by combining flat, gable or hipped roofs with each other. In order to combine these CSGs a complex building has to be divided into smaller parts using ground plan information, which is not trivial for building complexes. Once the complex is split up, the primitive has to fit in the roof. Süveg experienced here problems with inconsistent solutions. In this work it was also made clear that the used styles of CSG models should be extended to further improve results.

Line-based approaches are more diverse in literature: A method using ground plan information is presented in [Vosselman2001]. All planes are intersected with each other, but only those intersection lines remain, which have ALS points in their direct surrounding. Ground plan information is used to limit these lines. Reasons for not reconstructed building models are given with the outline of the building, which was not rectangular, or the shape of the reconstructed outline.

[Brenner2000] developed a method, which compares intersection situations of three lines with predefined junction models. Using a probabilistic decision model, junctions that do not agree with the ground plan information are dismissed. Single examples show achievements of the method.

LiDAR data only is used in the following three approaches: [Haala1997] briefly introduces his decision model on the grouping of planes, which are classified in roof and wall planes. In order to aid the decision model Haala creates adjacency graphs that symbolise the

connection of the roof faces and walls to each other similar to the approach described by Brenner.

Another grouping algorithm is also mentioned in [Forlani2003]. Here, intersection points are classified as either internal or external nodes by their number of lines meeting in the intersection point and their position in the building outline. No information on the performance of the method is provided.

The intersection strategy developed by [Schwalbe2004] is similar to Vosselman's strategy. Instead of ground plan information the roof face boxes themselves are used to delimit lines in their extension. A roof topology is not built up in this approach.

From the above named approaches it becomes clear that a method based on CSGs will always be limited in its results. First, complexes have to be split up correctly. Second, these small parts still need a large number of models to reconstruct any building's shape. Furthermore, a method which would try to fit a hypothesis model taken from a building model library into a point cloud, would fail for many complex building structures. In many other cases, it would generalise asymmetrical roof structures.

A rule based method similar to those of Brenner and Forlani has the advantage to be able to process also complex roof structures. The method would not be limited to a certain complexity but to ambiguous situations. The task is here to find clear rules for these situations.

#### **3.4.2 Analysis of Available Information**

The core of the grouping procedure is the knowledge on roof planes within the actually analysed LiDAR point cloud. There is, however, no knowledge on the input roof style or roof structure available. The task is to interpret the constellation of planes and to find relationships between these planes. As soon as the relationship is established, the actual intersection is performed and the building model is reconstructed. The ideal algorithm for this task should be able to give good results for any combination of roof faces. The simplest application would be a gable roof and a more difficult one multiple detached houses with different roof types.

Before addressing the intersection procedure itself, it is important to know which constellations two planes can have to each other. Figure 3-22 provides an overview about common situations.

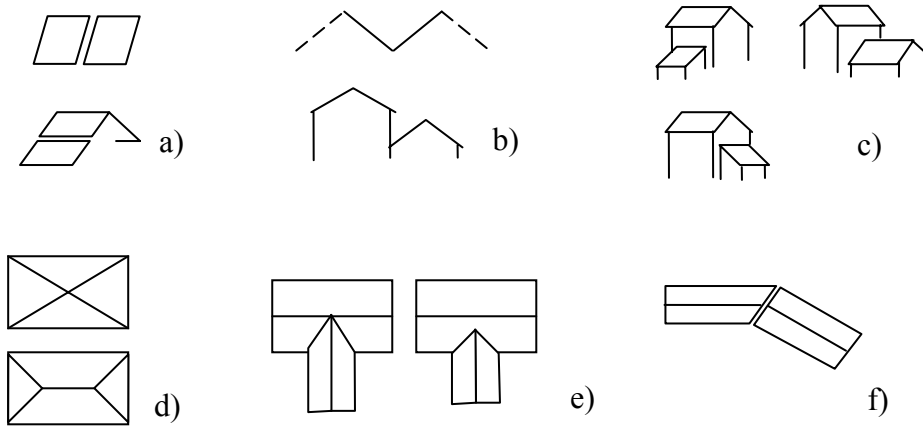


Figure 3-22: Possible constellations of roof faces a) coplanar roof faces, b) roof faces with opposite orientations ( $\pm 180$  degrees), c) planes intersected with walls, d), e) and f) planes of couples with side neighbours, which may belong to a couple themselves

A grouping algorithm should be able to recognise those situations, though they may exist in combinations, and intersect them accordingly. The first step in recognising would be to identify planes of a given group, which are direct neighbours.

In order to clarify what a neighbour is, Figure 3-23 is taken as an example. The building within this figure has three ridge directions. Each ridge is formed by two planes having opposite orientations – a couple. All three couples have hipped ends. The plane representing the hipped end is a neighbour to the couple and thus to the planes of the couple. It forms a pair with each of the planes of the couple. The couples may be neighbours in common sense, but for grouping matters only the indicated sites are neighbours in terms of “to be intersected”. Consequently, the according planes are grouped in pairs.

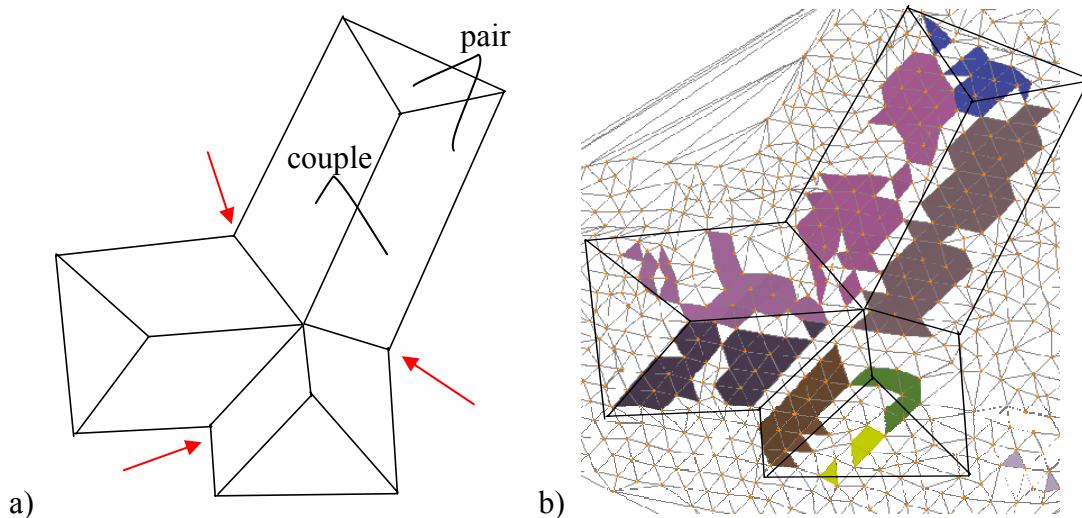


Figure 3-23: a) Group of planes, b) Group of planes with underlaid TIN-structure

The next task is to clarify the characteristics two planes must have to be neighbours. In Figure 3-23 b) those triangles are coloured, which were detected using cluster analysis. These triangles also determine a vague roof face bounding box delimiting the proposing roof face plane. Details to the roof face bounding box can be found under section 3.5.1

page 50 ff. The points defining the triangles are used to label proximities between planes and thus the neighbourhood.

From the different options which can be used to define distances the following two are applied. First, all planes are checked whether there are neighbours to a couple or not. If this is the case, two neighbouring planes are called a pair. Afterwards all remaining possible pairs are tested. If a plane is a neighbour to a couple or to a plane of a couple can be tested as visualised in Figure 3-24. The dots symbolise here the upper corners of the roof planes.

If one or two upper corners of a plane are within the dashed area of a couple, one of these basic combinations is apparent. Referring this strategy to the example of Figure 3-23 three hipped ends and three L-House combinations should be detected.

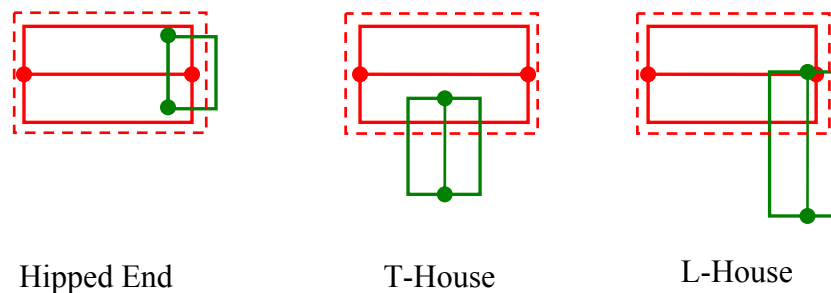


Figure 3-24: Basic combinations of planes and couples

For any other pair that may exist in a group of planes a simple minimum distance between two ALS points, which belong to the two roof faces, is accepted as indicator of neighbours. If this planimetric distance is lower than a user set threshold, which is the mean point spacing in the later analysed data sets, the planes are approved as neighbours.

When defining neighbours, also the position of planes to each other must be taken into account. It must be tested on which sides the two planes are adjacent to each other. Presuming a roof face having four sides, a plane can be positioned above, below, left or right of another plane. The position indicates then the side, the plane is intersected with the according neighbour.

With the above described test the following information is now available on the constellations of planes within a group of planes:

- Number of planes and their orientation in space (three orientation parameters)
- Couples: amount and named planes
- Pairs: amount, named planes, and intersection sides.

In case that multiple intersections have to be performed, they should follow a defined order. Best results for complex roof structures were obtained by starting to intersect those planes that have the smallest distance to each other. All other pairs are intersected in increasing distance order. If one of the planes of the actual pair belongs to a couple, that pair is simultaneously intersected. This means that the plane is intersected with both planes of the couple; even if the second distance is not the next in row.

Comprising the above explained facts, the proposed model is a plane-based approach, as the orientation of a plane in object space is most relevant for the grouping and the

intersection. The approach follows rules that have been developed in order to have a grouping algorithm that is as flexible as possible. The rules are only defined by facts, which describe possible constellations of roof faces. The rules have been varied in order to find the optimal algorithm, which is presented in Figure 3-38 on page 57. The next two sections describe two main approaches, which have been tested.

### 3.4.3 A Grouping Strategy by Means of Couples

The workflow of the grouping procedure described in this section consists of three steps: find dormers, group ridges and group sides. At each step of the grouping a code is assigned to the examined pair. A dormer means that a smaller plane is located within the x,y-projection of a larger plane. Two roof planes, which have opposite orientations and which intersect at the top and form a ridge, are a couple. A neighbour would be any other adjacent plane. Also, a basic rule was set: Once gained intersection lines remain as they are. Only the corner coordinates can be changed by moving them along the intersection line.

The task of the first step, the detection of any dormers, is to find planes with similar orientation parameters which are within each other. In a second step, those planes are associated that should be intersected at the ridge – couples. The planes are intersected and the new corner coordinates of the ridge are saved. If there are more than two planes, it is presumed that at least two of them form a gable roof. So, all roof faces are checked if there is/are one or more partners with opposite orientation that is/are within a certain distance and that has/have an overlapping area with the roof face worked on. These partners are listed in descending order by their overlapping lengths. Figure 3-32 on page 53 visualises this. Intersecting firstly those planes with the longest overlapping length will create the ridge of the two roof faces. Other bordering partners are intersected with the appropriate roof side. If no partner was found or none exists there will be, of course, no intersection.

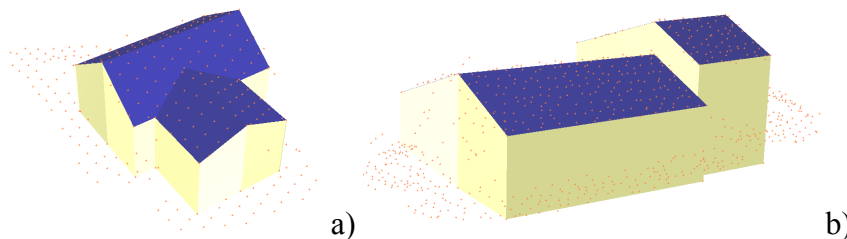


Figure 3-25: Examples of successfully reconstructed buildings with sideways-connected roof faces

The third step is the grouping of sideways neighbouring planes in order to intersect (Figure 3-25 a) or trim (Figure 3-25 b) them accordingly to their position to each other. The strategy which has been developed is: All roof planes are sorted in descending order by their size. The adjacent planes of each plane are detected and their connection type, as indicated in Figure 3-26, is recognised. All neighbouring planes are also sorted by their size. The intersection starts with the largest plane and its largest neighbour. Basically, three different intersection cases with couples can occur. Figure 3-26 illustrates them.

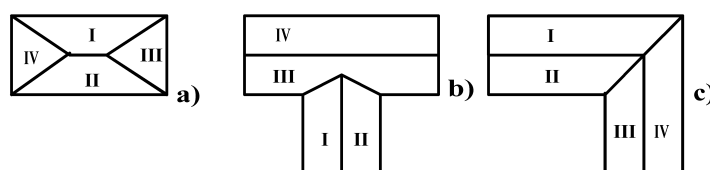


Figure 3-26: Types of possible sideways intersection

As the algorithm has to make the decision without knowledge of the buildings shape, a rule has to be set defining when to intersect all three planes or just plane II and I. If after intersecting all three planes with each other, one of them is covered by the other two planes (that would be the case for plane III of Figure 3-26 b), it should keep its original corner coordinates. Failing that, the appropriate sides of the three planes are blended.

Trimming planes is taken here as extending those sides of two adjacent parallel planes that are closest to each other in a way that they can be connected with one vertical wall. In some cases, such as storehouses, it is necessary to intersect the lower roof sides, the gutters, as well. This procedure is similar to the others. Planes next to each other with opposite orientations, which are not a couple, are intersected and the new lower end points are saved.

If all intersection steps are finished, walls are added to the building model. A wall element is created along each edge of the roof faces. The roof's eaves give the top line of the walls. The lower edge of the wall is derived from the DTM of the building's surrounding. The lowest point is chosen in order to please the eye in visualisations where also the terrain model is included. The reconstructed building model is now complete.

This approach especially showed good results for defined complexes, such as seen in Figure 3-26, but failed for various combinations of roof faces.

#### **3.4.4 Intersection Strategy Using Couples and Pairs**

The strategy described in the previous section was modified in order to process also very complex roof structures, such as seen in Figure 3-27, besides the defined roof structures shown in Figure 3-26. In order to accomplish this, the procedure of grouping side neighbours was extended. The first steps of detecting dormers and grouping ridges were not changed. For the grouping all planes were tested if they fulfil one of the following criteria:

- Orientation parameters of both planes are similar
- The planes have opposite orientations and meet at their lower edges
- One of the planes is connected to a wall or is a dormer
- Each of the planes belongs to a couple
- One of the planes belongs to a couple
- Any other combinations.

In order to ensure that those pairs, which meet more than one of these criteria, are processed correctly the arrangement of the criteria is of high importance. Best results were achieved, if all pairs are sorted in increasing order by their distances and then processed, as mentioned in section 3.4.2, obeying this order. Each pair is, of course, processed only once. A more detailed description is provided in section 3.5.5 on page 57 as part of the explanations to the whole building reconstruction algorithm.



Figure 3-27: Point cloud and picture of the Tillich-Bau of the Dresden University of Technology

In general, this approach showed better results for data with varying appearances of hipped roofs. T- and L-shaped intersections could not always be interpreted correctly. Section 3.5.10 discusses the reasons for this.

### 3.5 Reconstruction of Building Models

Having introduced the derivation of planes of an ALS point cloud and the problems of automated plane grouping procedures, the reconstruction process of the building models shall now be described.

The basic idea of the suggested approach is first to organise the planes and then to intersect them. However, the organisation as well as intersection is done here in an iterative manner: At the beginning, planes that have a similar orientation in object space and that overlap are divided into three groups. They might be dormers, failures or neighbouring planes, which accidentally have laser scanner points in common with each other. In the next step, neighbouring planes with opposite orientations in space are collected and the ridge is obtained by intersecting the planes. Afterwards, the gable ends of the roofs are aligned. This is followed by the actual grouping and intersection procedure.

The user may now decide if the gable ends of the buildings should be linearised and if the gutters and dormers should be adjusted. In order to complete the virtual model of the building, the walls are created and the result is written to a Vrml-File. Figure 3-28 lists the single steps, which are also explained in detail in the following.

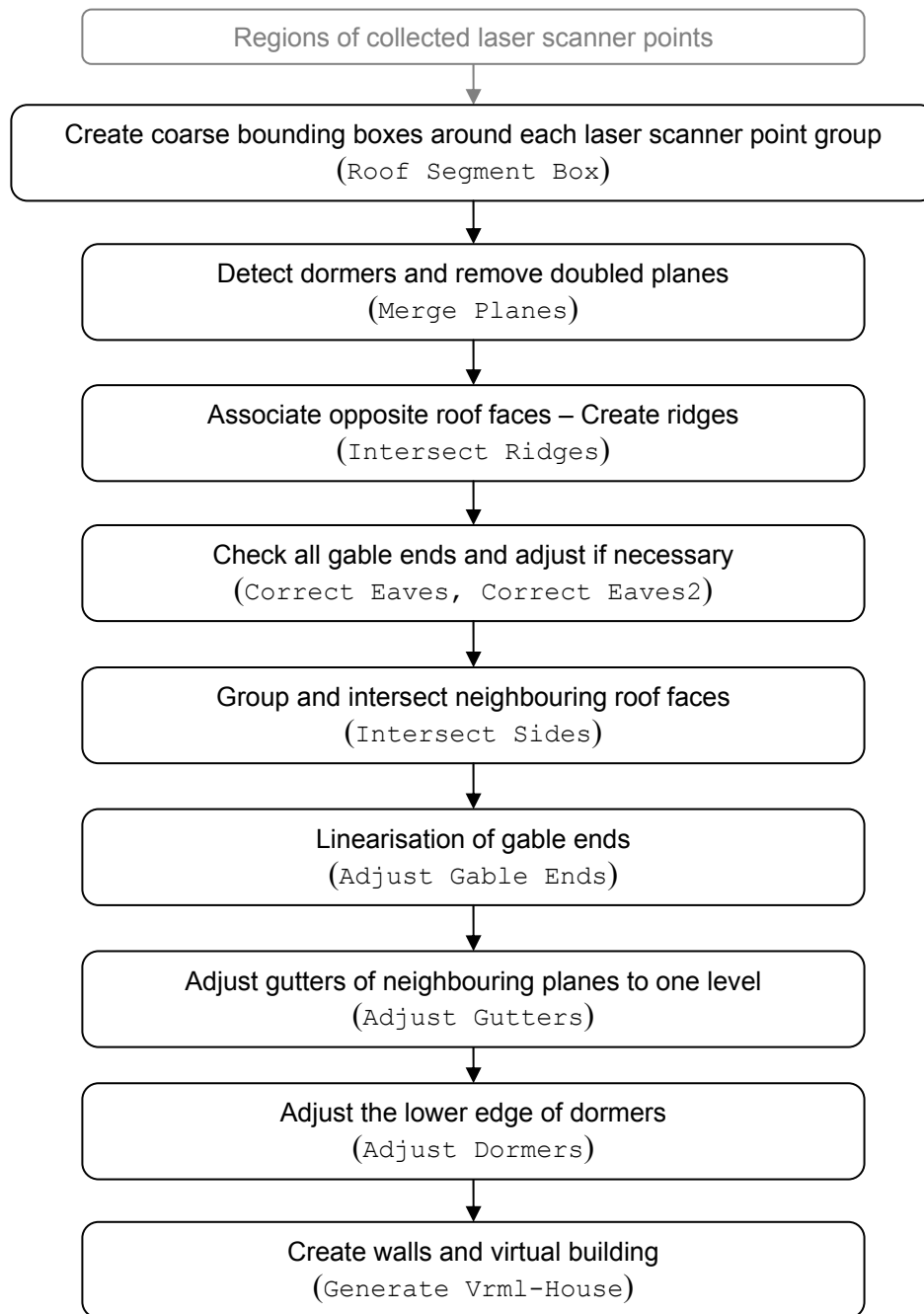


Figure 3-28: Flow chart of building model reconstruction

The whole process was designed in a way that different characteristics and attributes of LiDAR data may be handled. If strip information is provided with the LiDAR data, the strip is chosen that holds the most points within a point cloud. It is presumed that using this strip it is most likely to obtain a positive result. The adjustment of gutters and the adjustment of the gable ends are performed with all points provided in the LiDAR point cloud.

### 3.5.1 Roof Plane Bounding Box

A roof is geometrically modelled by connecting planar faces (patches). These patches are usually rectangular. Since quadrangular patches are very common for building roofs, the data structure will store the boundary information of a roof face with four points, whereby the four points must not have different coordinates. As a consequence, a triangular patch, which may describe a hipped roof end, can be described by the four points as well.

For every patch a bounding box (see Figure 3-29) describing the coarse outline of the ALS point group of the interpolated plane is generated. Figure 3-29 gives an example of a simple roof structure. In the right view of this figure, shaded triangles are visible through the patches. These triangles are the ones found using cluster analysis.

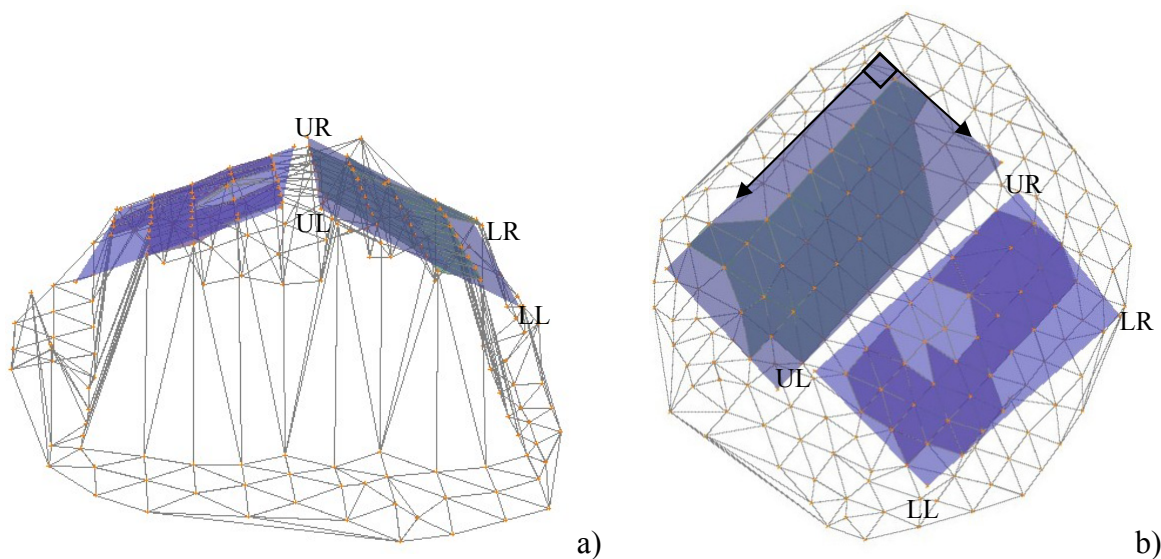


Figure 3-29: Example TIN-structure of a building with gable roof and bounding boxes  
a) front view; b) top view

A roof plane bounding box is created by putting a horizontal line, which is also within the plane, through the lowest and another one through the highest point of the roof face. These new horizontal lines represent a preliminary gutter and ridge. For the time being, the gable end sides of the roof face are defined by setting up lines through the points that are on the furthest right and left sides of the point cloud, respectively. These lines are forced to fit in the plane and to be perpendicular to the preliminary ridge and gutter. The new corner coordinates: UL upper left, UR upper right, LL lower left and LR lower right are saved. Thus, the lines can be retraced at any time.

### 3.5.2 Detect Dormers and Remove Doubled Planes

This sub-process aims to identify patches, which overlap or which are within each other as it would be the case for dormers. Figure 3-30 contains the decision tree that outlines the procedure. Two main cases have to be taken into account: On the one hand, a smaller patch can be fully within a larger patch. The smaller patch can describe a dormer or a failure. A dormer is a patch that either has an orientation that is similar to the larger patch (flat dormer) or the orientation difference is approximately 90 degree (pitched dormer). A failure would be any other smaller patch. On the other hand, two patches with similar orientations can overlap each other by some extent. In order to reduce this overlap the

smaller plane is trimmed to meet the larger plane. The procedure to draw these decisions is as follows:

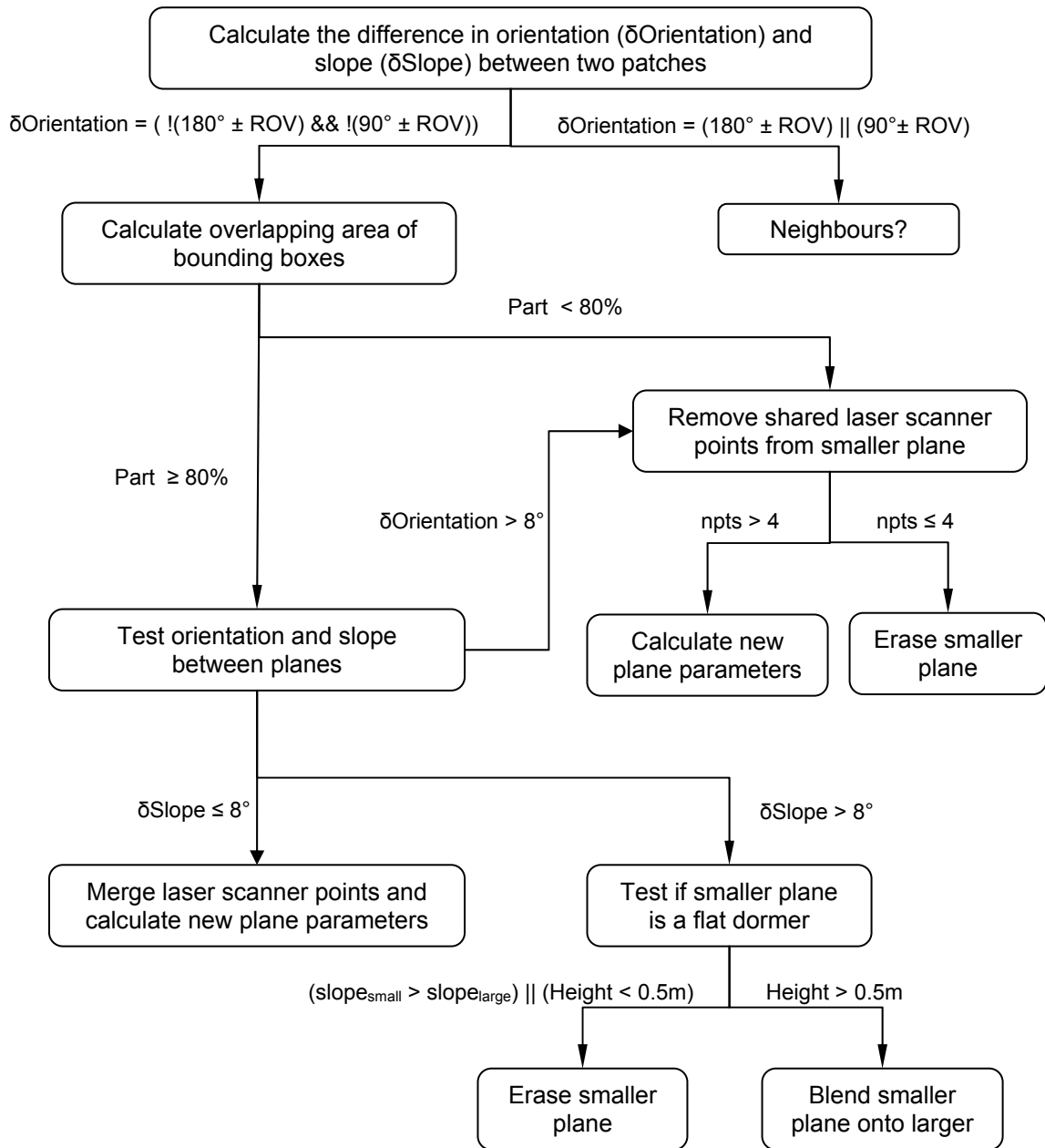


Figure 3-30: Flow chart of merge planes process

First, all patches are tested pair-wise if they have similar orientations. If this is the case, the overlapping area, in terms of the percentage of shared ALS points, is determined. As neighbouring triangles, which may belong to different patches, share the ALS points, one ALS point can be held in two planes. Thus, small patches that are positioned in larger patches can share up to 100% of the laser scanner points. This may happen when the problem of waviness occurs in the laser scanner data. It can be caused by a false scan line registration. Figure 3-31 shows an example. The right roof face is covered by two regions. Creating the roof segment boxes from both regions would create two overlapping patches. The patches have similar orientations in space and they share about 90% of the laser scanner points, but neither of them is a dormer.

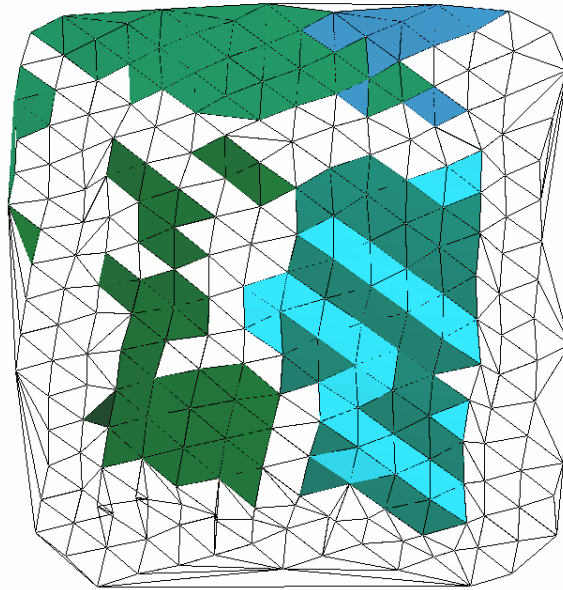


Figure 3-31: TIN-structure of a building with a gable roof, view from top

In any case, both patches have to be analysed to check if they should be merged or one of them trimmed or even eliminated. The patches are merged, if the plane characteristics are very similar, according to the thresholds given in Figure 3-30, and if they overlap by at least 80%. If the plane characteristics are not similar the smaller patches might then be either a failure or a dormer. A dormer is characterised by having a certain height relative to the larger patches on its lower edge. If this height is not reached, the smaller patch is defined as a failure and is eliminated. A patch that was identified as a flat dormer is excluded from the ridge and side intersection steps. Any other dormer faces are treated as small roof faces. If two patches overlap by less than 80%, the smaller patch is trimmed in a way that it will not share any points with the larger patch anymore. The whole sequence is repeated until no changes occurred in the data anymore.

If the user wishes to eliminate smaller patch via a size criterion, he or she may do so. For further analysis this option was not used, as it is of interest which planes can be detected.

### 3.5.3 Intersect Ridges

In order to obtain ridges, all patches combinations are compared pair-wise. If two patches have a difference in orientation of  $180 \text{ degree} \pm ROV$  and their upper lines are close to each other, the patches are considered a couple in terms of forming a ridge. *ROV* is the roof orientation variation threshold, which is caused by a tilting angle of the roof faces of the real roof and was empirically found to be 15 degree. *ROV* is necessary to enable the entire reconstruction of the building model. For good data sets *ROV* is sufficiently set with 5 degree.

Two patches are considered to be close to each other, if their upper lines are not further apart than twice the mean point distance and 1m in height. Besides, the fact that a patch can have more than one partner has to be taken into account; see Figure 3-32. If this is the case, the pair that has the longer overlapping length is the main couple and any other patches are made to fit that partner (see Figure 3-32). Here the rule applies that once created intersection lines remain.

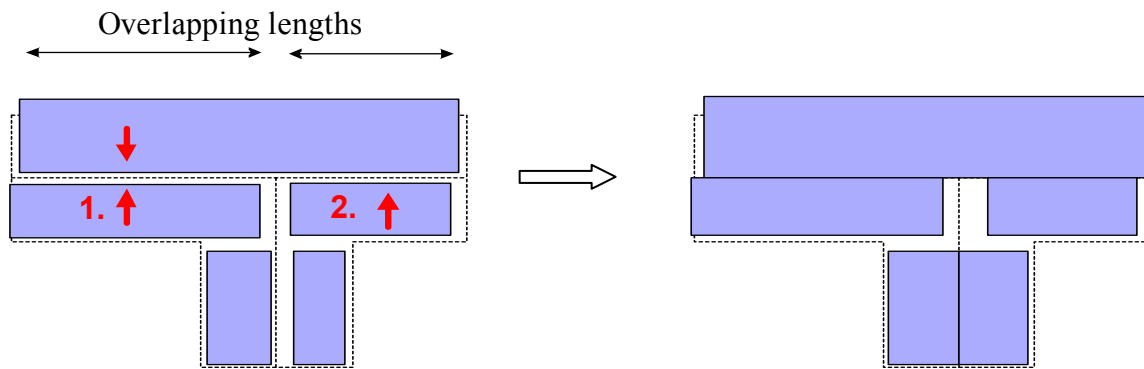


Figure 3-32: Order for ridge intersection

At this point, the ridge is not forced to be horizontal. If the user desires to apply such a rule to the building model, he or she may do so at a later point. It is recommended to execute such regulations after all patches have been grouped and intersected.

### 3.5.4 Adjust Gable Ends of Roof Faces

The eaves along the gable ends of the roof face must be adjusted in cases where the gable ends of the roof faces are not along one line (see Figure 3-33). As the grouping and side intersection has still to be carried out, the adjustment of the gable ends is performed before.

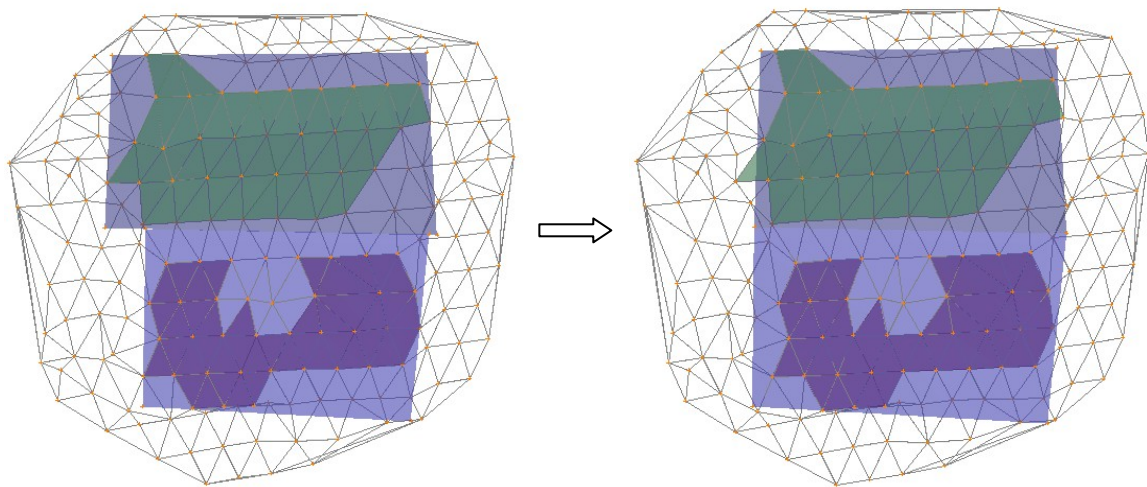


Figure 3-33: Adjustment of gable ends (Testhouse5572)

At each gable end side of a couple preliminary bounding boxes, one per roof face and gable end, are created and the gable end sides are analysed stepwise. Figure 3-34 visualises such bounding boxes. If the width of such a bounding box is less than the mean point spacing, then the pair of roof edges can be adjusted by simply applying a mean line that fits both lines (Figure 3-33 right gable end). Failing that, the content of the bounding boxes is checked. If the distance is greater than the mean point spacing (Figure 3-33 left gable end), it is presumed that either one or the other patch is not the correct size. To find out which one is more correct, buffers, as illustrated in Figure 3-34, are placed around these gable ends. A corridor is placed along each buffer. The corridor's height is the accuracy of the laser scanner data. The number of points within each of the corridors are counted and analysed; at least one point should be found. This is the point that defines the original gable

end. If there are any other points in these corridors, they should belong to the roof. The new gable lines are derived using the outermost point in each of the corridors as a new gable. Then, all points that are within mean point distance are collected and a regression line is generated. These new gable ends are compared. If the distance between both is smaller than twice the mean point distance one new mean line is generated for both roof faces. Failing that, an additional roof face is created from the larger roof face. The main gable end is determined via the shorter roof face of the couple (Figure 3-35).

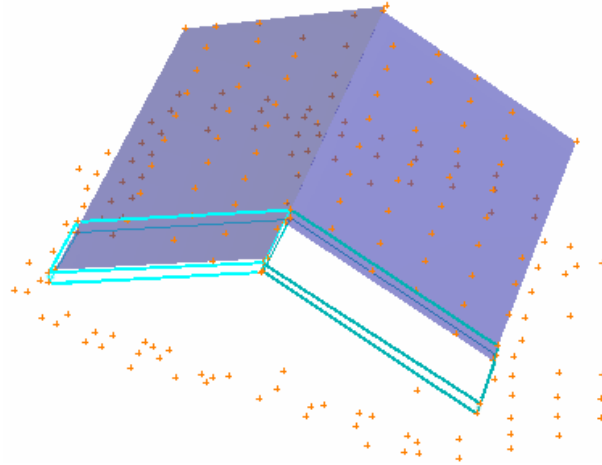


Figure 3-34: Visualization of corridors as used to look for points belonging to the roof (bird's eye view)

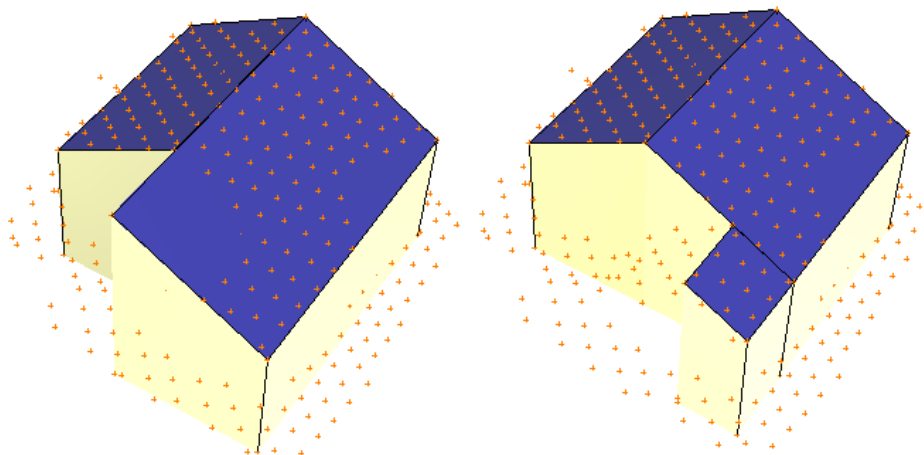


Figure 3-35: Example in which an additional patch (right) is created from a roof face (left), which is too large

Points which are outside of the corridors and which may belong to a roof face as well are not collected using this strategy. It may also occur that by editing the gable end lines of detached roof faces an overlapping area is created. The overlapped patch is shortened to fit the extended gable end line as Figure 3-35 demonstrates. The adjustment is performed even if it is not clear whether the gable ends are gable ends or if they will be intersected with another roof face. This has the advantage that roof faces that have not been detected properly are completed in this way. The disadvantage is that roof faces may be shortened although the found points belong to the roof face, as it can be seen in Figure 3-36.

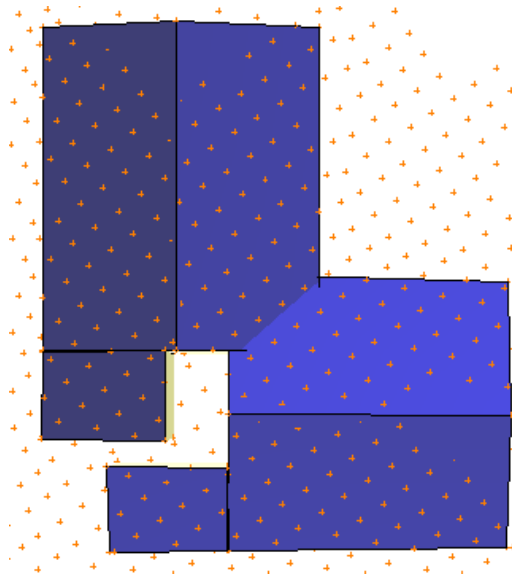


Figure 3-36: Example of the disadvantage of adding an additional patch, the constellation of patches becomes more complicated

### 3.5.5 Grouping of Planes and Intersecting Sides

The next step is the grouping and intersection of neighbouring planes. The difficulty here is to find a grouping scheme that can be applied to any number of roof planes. In order to accomplish this, the relation of the patches to their neighbours is established first and then the pairs are intersected. Here, a pair is a plane and one of its neighbours.

#### *Grouping of Planes*

Within this task the adjacent patches to each patch are detected and their connection type is recognised. Using the connection type the roof topology is established. Neighbouring patches and their position will be known. A neighbouring patch is defined as a patch that has at least one point that is closer than the mean point spacing to the other patch's bounding box. Two patches are called a pair, which are neighbours. A couple is a special type of a pair. All neighbouring patches are also sorted by their distance (attribute length) to each other. The actual intersection takes place by starting with the pair, which has the smallest distance. The type of connection is determined by the analysis of the position that two patches have relative to each other. Seven cases can be distinguished:

- Type 0 Dormer: more than 90% of a patch's points are within the boundary the projection of another patch
- Type 1 Ridge: two patches meet at their upper edges and have, as described in the section 3.5.3, a difference in orientation of approximately 180 degrees
- Type 2 Neighbours: two patches meet at their eaves
- Type 3 No connection at all
- Type 4 Bottom: two patches meet at their bottom edges
- Type 5 Lower/Upper: the patches are positioned on top of each other; the lower edge of the one patch meets the upper edge of the other patch
- Type 6 Wall neighbours: a roof plane intersecting a neighbouring wall

Those edges of two neighbouring patches – of a pair, which are closest to each other, are detected and the information is retained in a data structure. The structure of a pair is given with Figure 3-37:

pair[i].fir	patch
.sec	neighbour
.typefir	edge of patch to be modified if intersected with neighbour
.typesec	edge of neighbour to be modified if intersected with patch
.length	smallest distance between patch and neighbour
.type	type of connection
.done	marker if intersection was done

Figure 3-37: Data structure of pairs

If there is an ambiguous result in identifying the nearest edge, then no edge is stored and this patch's outline is not changed when intersected with its neighbour. In the case that no edge can be identified on both patches, there will be no intersection. If two pairs have the same length attribute, the attribute of the pair with the smaller patches is slightly increased, to make sure the intersection order is correct. Now, each pair has the information about which edge is modified when intersecting the roof faces with each other.

### *Intersecting Sides*

The most difficult part of building reconstruction, the assignment of possible intersection rules, is rarely described in literature (see section 3.4.1). Since the approach proposed in this work is to succeed without additional information a rule-based procedure was developed. Within this procedure all pairs are sorted by the attribute length. The intersection itself starts with the shortest number and thus with the pair which is closest to each other. Each pair runs through the decision tree that is shown in Figure 3-38. If the pair fulfils the requirements, its planes are intersected. Once an intersection is performed, the next pair is processed.

The decision tree was built up in order to prevent false intersection decisions. So, it starts with deciding how to intersect patches by their position relative to each other. This is followed by working with potential wall neighbours. If a pair has not been treated at that point, the couple information is taken into account as well.

If both neighbouring patches are part of a couple a roof structures, such as illustrated in Figure 3-38, may be present. The routine checks the position of the ridge end points of one couple to the other couple. In case of L-shaped roof structures one end point of each couple is within the area of the other couple. For a tent roof both end points of both couples are within the other couple's area. A T-shaped roof structure is recognised when only one end point is in the appropriate couple's area. The intersection itself is aided by the recipe developed within the grouping procedure described in section 3.4.2.

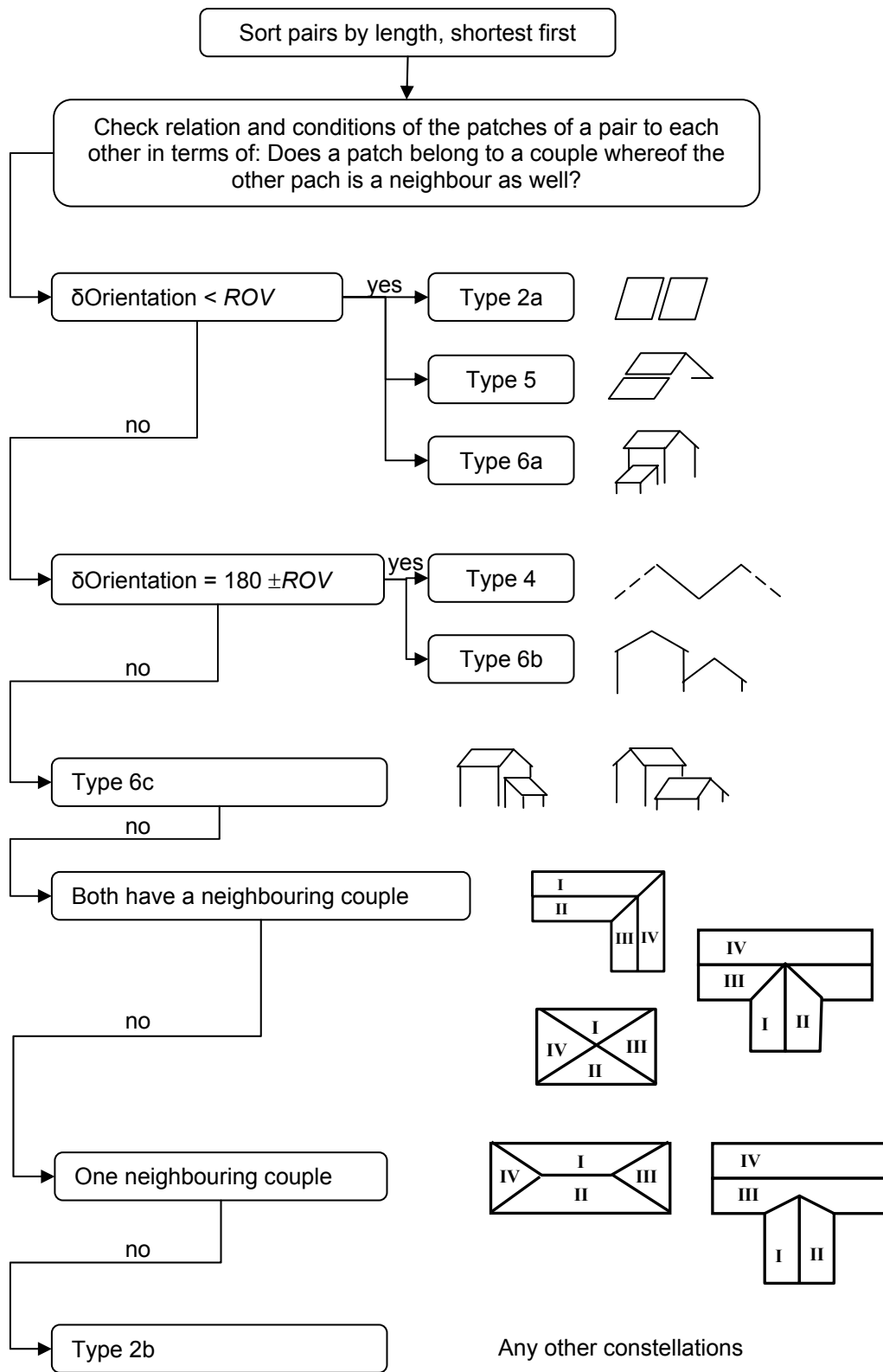


Figure 3-38: Part of decision tree of side intersection

If one out of two neighbouring patches belongs to a neighbouring couple, than the three roof faces can either form a hipped roof or an attached roof, as illustrated in Figure 3-38. The situation both examples have in common is that a patch is a neighbour to a couple. In the one example the neighbour is intersected with the couple, but in the other it is not. The plane's attribute of the according pair indicates if the neighbour is to be modified or not. If so, the ridge of the couple fixes the new upper corner coordinates of the neighbour and the sides are blended with their according neighbour of the couple.

Any other “type 2” constellation is processed as suggested by the pair's attributes.

Figure 3-39 shows an intersection result from a building complex. Three sides have not been intersected, because they have not been interpreted as neighbours. In this example the linearization of gable ends, which is described in the following section, has not yet taken part. It can also be observed that the lower roof edges, the gutters, are not levelled. This is described in the section that follows the next section.

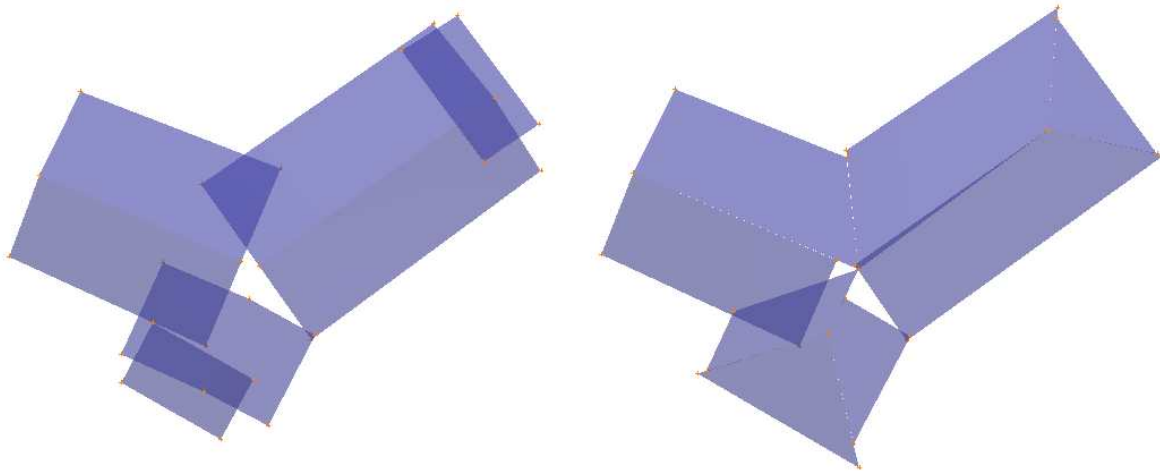


Figure 3-39: Left: group of planes as input in the intersection algorithm, Right: output of the intersection algorithm

### 3.5.6 Linearization of Gable Ends

At this stage of the 3D building model generation all neighbouring patches should be intersected. The gable end lines are still perpendicular to the gutter direction. Thus, the lines of coupled roof faces, which are on one gable end, must not be parallel. If it is desired to enforce parallelism of those lines, then the gable end lines can be adjusted. The adjustment is done by selecting the lower and upper points of one gable end. A mean line is calculated in the x, y-projection of these three points and the gable end lines can be adjusted accordingly to this mean line.

### 3.5.7 Adjustment of Gutters

Adjustment of gutters means here the levelling of the lower edges of neighbouring patches. Usually, neighbouring roof faces, except couples, have matching gutter heights. However, the lowest ALS point found within a patch may not have the same height as that of a neighbouring patch. Then the question arises, if these two heights should be adjusted. Figure 3-41 shows two examples where an adjustment would rectify or falsify the result. A

rule has to be found in order to draw the most likely decision. For building up such a rule, the following points can be taken as a fact:

- Gutters are horizontal.
- The mean point spacing determines the object size that can be identified and the details that can be recognized.
- The lowest edge of neighbouring planes indicates the lowest extension of the roof.

Considering these facts, neighbouring gutters will be adjusted, if the distance  $d$  (see Figure 3-41) is smaller than the mean point spacing. If  $d$  is larger than the mean point spacing, there was no laser point, which fits in the roof plane found and which is lower than the gutter. Along these lines, there is no information about the continuation of the roof face.

Given a certain point spacing of the ALS data, the lowest point at a patch may have hit the gutter or some point above it. Thus, using the lowest point of neighbouring patches, as a reference to adjust the other lower roof edges to it, would be a logical step. Figure 3-41 illustrates that all roof faces whose gutters are linked to a lower neighbour are adjusted to the lowest gutter in the connection, although that must not necessarily be its direct neighbour. The right roof structure of this figure also shows an example where the adjustment is not applied, as the distance  $d$  is larger than the mean point spacing.

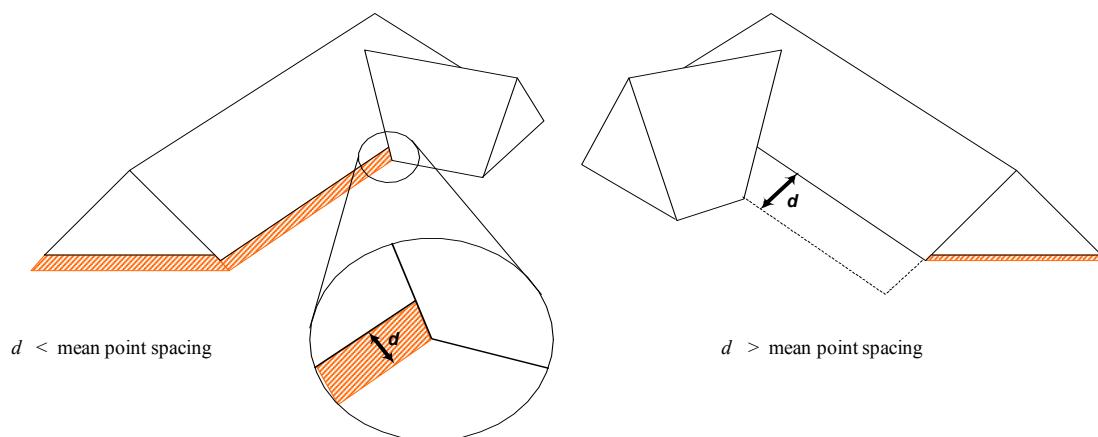


Figure 3-40: Principle of gutter adjustment

### 3.5.8 Adjustment of Dormers

Usually flat dormers are small rectangular features on a roof. But, being small or longish increases the chance of an insufficient estimation of plane parameters. The interpolated plane may be positioned slant to the larger roof face. Some users may wish to adjust the plane in a way that it has the same orientation as the roof face. In the building reconstruction algorithm therefore a switch is included that forces the gutter of a flat dormer, as illustrated in Figure 3-42, to be parallel to the gutter of the roof face and that forces the upper edge of the dormer to be horizontal within the roof face.

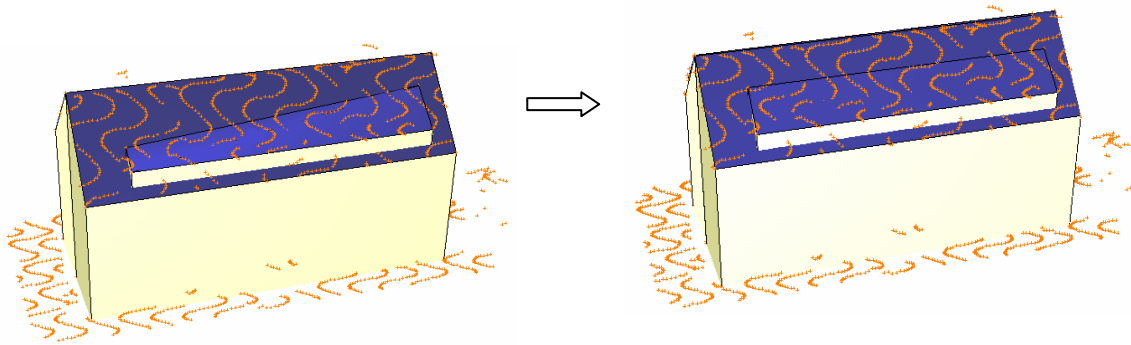


Figure 3-41: Example of a building model without adjusted dormers (left) and with adjusted dormer (right)

### 3.5.9 Determining the Outline of the Roof

Determining the outline of a roof is a task necessary for mapping 2D building information. With the provided roof topology of the proposed approach the outline of a building's roof can be retrieved by following those edges of the roof structure, which have not been intersected with other roof faces. Starting with the lowest roof edge the algorithm can then continue around the roof face in direction given by the edge. The edges of the roof face are checked to see whether they have been intersected with another roof face or not. If the edge was intersected with another roof face, the previous edge is taken. It is clear now that the outline information should be retrieved from the plane the just rejected edge was intersected with. Figure 3-43 exemplifies this. This procedure requires a complete and correct roof topology.

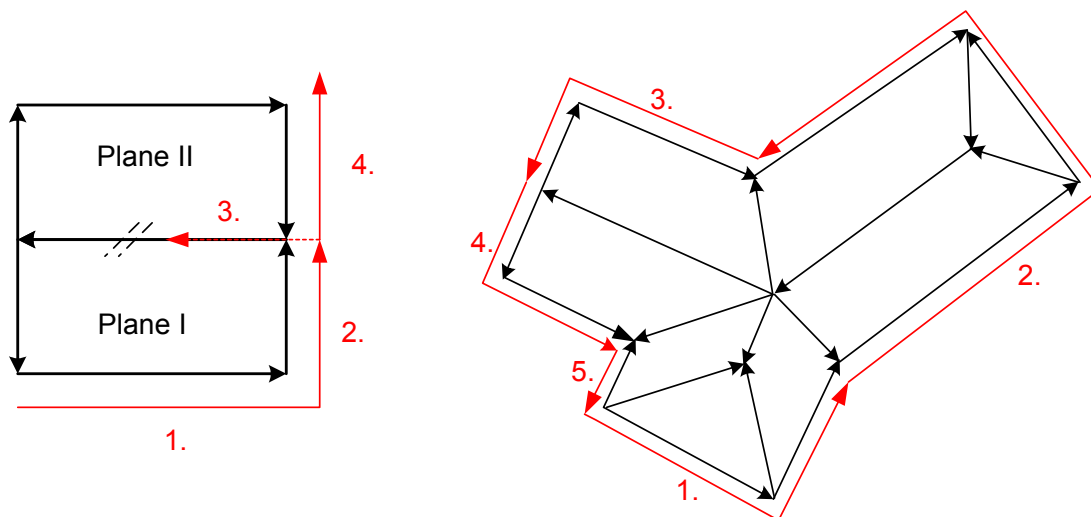


Figure 3-42: Suggestion of a procedure for deriving the building outline (black: roof face polygons, red: outline)

### 3.5.10 Discussion of the Intersection Algorithm

The two main parameters *meanPtDist* and *Acc*, which have been introduced in section 3.2.3, have not only an influence on the cluster analysis but also on certain decisions within the intersection algorithm. Such decisions mainly take place if the relation and position of two patches to each other are in question. The following routines use the knowledge on the

mean point spacing as well as the proclaimed accuracy in order to establish parts of the roof topology or to ascertain plane outlines.

- Intersect Ridges – the maximal distance two patches should have at their top to be intersected is equivalent to the meanPtdist.
- Adjust Gable Ends – meanPtdist is the measure to check for further points along the gable ends, which are within *Acc* distance around the plane. *Acc* stimulates the point selection in the adjustment of the gable ends (Correct Eaves), though, the influence is marginal. The larger the *Acc* value is the more eager is the routine to find points that may belong to the plane.
- Find Neighbours – meanPtdist defines the maximal planimetric threshold two neighbouring patches should not exceed.
- Adjust Gutters – combining the roofs inclination with meanPtdist results in a measure, which is used to decide if neighbouring gutters are levelled

Before the intersection algorithm was set up in its present form, the placement of the “adjust gable end” routine was considered. Its actual position, before the grouping algorithm, has certain advantages and also disadvantages in comparison to an implementation after the `Intersect Sides` routine. The advantage is that roof planes, which are too small, may be extended by the adjustment. But, vice versa, it may be the case that they are slightly shortened and a neighbourhood to a plan can not be created anymore. In practice, performing the adjustment prior to the grouping showed better results under the condition that adjusted gable ends may be intersected.

Grouping patches is the most important procedure within the intersection algorithm. It is essential that all patches of a roof have been detected correctly and that there are no false patches within a group of planes, which is to be intersected. If a patch is assigned falsely within this routine, the intersection will not provide proper results. The ambiguous situations that may arise in practice are explained on the following example:

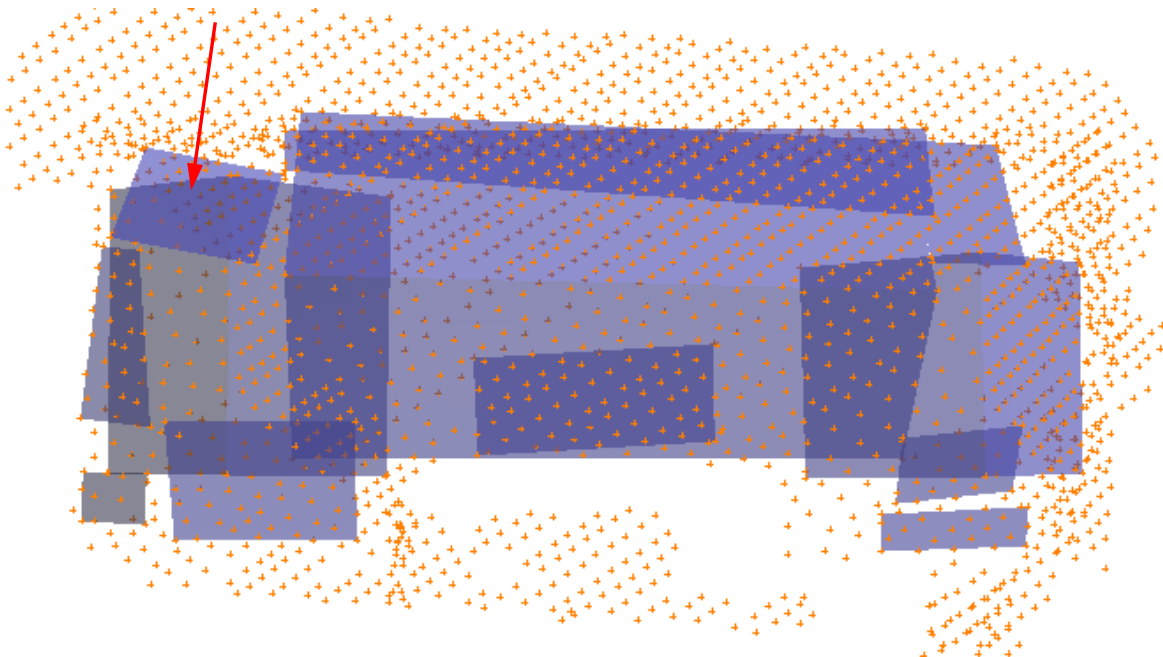


Figure 3-43: Top: Group of patches with underlaid ALS point cloud

Figure 3-44 shows the group of patches of a building complex as it is put in the `Find Neighbour and Side Intersection` procedure. Besides the patch, which is indicated, all roof faces have been detected correctly. The tilting of this patch is due to an irregularity of the laser scanner data itself. This causes then the extension of couple that forms the left wing to this side of the roof, where the incomplete triangle group is. The correct result is shown at the right wing of the building.

The following figure (Figure 3-45) shows the main problem of the grouping and intersection of the group of patches of Figure 3-44: the obvious false assignment of neighbours. The inner roof face of both wings was falsely intersected with the other roof side. In both cases a decision, as suggested in [Vosselman2001], which relies on existing points along intersection lines, would have failed as well. The reason that both wings have not been intersected correctly with the couple forming the main ridge originates from the distance of the upper left/right corner coordinates of the “wing couples” to the “main ridge couple”. In this case the intersection algorithm interpreted in (a) a T-House and in (b) a hipped end. (The gutters are adjusted after the intersection.)

All parameters of the intersection algorithm were set in order to rather not intersect planes in case of an ambiguous result. Doing so, the 3D building models may look incomplete, but editing is easier for these models than for falsely intersected planes.

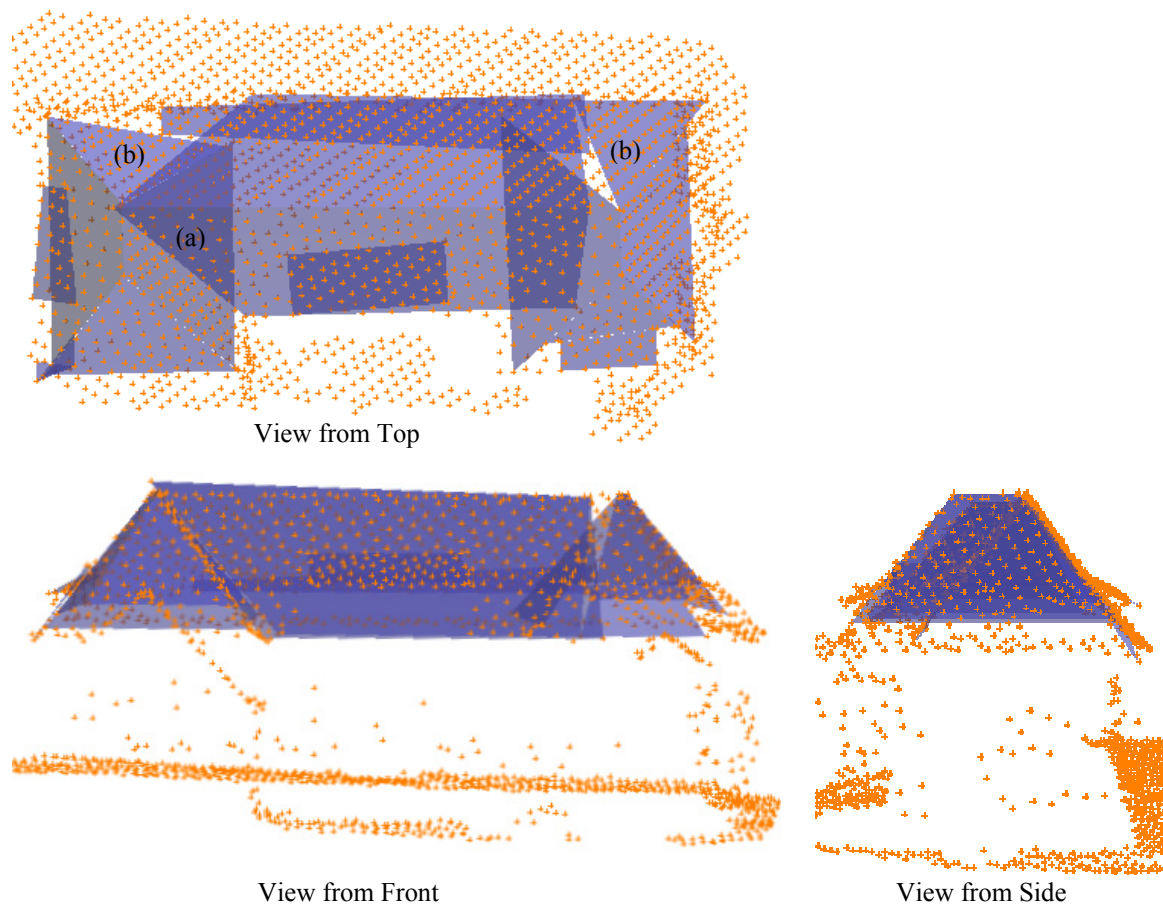


Figure 3-44: Intersection result of Figure 3-44

In case of two neighbouring couples, which have similar orientations (Figure 3-46), the intersection is carried out in a way that the couple having the smaller roof faces is extended

until it reaches the gable ends of the larger couple. This is necessary, as both couples may not have the same orientation.

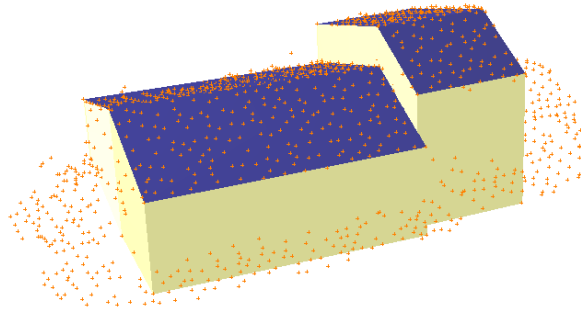


Figure 3-45: Intersected building consisting of two couples with similar orientations

Using the described approach, flat roofs may not be reconstructed correctly as the approach outlining a roof plane bases on a minimal roof inclination of three degree. The approach has to be extended in order to outline also flat roof structures. Another feature that was not implemented in the approach is the adjustment of all assumptions. Within this feature opposite roof faces may be forced to have a difference in orientation of 180 degree.

In reference to the limitation of a roof plane having maximal four corner coordinates, using a polygon data structure would allow cut outs within a roof plane. Momentarily, roof faces having more than four corners are split into smaller roof patches with each having four corner coordinates.

## 4 Laser Scanner Data Sets Used for Practical Testing

There are various laser scanner systems on the market. Their basic principle of deriving x, y, z-point information of the earth's surface is quite similar, as they measure the time a laser impulse needs to travel to the surface and back. The laser pulse is directed via a mirror system. The x,y,z-point information of the surface is retraced using GPS and INS on board and combining this information with the direction the impulse was given, the time it needed to reach the system again and system calibration parameters. Further information on the work flow of airborne laser scanner systems can be found in [Wehr1999].

For the time being, it shall only be of interest that the different laser scanner systems provide the user with different point patterns and accuracies. In section 1.1 it was stated that an ideal building model reconstruction system should be able to process laser scanner point information of a wide range of systems. In order to prove the potential of the presented method, five different data sets have been tested. The following section will make the reader familiar with the laser scanner data sets and their difficulties.

### 4.1 Airborne Laser Scanner Sensor Systems

The obtained laser scanner data sets originate from three different laser scanner sensor systems, which are introduced in the following:

#### *ALTIMS by TerraPoint*

The data set "Brienz" that has been taken with the ALTIMS laser scanner system operated by TerraPoint for the Swissphoto Group AG within the "LWN" project with the Swiss Federal Office of Topography (LTOP). The laser scanner uses a multifaceted rotating mirror, which creates its point pattern as parallel lines. Detailed information on the system can be read in [Baltsavias1999b]. The point pattern of a section of one strip is visualised in Figure 4-1. It can be described as regular and uniformly distributed. The mean point spacing, as given in Table 4-1 on page 67, is approximately 1.5m within one strip. The standard deviation of the laser scanner points within one strip is known with 0.1m.

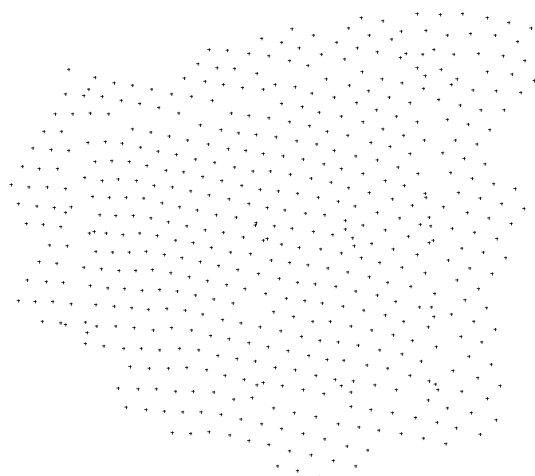


Figure 4-1: Point pattern of the ALTIMS laser scanner by Optech

*LMS-Q140i-80 by RiegI*

The LMS-Q140i-80 scanner manufactured by RiegI is operated by Milan Flug GmbH and was used to obtain the data sets “Freiberg” and “Dresden”. The scanner uses a homogeneously rotating 3-side polygon wheel. As it can be seen in Figure 4-2, the point pattern of one strip appears to be quite regular in x and y, however points are missing along the scan lines. The mean point spacing is 0.9m per strip and the standard deviation in z is approximately with 0.2m. This is because the exactness of the points may vary within one scan line. More information on the system is given in [DASilbermann].

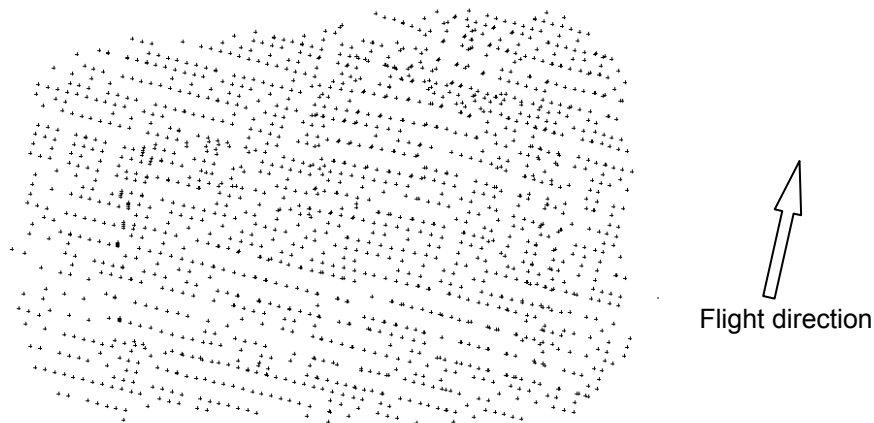


Figure 4-2: Point pattern of the LMS-Q140i-80 laser scanner by RiegI with indicated flight direction of the “Freiberg” data set

*FALCON II with swing-mode by Toposys*

The FALCON II scanner system is manufactured and operated by TopoSys. It uses a so called fibre scanner, as the light is directed and transmitted to the ground via a bundle of glass fibre. Another bundle of glass fibres receives the light. The individual beam directions are firmly aligned due to a mechanically solid orientation of the fibres. Detailed information can be obtained from [TopoSys]. In order to optimise the scan pattern a swing mode was implemented. The resulting point pattern can be seen in Figure 4-3. The point spacing within the data set “Friedrichshafen” is in average 0.3m in flight direction and 2.3m across flight direction. The standard deviation of the laser scanner points is 0.1m.

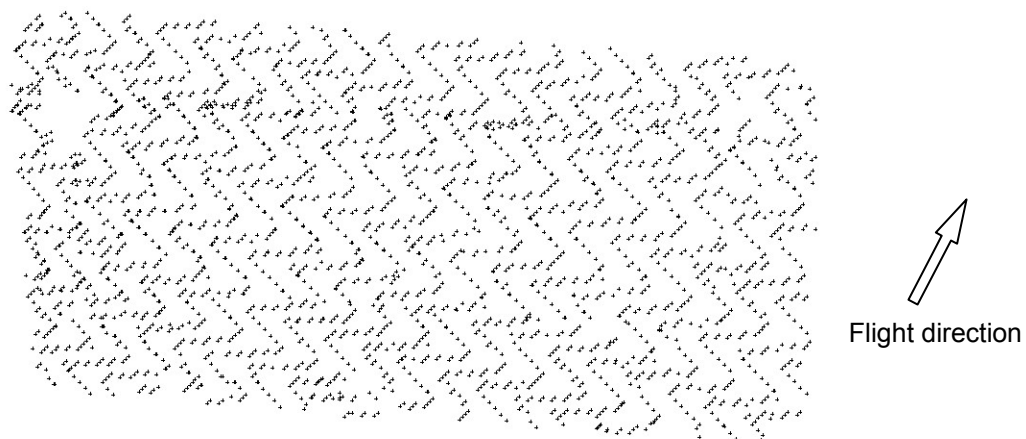


Figure 4-3: Point pattern of the FALCON laser scanner with swing mode by Toposys

*TopEye MKII by TopEye AB*

The “Lingköping” data set was kindly provided by the FOI Swedish defence research agency. The system has fiber laser technology [TopEye] and was mounted on a helicopter for this project. As no direct strip information was given with the data and as the area was covered patchily, the point pattern is consequently irregular. The mean point spacing is approximately 0.7m and the standard deviation of the points in height with 0.1m.

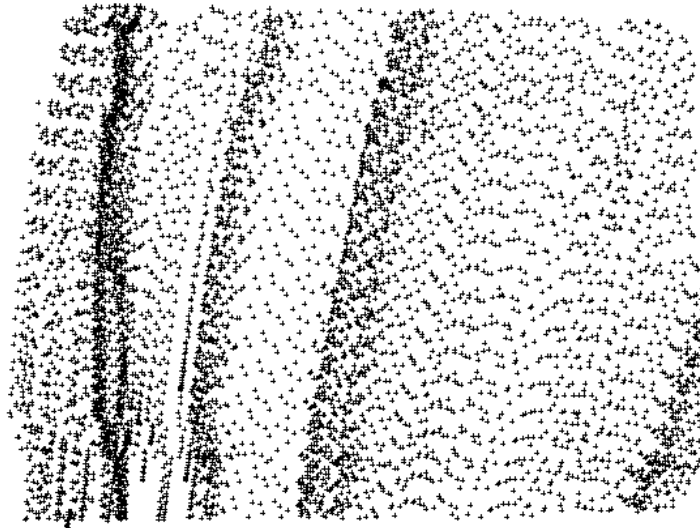


Figure 4-4: Point pattern of the TopEye MK II mounted on a helicopter

Table 4-1 summarises the main characteristics of these five available data sets.

In principal, building model reconstruction from geometry data, whatever source they come from, is reasonable if enough information is available to retrace the original structure. In analogy to the sampling theory, only those features can be reconstructed which have a certain size to point spacing ratio. Theoretically, it takes three points to define a plane that represents a planar surface. In practice, it takes at least five points to identify a plane reliably, as already discussed in section 3.2.1. As a consequence, the point spacing of a data set determines the minimal size of a planar surface that can be detected. Besides the point spacing, the point pattern has great influence as well. A TIN-structure calculated in an irregular point pattern will have triangles, which have large variations in size and shape. Applying a constant point standard deviation in z, orientation parameters will vary strongly for triangles, which are actually on one planar surface. This will aggravate the cluster analysis. In this way, the chosen data sets will test the proposed method to its limits.

Number of Buildings	Area	Standard deviation in z	Strip overlap	Strip information	Point spacing per strip	Provider / Company	Laser scanner system	
177	country	0.5m	50%	yes	1.5m	LTOP / Terra Point	ALTMS (TerraPoint)	Brienz
243	city	n.i.	n.i.	no	1m (interpolated to grid)	Milan-Flug GmbH	LMS-Q140i-80 (Riegl)	Dresden
134	city	0.2m	80%	yes	0.9m	Milan-Flug GmbH	LMS-Q140i-80 (Riegl)	Freiberg
328	city/ country	0.15	~20%	yes	2.3m / 0.3m	TopoSys	FALCON swing-mode (TopoSys)	Friedrichshafen
48	city	0.1m	n.i.	no	~0.7m	FOI / TopoEye AB	TopEye (TopoEye AB)	Lingköping

Table 4-1: Key information of used laser scanner data

## 4.2 Characteristics of the Data Sets

The five different data sets not only have different point patterns as shown in the previous section, but they also contain diverse building styles, which are common for their areas. All five laser scanner data sets cover areas of several square kilometres. Smaller regions, which are representative for the whole data set, were extracted out of these areas in order to reduce the time spend on analyses. The point clouds were extracted as explained in chapter 2 and checked for their quality. Point clouds with very peculiar roof structures were also excluded from the analysis. Each analysed data set has between 40 and 330 point clouds representing buildings. This section will introduce the characteristics and appearance of these sub-data sets.

### *Brienz*

The study area of Brienz contains data of two areas at the “Brienzer See” east of Bern in Switzerland. Both areas are situated in an alpine rural region. The main building style is a single standing building with a gable roof (see Table 4-2 and Figure 4-5). Hipped buildings are not and complexes are rarely seen. Due to the alpine terrain, some buildings have been built on a slope. Thus, it can be predicted that problems will occur at roof ends close to the hillside. In general, the roof faces are sufficiently large for a point spacing of 1.5m and they are only occasionally disconnected by dormers. The data set has, as presented in section 4.1, strip information. If a building is continued in multiple strips, the reconstruction algorithm chooses the strip with the highest point density. The strips are not merged to avoid inconsistencies emerging from height discrepancies between the strips.

Roof type / Number of Buildings	Sum	Flat	Pent	Gable	Hipped	Complex
Brienz	176	0	5	130	0	31

Table 4-2: Statistics to roof types of the data set “Brienz”



Figure 4-5: Example of typical buildings of the data set “Brienz”

### *Freiberg and Dresden*

Freiberg and Dresden are two cities in Saxony. The type of buildings found in these data sets is quite different. In Freiberg, larger buildings, such as storehouses or apartment houses,

dominate the scene. The storehouses mainly have flat gable roofs. The apartment houses may have any roof type. Table 4-3 summarises the occurrences of the different roof types.

The study area Dresden is restricted to the district “Südvorstadt”. This area is dominated by villas with hipped roofs or complex roof structures and apartment houses with gable roofs. The roofs of the villas often have dormers, roof gardens or mansard-like shapes, as the upper left example of Figure 4-6 shows. Beside these typical residential houses, there are also larger buildings with pent roofs.

Roof type / Number of Buildings	Sum	Flat	Pent	Gable	Hipped	Complex
Freiberg	134	0	5	66	37	26
Dresden	243	3	13	69	99	59

Table 4-3: Statistics to roof types of the data set “Freiberg” and “Dresden”



Figure 4-6: Examples of typical buildings of the study area Dresden (top) and Freiberg (bottom)

Both study areas have non-trivial roof structures, whereby the Dresden data set has the more demanding roof structures, taking into consideration that the roof features may be too small to be identified with the provided point spacing (1m grid). The LiDAR data of “Freiberg” have a low accuracy in  $z$ , even within one strip. On account of this the triangles’ plane parameters vary widely and the cluster analysis may not perform well.

### *Friedrichshafen*

The study area Friedrichshafen in Baden-Württemberg is situated on flat terrain close to the city centre. The area is mainly residential and dominated by small gable and hipped roofs with dormers (see Figure 4-7). The dormers may be as long as the roof face is. Many of the gable and hipped roofs show a tilt change at the gutters. The roof structures are simple in comparison to “Dresden”, but many houses have rather small sizes.

Roof type	Sum	Flat	Pent	Gable	Hipped	Complex
Number of Buildings	328	0	5	236	67	20

Table 4-4: Statistics to roof types of the data set “Friedrichshafen”

Figure 4-7: Left: Example of an ALS-point cloud of the data set “Friedrichshafen”,  
Right: Example of the typical building style

The most interesting fact of this data set is the point pattern as shown in section 4.1. Because of its inhomogeneous point spacing, triangles will vary in size immensely (see Figure 5-12 at page 83) and the resulting parameter space will be rather diffuse. This may cause problems in the cluster analysis algorithm.

### *Linköping*

Linköping is a city in Östergötland, Sweden. The provided data set covers part of the inner city. Besides contemporary roof structures, also old styled Swedish roof structures can be found within the data set. An old style Swedish roof is a gambrel roof with ornaments at the ridge points as it can be recognised in Figure 4-8. The contemporary roof shapes resample common European roof structures. All together, the roof structures are as complicated as those in the Dresden data set. Table 4-5 summarises the number of roof types.

Roof type	Sum	Flat	Pent	Gable	Hipped	Complex
Number of Buildings	48	3	1	23	9	12

Table 4-5: Statistics to roof types of the data set “Linköping”

The LiDAR data of this data set has been taken from a helicopter. The strip information can not be retrieved completely. Thus, the data set provides poor conditions in terms of the ratio triangle size to accuracy in  $z$ .



Figure 4-8: Front view of a gambrel roof in old Swedish style

Finally, Figure 4-9 provides the statistics, which compares the composition of the five study areas:

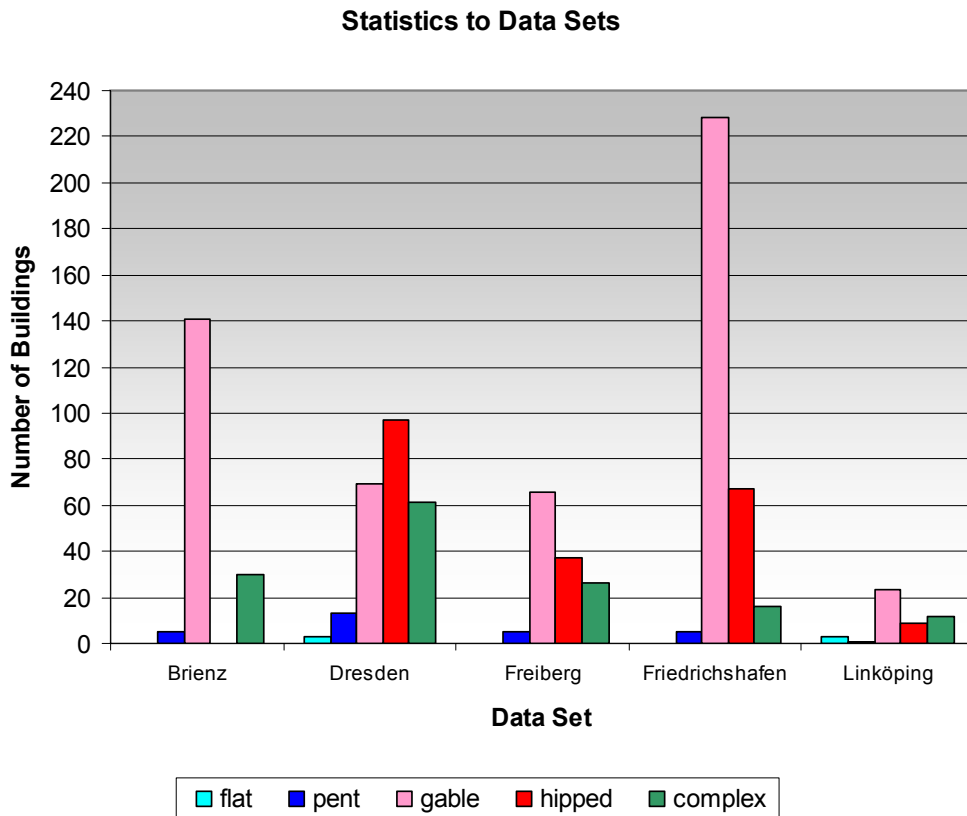


Figure 4-9: Statistics of roof types to the study areas

*Benchmark Data Set of the Institute of Photogrammetry and Remote Sensing (IPF)*

In order to test the reconstruction algorithms, a collection of point clouds was used while developing the approach. The collection represents various types of data and buildings. It contains buildings of the data sets Brienz, Gruyères and Dresden. Within this collection of

buildings, the height accuracy varies between 0.1m and 0.15m and the point spacing varies between 1m and 2m. The buildings were collected to exemplify a quite wide variety of roof shapes and combinations. The 58 gable roofs represent different inclinations and sizes. The complexes contain T-shaped buildings, detached houses and a mixture of combined gable and hipped houses. In order to prove the versatility of the developed techniques, all point clouds were processed with the same roof reconstruction algorithm scheme.

## 5 Verification of Reconstructed Building Models

The proposed method was developed with the aim of being able to derive building models from any point spacing and point pattern. In order to verify the achievement of this goal data sets, such as described in chapter 4, have been processed. In addition to providing different qualities, the data sets also contain different styles of buildings. The buildings have been divided into five main categories: flat, pent, gable, hipped roof and complexes. Section 1.2.1 defines these.

This chapter will analyse the results of the building model reconstruction scheme with regard to the geometric correctness (section 5.1) of the reconstructed roof structures and their geometric accuracy in position and height (section 5.2). The limitations of the cluster analysis approach as well as the building model reconstruction approach are investigated and discussed. The quality of the reconstructed building models will be evaluated. The following issues shall be discussed:

- The percentage of completely detected and reconstructed roof faces.
- Reasons for incompletely detected roof faces.
- Limitations of the grouping and intersection algorithm.

In addition to that, the applicability of the procedure is examined. Within the accuracy verification the relative as well as absolute accuracy of selected reconstructed building models shall be of interest. The relative accuracy is determined analysing roof parameters, such as the roof width, height and steepness. The absolute accuracy is ascertained by comparing a selection of building models to either photogrammetric or terrestrial measurements.

### 5.1 Quality Verification of Reconstructed Building Models

When discussing the quality of a building model, its completeness in respect to fully reconstructed roof faces is meant. Furthermore, the smallest feature that can be reconstructed from the provided data must be defined. From chapter 3 it is known that a cluster in parameter space is detected as a roof plane cluster, if it has certain characteristics and input of at least five triangles. Considering the mean point spacing of the ALS data, the minimum size of detectable features can be estimated.

In addition to producing complete roof faces, a reconstructed building model should not contain double surfaces or holes. The reconstructed building models are evaluated visually concerning their completeness in respect to the minimum detectable feature size as well as a complete intersection, i.e. connection of roof faces. Regarding their completeness, the building models have been divided into five categories 100%, 75%, 50%, 25% and 0%. The categories are arranged into four groups: correct (100%), mostly ( $\geq 75\%$ ) and partially ( $\geq 50\%$ ) correct reconstructed and not useful building models ( $< 50\%$ ).

Practical aspects are the motivation for the establishment of these groups. The reconstruction algorithm is supposed to generate correct building models, of course. Still, there are models which are not correct, but which may have correct features. Using a

software tool, which allows manual editing of generated 3D building models, mostly and partially correct building models could be completed spending less time than creating the entire building model manually. Editing building models may be done, for instance, by correcting corners of roof faces using a drag-and-drop tool. Since each roof face of an output building model is momentarily represented as a polygon, functions as provided in general construction software (e.g. AutoCad) may be used to correct corners of roof faces. The four groups were defined considering this method of editing building models. Examples of these groups are given in the following.

Allowing manual editing of generated building models may denote a semi-automatic system. However, this is not desired nor does it fulfil the task. The developed reconstruction algorithm works automatically. Its results are evaluated in respect of their degree of completeness and accuracy. Moreover, evaluating completeness may not be done without bearing practical aspects in mind, which have the aim of introducing categories of completeness and groups of useful building models. None of the reconstructed building models were edited manually. If interaction in terms of editing is a desired future task, the procedure may then be described as semi-automatic.

A “correct” building model can be qualified as a model with complete (100%) correct features, such as Figure 5-1 illustrates.

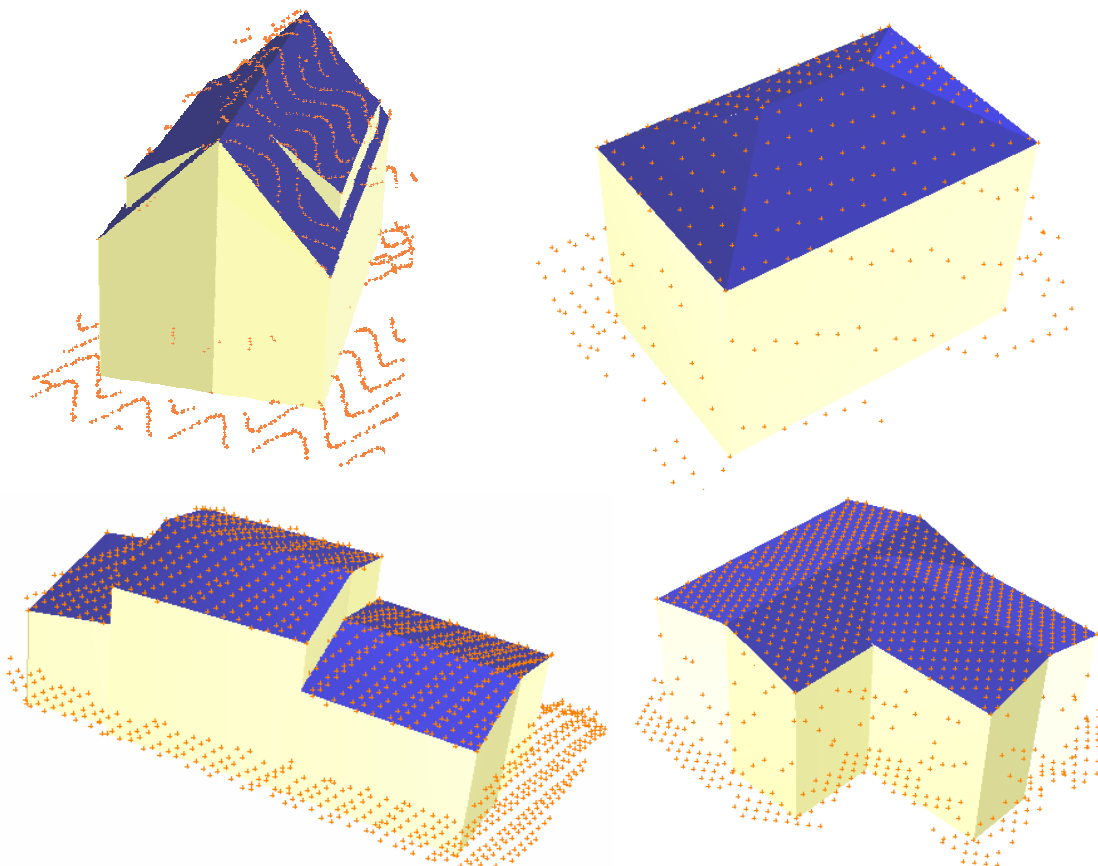


Figure 5-1: Examples of correct reconstructed building models (100%). The left examples originate from the Dresden data set and show interpolated points at the walls.

A “mostly correct” building model is a result, which is over 75% complete. If the model was to be edited manually, only a few steps would be necessary to transform the

incomplete model into a complete one. Figure 5-2 gives examples of “mostly correct” reconstructed building models.

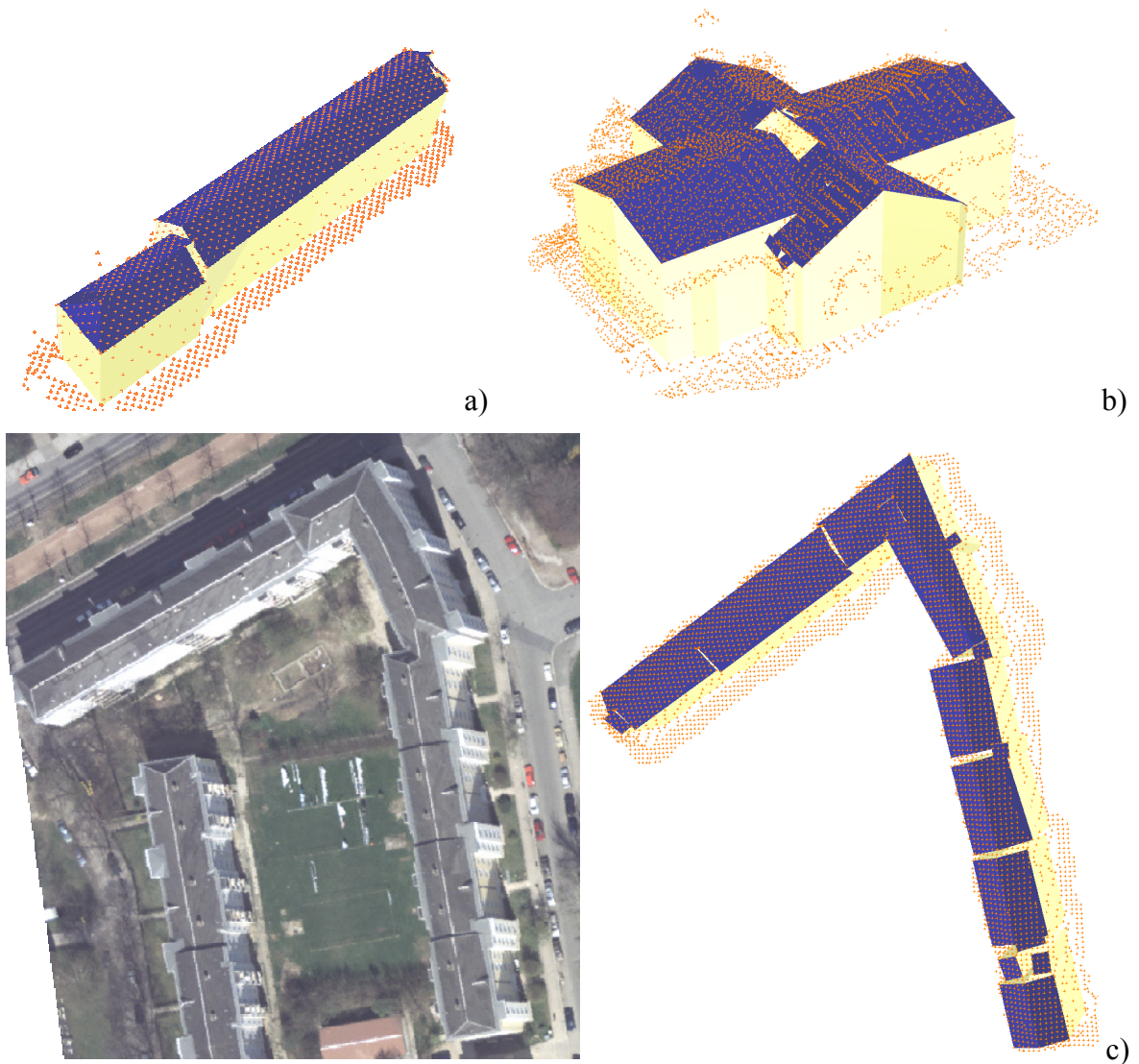


Figure 5-2: Examples of mostly correct reconstructed building models ( $\geq 75\%$ )

“Partially correct” (50%) reconstructed building models are shown in Figure 5-3. It can be seen, that editing is necessary, but using a suitable user interface it can be done in less time than needed to create the building model manually. In the given examples of Figure 5-3 all planes, except one, are detected and the intersection was not complete.

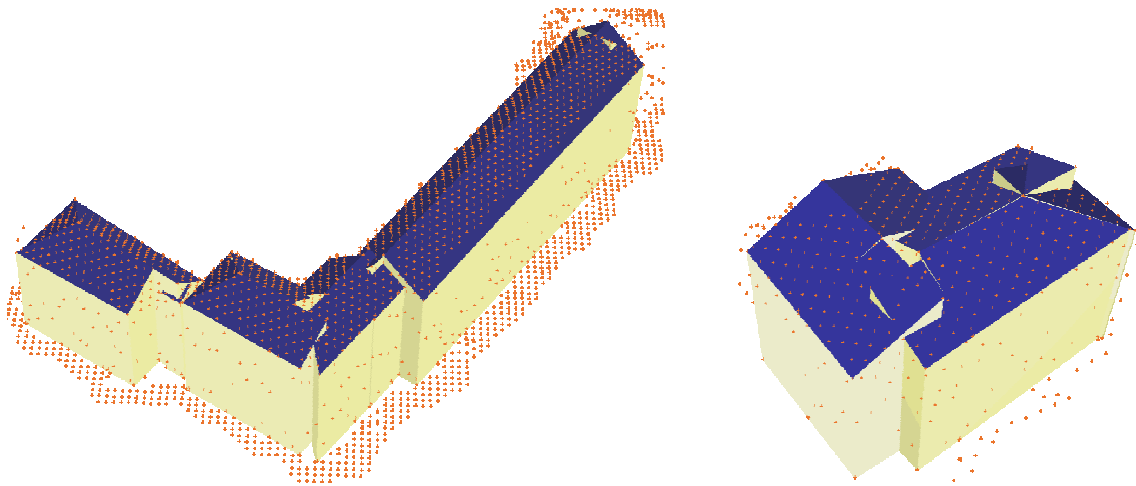


Figure 5-3: Examples of partially correct reconstructed building models ( $\geq 50\%$ )

If less than 50% of the information is available the models, such as those in Figure 5-4, are discarded. For statistical analyses these models will be divided into two categories: more than 25% and 0% reconstructed in the next section.

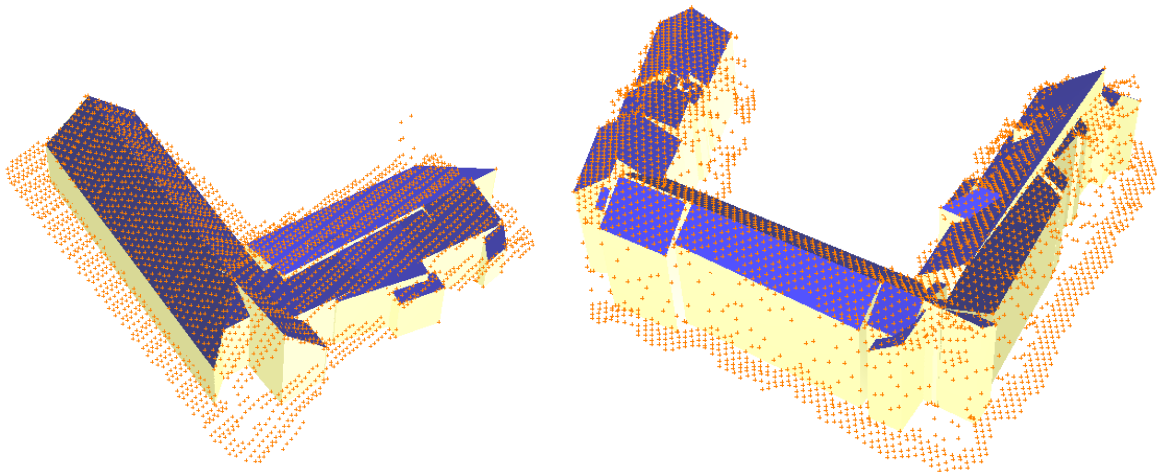


Figure 5-4: Examples of not useful building models Left:  $\leq 50\%$ , Right:  $\leq 25\%$

### 5.1.1 Statistics on Study Areas

This section summarises the results obtained from the building model scheme for each study area. Figure 5-5 gives an overall statistics of the achieved results and Table 5-1 contains the percentages of the graphs in Figure 5-5. It can be seen that the data set “Brienz” has the best results with 64% completely reconstructed building models. The lowest rate of complete reconstructed building models was obtained in the data set “Linköping”.

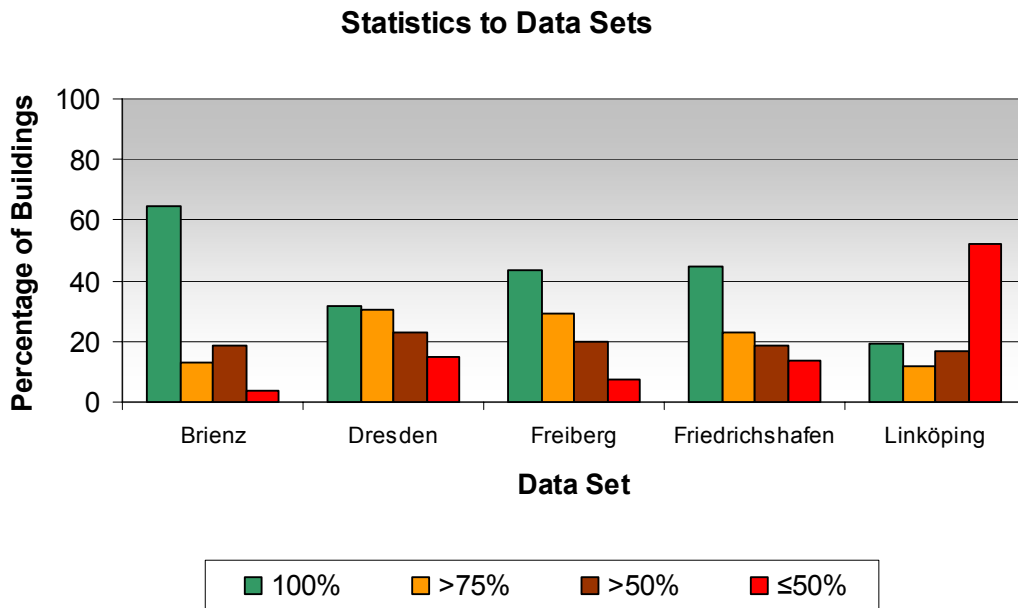


Figure 5-5: Overall statistics for reconstructed building models of the five data sets

Data set	Completely	Mostly	Partially	Not useful
Brienz	64%	13%	19%	4%
Dresden	32%	31%	23%	15%
Freiberg	43%	29%	20%	8%
Friedrichshafen	45%	23%	18%	14%
Linköping	22%	11%	18%	49%

Table 5-1: Numbers of the overall statistics for reconstructed building models of the five data sets

In the following, the results of the tested data sets are analysed. Each data set is summarised by figures showing the percentage of buildings, which were reconstructed completely (100%), mostly (75%), partially (50%) and not useful (25% and 0%). To each figure a table names the number of buildings which was processed of each roof type.

### *Brienz*

As already mentioned, this data set has the best results: the majority of the buildings have been reconstructed correctly (see Figure 5-6). Their characteristics have earlier been described as relatively simple. Table 5-2 reveals again that most of the roof structures are gable roofs.

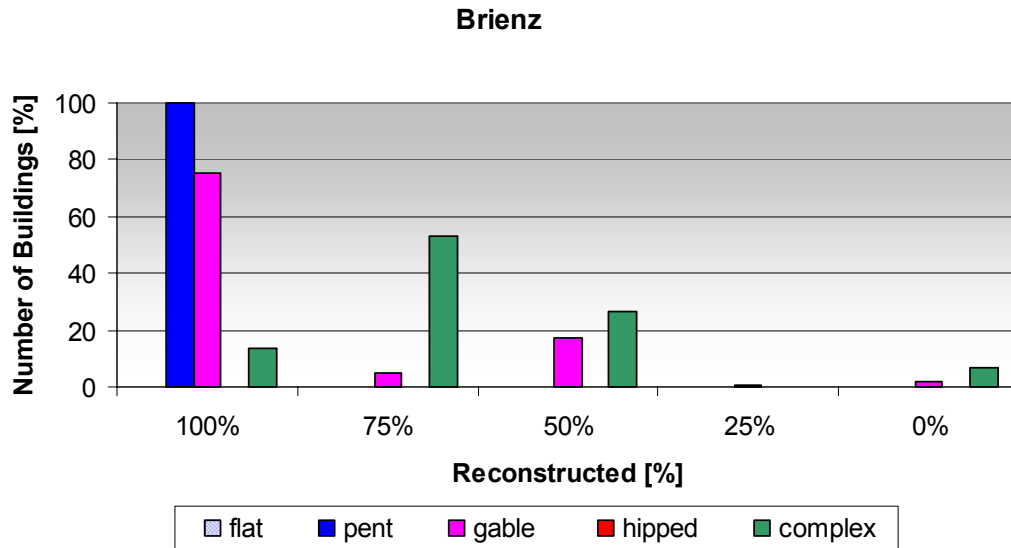


Figure 5-6: Percentage of reconstructed roof types in the study area Brienz

Roof type / Number of Buildings	Sum	Flat	Pent	Gable	Hipped	Complex
Brienz	176	0	5	130	0	31

Table 5-2: Statistics for roof types of the data set “Brienz”

The smallest detectable feature size for this data set would be approximately  $16\text{m}^2$ . Figure 5-7 a) shows a building, which contains two features larger than  $16\text{m}^2$  shaded in green colours and two features of approximately  $15\text{m}^2$  outlined in blue. The assumed cluster positions of the two smaller features are indicated in the parameter space plot below, but they might not be recognised as clusters at all. Thus, the method is not expected to detect these small features and the building is reconstructed correctly as shown in Figure 5-7c. Still, if a gable roof has only one roof face large enough to be detected, the method is expected to find the opposite partner of it.

Half of the “partially correct” reconstructed building models had at least one roof face which is too small to be detected. For the other half no specific cause could be identified. The main problem that caused “mostly correct” reconstructed building models is predominantly the incompleteness of smaller roof features.

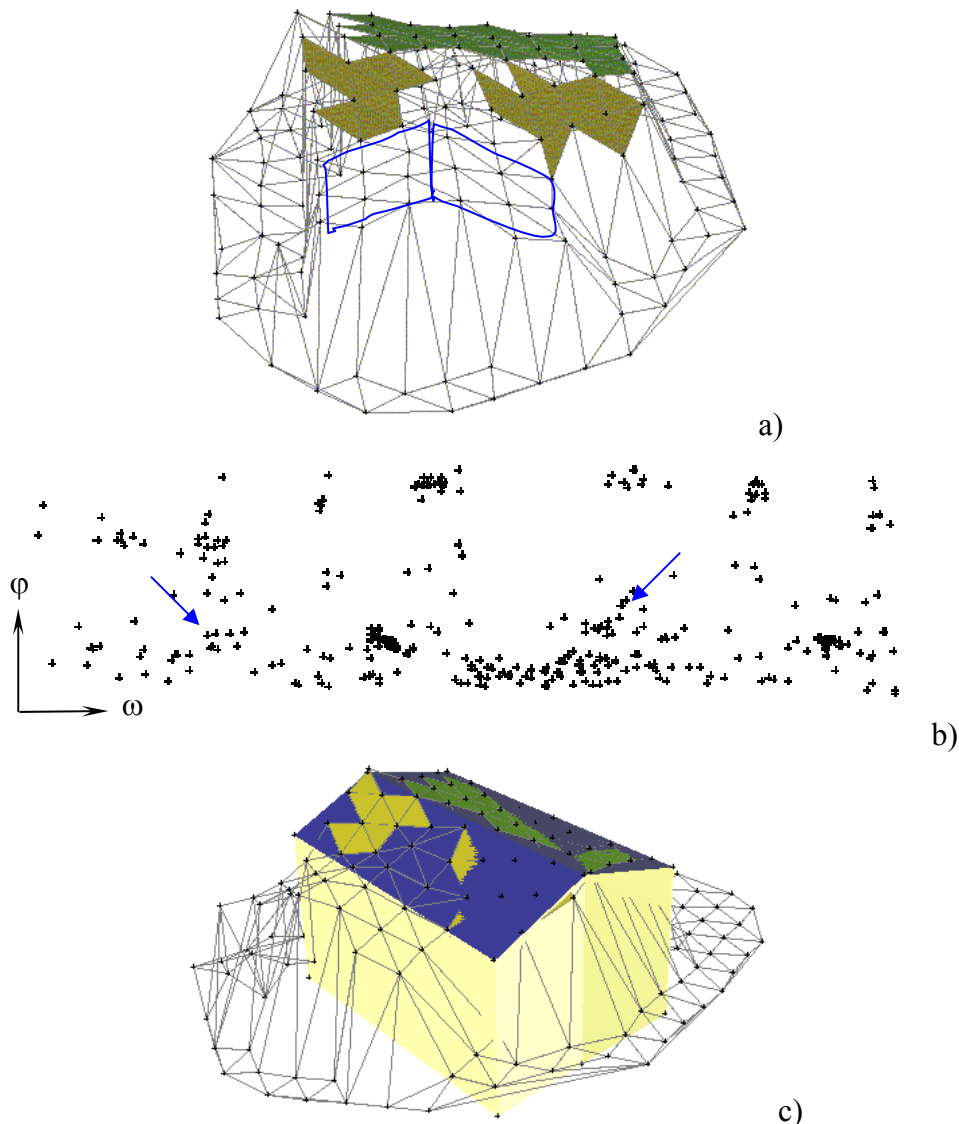


Figure 5-7: a) Shaded TIN-structure of a building b) Parameter space of TIN-structure c) building model

### *Dresden*

As mentioned before, the ALS data of “Dresden” were only available as interpolated 1m grid. The original mean point spacing is not known. By interpolating the original information to a 1m grid, break lines and edges are blurred. This means, for building reconstruction purposes, that the smallest detectable feature size would be increased by the interpolation to 15m<sup>2</sup>.

In section 3.2 the processing of flat roofs was discussed. For the reason that surfaces with extremely low inclinations cannot be properly defined in the parameter space, those with less than three degrees were excluded from the analysis. A pent roof was defined as a roof face with an inclination of more than four degrees, only three flat roofs were entered into the processing algorithm. Two out of these three examples were not reconstructed correctly, as the outlines were not true. This is due to the roof plane bounding box algorithm. For pent roofs the reasons of insufficiently reconstructed building models are mainly because of false intersections with other roof planes.

Similar to the “Brienz” data set most of the gable roofs have been reconstructed completely. Those, which were not reconstructed completely, mainly have roof faces that are interrupted by dormers or that are not flat, but curved.

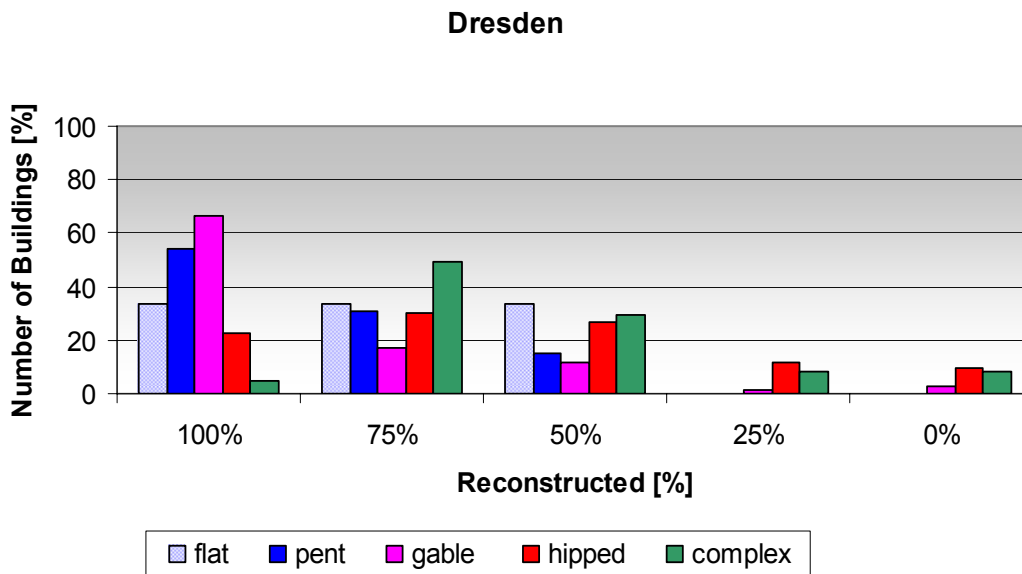


Figure 5-8: Percentage of reconstructed roof types in the study area Dresden

Roof type / Number of Buildings	Sum	Flat	Pent	Gable	Hipped	Complex
Dresden	243	3	13	69	99	59

Table 5-3: Statistics for roof types of the data set “Dresden”

Within the study area Dresden, the most frequent roof styles are hipped roofs. One third of these roofs are tent roofs. Section 3.4.2 pointed out that these roofs demand an intersection strategy, which is different to the strategy used by general hipped roofs. Despite the different intersection strategies, the same problems caused insufficient results. Usually, for building models with 75% or 50% completeness, a smaller roof plane or a roof face with dormers was not or only partially detected. This leads to plane constellations, which are not unfavourable relating to the intersection. Figure 5-9 shows a representative building of the category “hipped roof”, of which 75% were reconstructed. As it can be seen in the photograph of Figure 5-9, small dormers are arranged along the lower ends of the roof. These dormers are usually hit by one or two ALS points (as indicated in Figure 5-9) and thus reduce the roof face area.

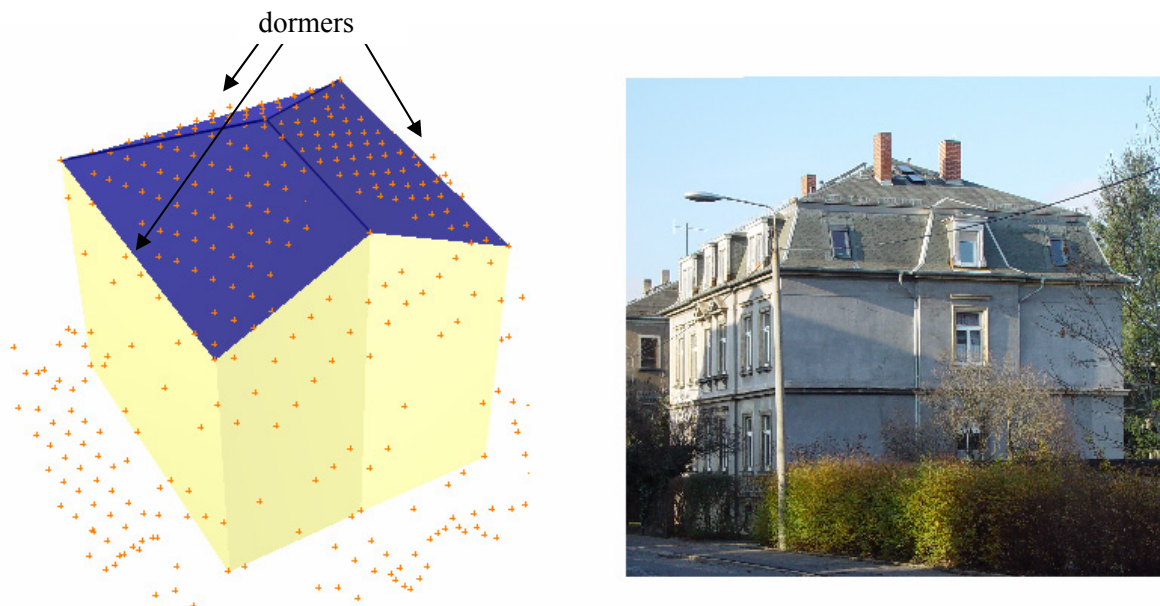


Figure 5-9: Example of a common hipped roof within the Dresden data set

Within this data set the occurring complex roof structures are the most difficult ones of all the data sets. The statistics shown in Figure 5-8 confirm this. Approximately 50% of the complex roof structures are mostly reconstructed and only 6% complete. Again, the main reason for incomplete building models of complexes is the intersection algorithm. Section 3.4.2 provided examples of indefinite constellations. Some complex roof structures could have been reconstructed correctly, if they were divided into smaller parts. The left example in Figure 5-3 was such a building. The other complexes, such as that in Figure 5-10, are hard to accomplish, as they contain roof faces smaller than 15m<sup>2</sup>, the smallest detectable size of this data set.



Figure 5-10: Example of an excluded building complex in the data set Dresden

### *Freiberg*

Although the composition of roof types of the data set Freiberg is slightly different to the data set Dresden, both data sets can be compared with each other in terms of similar roof structures. However, the buildings within the study area Freiberg do not have as many dormers as the buildings within the study area Dresden. The point spacing is with 0.9m –

also similar to that of the Dresden data. Thus the smallest detectable feature size is approximately 10m<sup>2</sup>.

In section 4.1 this particular data set was found to be irregular, to some extent. As a consequence, within a planar surface the parameters of triangles vary irregularly. In order to increase the chance of identifying smaller roof features the single point clouds were filtered with an edge-preserved filtering routine. The routine is described in [SAMeierhold]. Using this filtering technique, single outliers are removed. As a result, the number of detected roof planes could be increased.

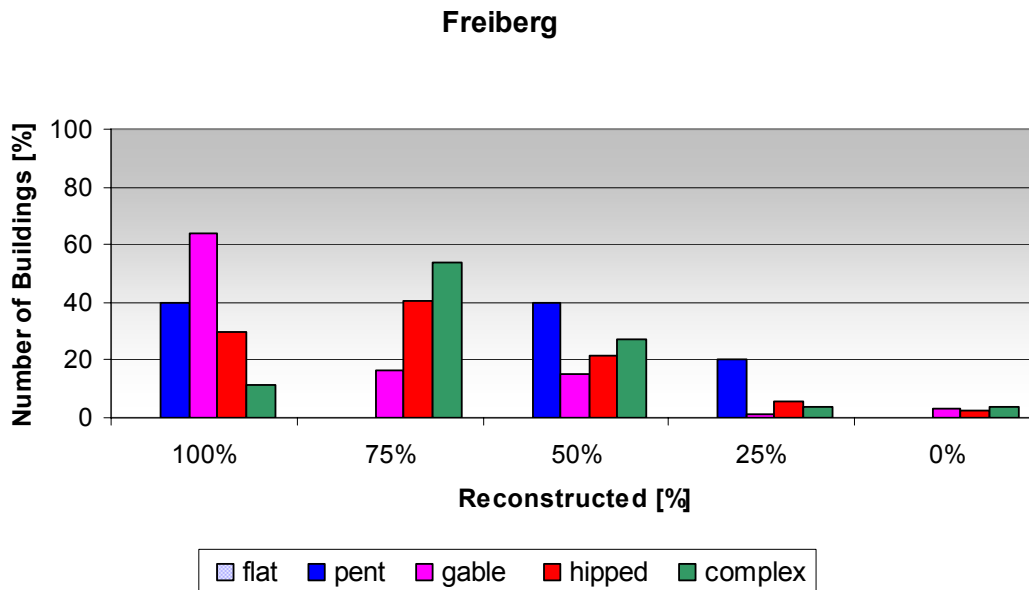


Figure 5-11: Percentage of reconstructed roof types in the study area Freiberg

Roof type / Number of Buildings	Sum	Flat	Pent	Gable	Hipped	Complex
Freiberg	134	0	5	66	37	26

Table 5-4: Statistics for roof types of the data set “Freiberg” and “Dresden”

On first view, the statistics illustrated in Figure 5-11 show improvement in comparison to the statistics of the Dresden data set. A higher percentage of pent and hipped roofs have been reconstructed “completely” and “mostly”. However, this may be on account of the generally larger roof features. The results for gable roofs and complexes resemble those of the Dresden data.

### *Friedrichshafen*

For this data it is quite difficult to determine the parameter of the mean point spacing for the reconstruction scheme. By counting the number of points within a certain area, a mean point spacing of 0.5m is obtained. Still, most triangles have sides which are longer than 2m, as shown in Figure 5-12 a).

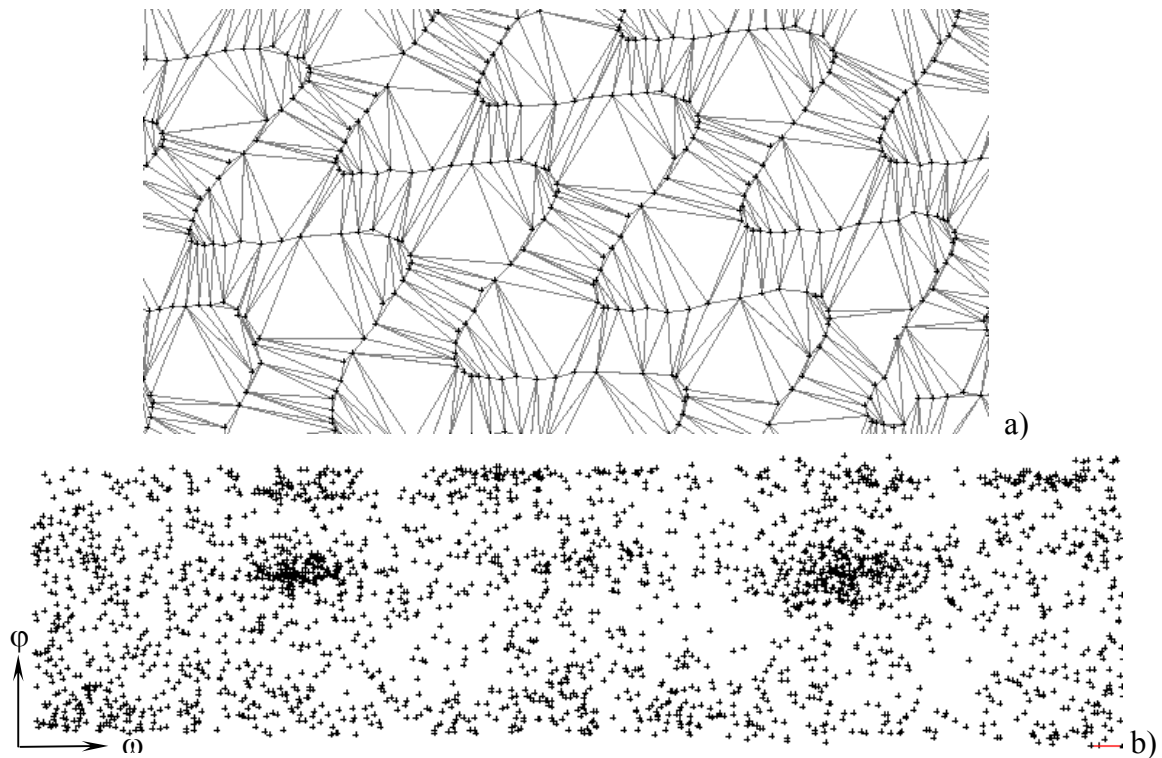


Figure 5-12: a) Part of a TIN-structure of the TopoSys data b) Whole parameter space of the TIN-structure

Assuming a constant accuracy in the laser scanner data, the variation of the triangles in slope ( $\varphi$ ) and in orientation ( $\omega$ ) will be much higher for the very small or narrow triangles than for the larger triangles. Figure 5-12 b) confirms this thought showing a typical parameter space with diffuse roof clusters. Actually, this parameter space contains the point cloud of a relatively steep hipped roof. It is obvious that two of the four clusters cannot be distinguished from random clusters. In addition to the complicated triangle pattern, most houses within the study area Friedrichshafen have dormers – even on smaller roof faces.

Concerning the parameter settings, best results were obtained with a mean point spacing of 1.7m and an accuracy of 0.15m. Consequently, the smallest detectable feature size is considered to be approximately 25m<sup>2</sup>. Nevertheless, houses with roof faces which are slightly smaller than 25m<sup>2</sup> have been processed. The statistics in Figure 5-13 confirm the predicted lower percentage of correct results for hipped roofs and complexes. The overall percentage seems acceptable enough, but the number of gable roofs is much higher than the number of the other roof structures. At the end of this section statistics are given comparing the results of all five data sets together.

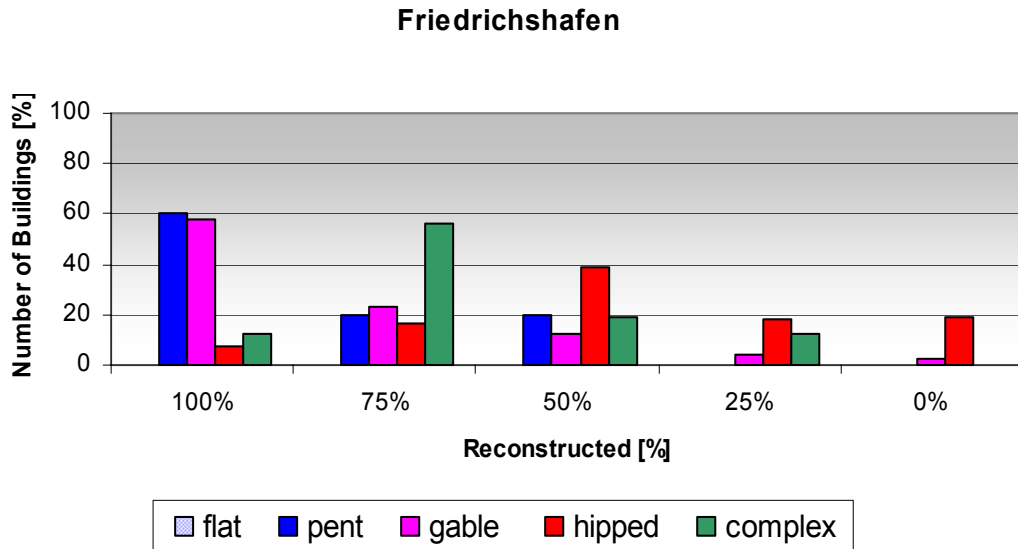


Figure 5-13: Percentage of reconstructed roof types in the study area Friedrichshafen

Roof type	Sum	Flat	Pent	Gable	Hipped	Complex
Number of Buildings	328	0	5	236	67	20

Table 5-5: Statistics for roof types of the data set “Friedrichshafen”

### Linköping

The statistics for the laser scanner data set of Linköping are summarised in Figure 5-14. The smallest detectable feature size was calculated to be approximately 4m<sup>2</sup>. This indicates that dormers should also be detected.

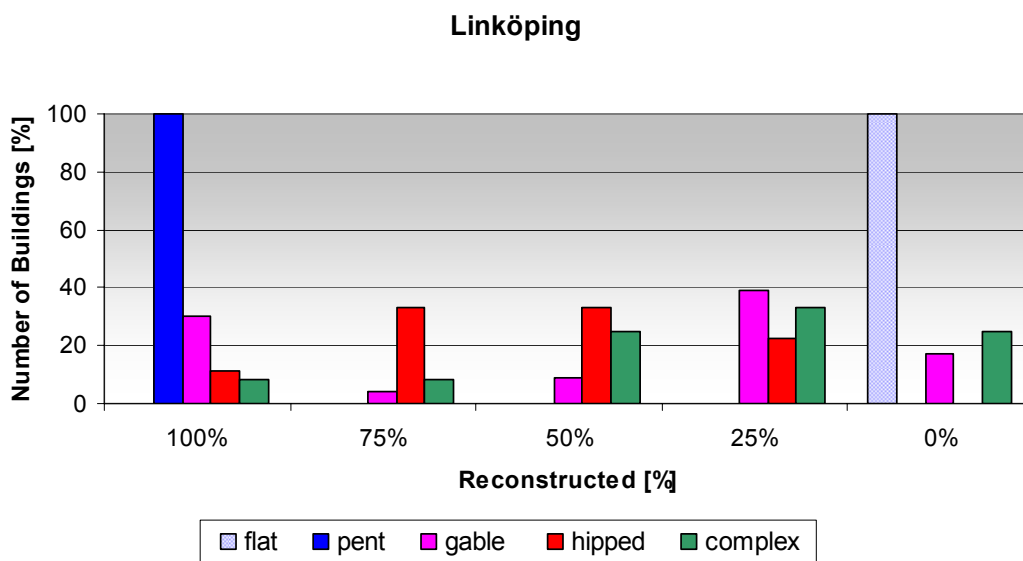


Figure 5-14: Percentage of reconstructed roof types in the study area Linköping

Roof type	Sum	Flat	Pent	Gable	Hipped	Complex
Number of Buildings	48	3	1	23	9	12

Table 5-6: Statistics for roof types of the data set “Linköping”

Within this study area, the percentage of completely reconstructed buildings is rather low. Nearly 50% of all buildings have “not useful” building models or no information at all was reconstructed. The following figure shows a parameter space of a gable roof with a low inclination within a point cloud (Figure 4-4) that is highly irregular:

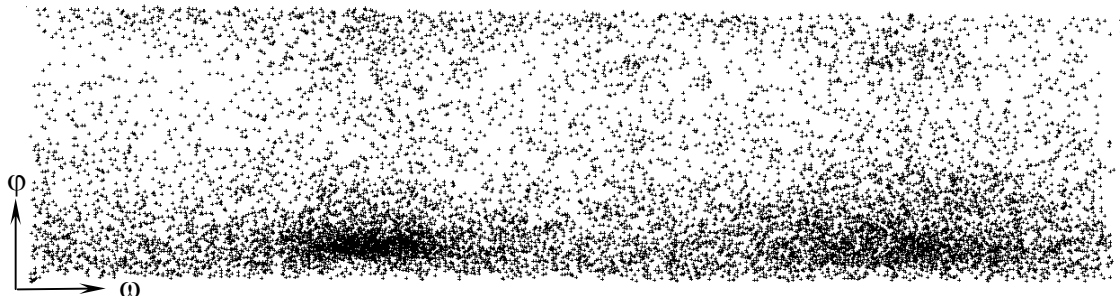


Figure 5-15: Parameter space of a flat gable roof within the Linköping study area

As well as the high number of points, which indicates a larger building, it can be seen that the borders of the clusters are even more diffuse than some parameter spaces of the Friedrichshafen data set. The reasons are the irregular ALS point distribution, which leads to inhomogeneous triangle parameters, and the higher influence of the accuracy in height if the ALS points form small triangles. Because of this, it is difficult to find optimal parameters for the cluster analysis and thus for the roof face detection. The problem increases if a building in such a point cloud has multiple roof faces with slightly different orientations. They cannot be separated and the building cannot be reconstructed completely. The main problem within this data set is then that single roof faces of larger point clouds cannot be detected in parameter space and thus get lost.

Although the LiDAR data has a low point spacing (0.7m), roof faces which are as small as 4m<sup>2</sup> were reconstructed only occasionally. The laser scanner data and thus its information could not be used by the method as it was expected.

In order to compare the results of the five study areas, they were scaled to an average city. The five cities have the average percentages of flat (2%), pent (3%), gable (55%) and hipped roofs (21%) and complexes (19%). The single results of the five data sets were scaled to this composition. Hence, the influence of the composition of roof types is eliminated for these statistics. The results are shown in Figure 5-16.

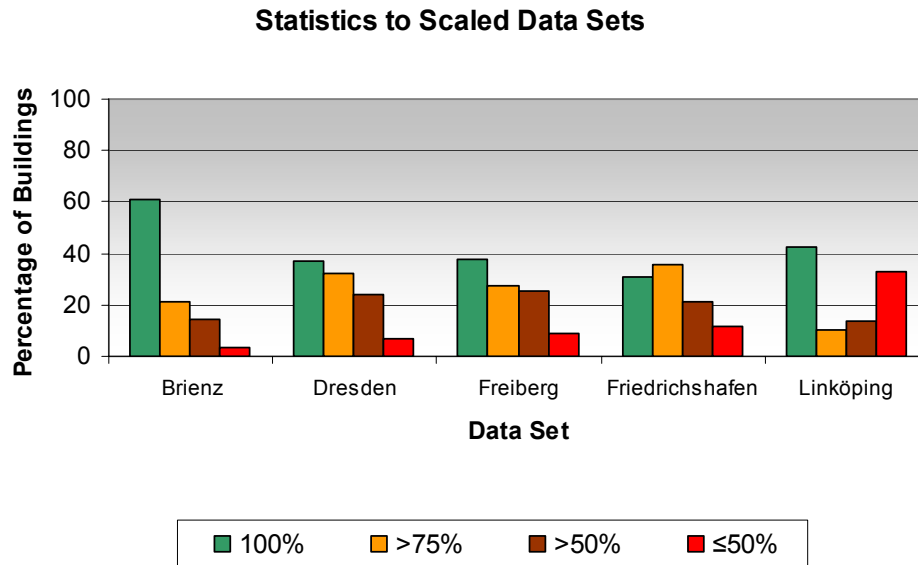


Figure 5-16: Statistics for the results of the five study areas scaled to an average city

The Swiss data set “Brienz” has best results in these statistics. Approximately 60% of the building models were reconstructed completely and there are only 3% of not useful building models. This data set has the best point spacing to feature size ratio. In addition to that, the ALS data have not been interpolated and they have a quite regular point pattern with a constant accuracy between ALS points of one strip.

The Dresden and Freiberg data, both coming from the same ALS system, have similar results when scaled to the average composition of roof types, although their actual results (shown in Figure 5-5) are not alike. It can be concluded that the Dresden data set has more difficult roof structures than the Freiberg data set.

From Figure 5-16 it may also be concluded that the ALS data of “Friedrichshafen” are not as suited for the method as a more regular point pattern. The lower percentage of “completely” reconstructed building models may have been caused by the irregularly distributed ALS points or by the very small difficult buildings.

Interesting results were obtained for the Linköping data. It appears that a building model could either be reconstructed completely or no information at all. Checking these values with the data, it was found that point clouds having a more regular point pattern were reconstructed completely and point clouds with highly irregular point density were not reconstructed at all. The irregular point density is due to the obvious inconsistent speed of the helicopter. In addition to this, insufficient strip information is provided. Up to now, it can be concluded, that the regularity of a point pattern has an influence on the results of the reconstruction algorithm. The next section will discuss the results of the reconstruction algorithm in detail.

### 5.1.2 Discussion of the Results

The results described above for each data set were analysed and are now discussed. This section aims to look at the results from a general point of view. It analyses the influence of the ALS data and the influence of parameter settings on the result as well as the reasons for failed intersections.

#### *Amendment of strip information to the reconstruction results*

As explained in [Maas2002], the relative accuracy of individual ALS points is approximately 4cm but, mainly due to GPS and INS, vertical discrepancies between single strips may be 20cm and horizontal discrepancies up to 70cm. A horizontal shift of this amount may have, depending on the surface inclination, a larger influence on the ALS data than a height shift of 20cm. If strip information is not provided, both discrepancies cause triangles in the TIN-structure, which do not represent the roof's surface, but appear as noise in the parameter space. From this point of view the use of strip information should be considered.

The planimetric discrepancies between strips of the ALS data of the data set Brienz are approximately 50cm and their accuracy in height is approximately 20cm. Statistics, which analyse the data set Brienz processed without using strip information, show that these results are worse than those obtained using strip information. Approximately 56% of the results are not useful and only 24% are completely reconstructed building models. These numbers reflect in general the results of the Linköping data set, which had no strip information available. In addition to this, the ALS data of the Linköping data set also contain the irregularities of a helicopter flight.

#### *Amendment of pre-filtering ALS data in order to enhance the cluster analysis*

It is not recommended to smooth the ALS point clouds using local average filter or any other filter with such an effect. One reason is that breaklines representing the outline of a building are blurred and triangles in those areas cannot be collected as they have parameters different from the roof plane. The breakline information of the original data would have to be transferred to the filtered data, which is not trivial. In addition, the parameter space would still be diffuse whether applying the filter or not. ALS data, which has high-frequency noise and is in need of smoothing (see Figure 5-17 as an example), may not be flattened without distorting height information of the ALS points.

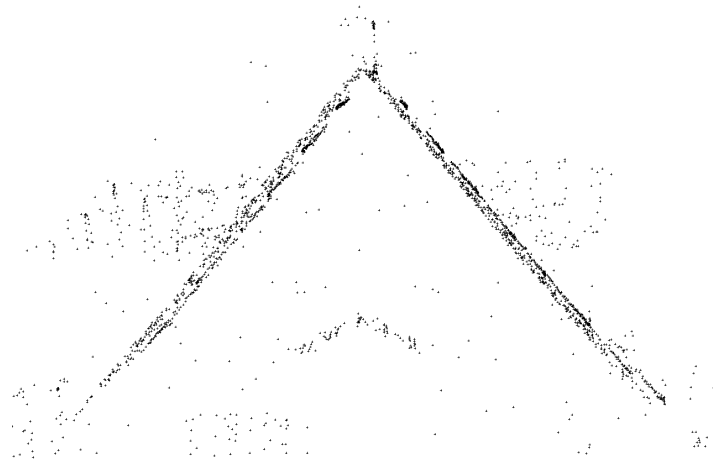


Figure 5-17: Point cloud from the Linköping data set

Filtering can be recommended, if it is desired to remove outliers (e.g. ALS points at chimneys) only. Edge-preserved filters or such [Lehmann97] eliminate single disturbances on a planar surface. Such a filter [SAMeierhold] was applied to all data sets except “Dresden” as it already is interpolated data. In using an edge-preserved filtering technique outliers are removed and the resulting gap is closed with triangles, which represent the surface.

#### *The influence of the point pattern on the minimal recognised roof face size*

When comparing buildings of the same size from the data set of the ALTMS (regular 1.5m point spacing) with FALCON II data (2.3m – 0.3m point spacing) it is more likely to detect small roof faces with the regular point information. Analysing the results of “Friedrichshafen”, it can be seen that small roof faces were only detected when their sides are longer than the point spacing across flight direction.

#### *Reasons for failing in complete reconstruction*

In general, half of the errors of reconstructed models originate from planes, which are not identified although they fulfil all requirements of a detectable planar surface. For instance, approximately 20% of the roof faces, which are large enough to be detected, are not identified or not sufficiently identified in “Brienz”. Altogether 36% of the buildings in “Brienz” were not reconstructed completely. Those 20% are roof faces, which are either not planar but slightly curved or which are disconnected by smaller features such as dormers or chimneys. In some cases an insufficient line registration of the ALS data was recognised. In any case, an incomplete roof plane set certainly causes failures in the intersection. The other falsely reconstructed building models arise from intersection errors by means of false or insufficient groupings.

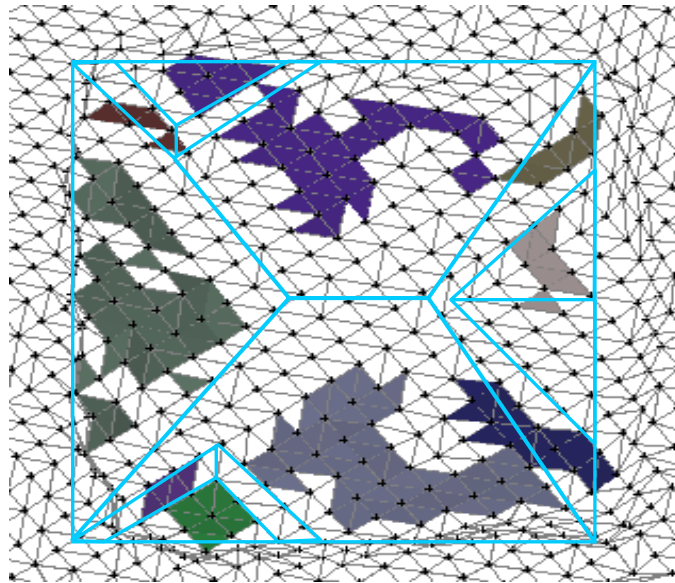


Figure 5-18: Shaded TIN-structure of a hipped roof, which has a pitched dormer and smaller roof features

False groupings have various reasons as well. Often, neighbouring planes exceeding a certain distance to each other have not been grouped. This was caused mainly by unidentified triangles, which may represent small areas of different orientation which connect two roof faces. Figure 5-18 shows a roof structure of the Dresden data set. All shaded triangles are identified. Obviously, those triangles that should be at breaklines could not be identified. The breakline area in the example in Figure 5-18 is wider than usual since breaklines were blurred by applying an interpolation when generating the 1m-grid data. Increasing thresholds to force an intersection of neighbouring planes may have bigger disadvantages in those cases where an intersection is not desired.

A specific situation that could not be reconstructed at all was not found. But there are constellations that are more likely to be misinterpreted such as those of the small roof features in Figure 5-18. Another situation may be an asymmetrical T-house, for example, which comes close to an L-House.

#### *On the importance of correct parameter settings*

The parameters *meanPtdist* and *Acc* mainly determine the collection of clusters as well as of ALS points for the plane interpolation. Usually, the mean point distance *meanPtdist* is given with the ALS data. Its influence was already discussed in section 3.2.3 on page 38 and in section 3.5.10 on page 60. *Acc*, the relative accuracy of the precision in height of individual ALS points, may not be provided with the data. If this is the case, the user has to find out the optimal value for *Acc*. In order to help understanding the influence of *Acc*, its use is briefly summarised.

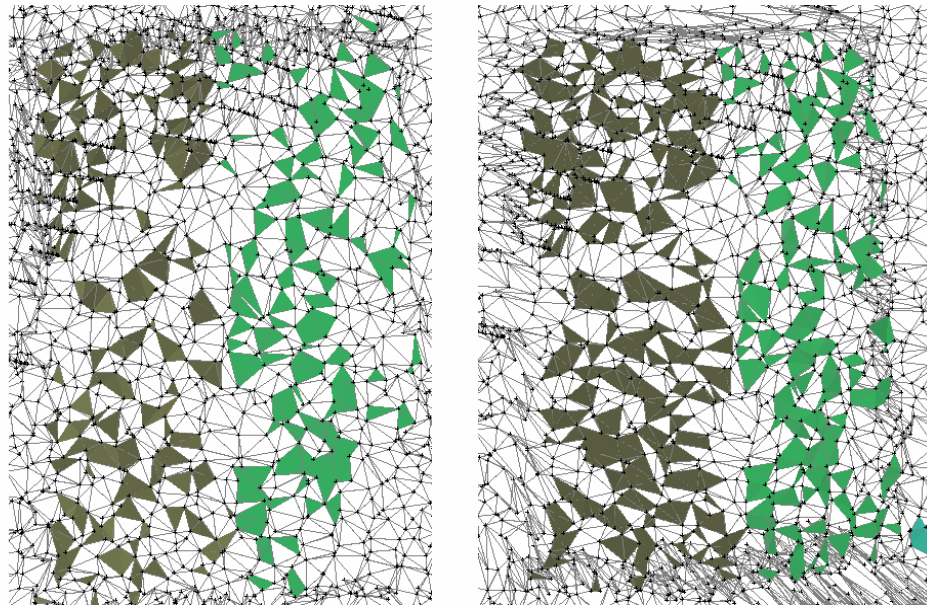


Figure 5-19: Shaded TIN-structure of an ALS data set. Left:  $Acc$  0.1m, Right:  $Acc$  0.13m

Cluster Analysis:  $Acc$  determines the variation of triangles in slope and orientation as a function of the slope itself. The larger  $Acc$  is set, the more likely it is that the algorithm assigns parameter points to a cluster. Consequently, the clusters are extended in size. This means, in reference to the object space, that more triangles are identified as belonging to a roof face, by increasing  $Acc$ . It follows that for low precision ALS data a greater value of  $Acc$  increases the chance of identifying “roof triangles”, as visualised in Figure 5-19. Accordingly, in a noisy parameter space, points can be collected which do not belong to the roof plane.

Collection of ALS Points: When transferring the collected parameter points into object space, ALS points of neighbouring triangles are tested to see they fit in the interpolated plane. Here,  $Acc$  is a direct measure of the maximum distance an ALS point must have to be included in the plane.

In order to test the influence of  $Acc$  the data set Friedrichshafen was processed with two different  $Acc$ s. One reason is that accuracy information was not provided with the data the other reason is to show the effects a change in settings has. In general, better results were obtained applying  $Acc = 0.15m$  than using  $Acc = 0.2m$  or  $0.1m$ . Using a higher accuracy value ( $0.2m$ ) the following problems occurred more often: The method produces small patches as roof faces, which are hard to associate to each other or to larger patches. Since it is more likely that triangles, which do not belong to the roof face, are collected, planes are interpolated falsely into the point cloud. This leads sometimes to not intersected planes which should form a ridge. Nevertheless, if  $Acc$  is set too low it may happen that not enough triangles are collected and that they are not uniformly distributed over the whole roof face area. An interpolated plane may not fit the actual roof face very well then. The next two figures compare the results obtained with either using  $Acc$  0.15m or 0.2m:

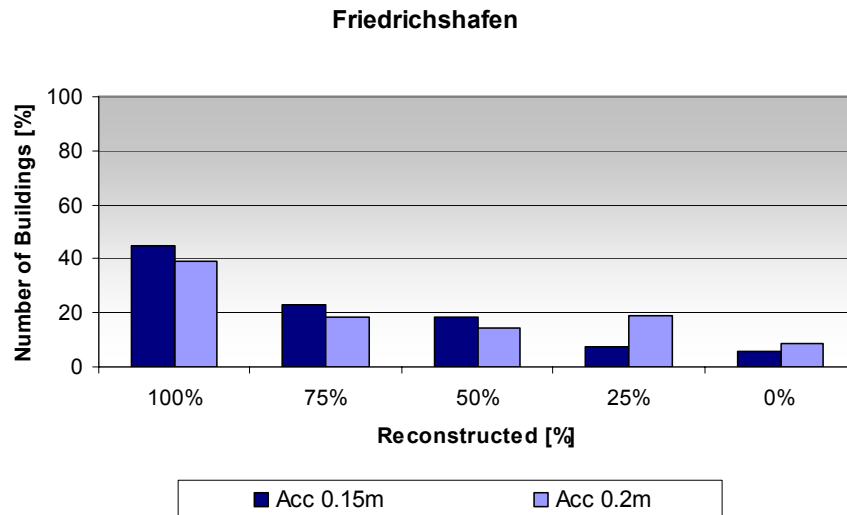


Figure 5-20: Reconstruction results when using Acc 0.15 and Acc 0.2

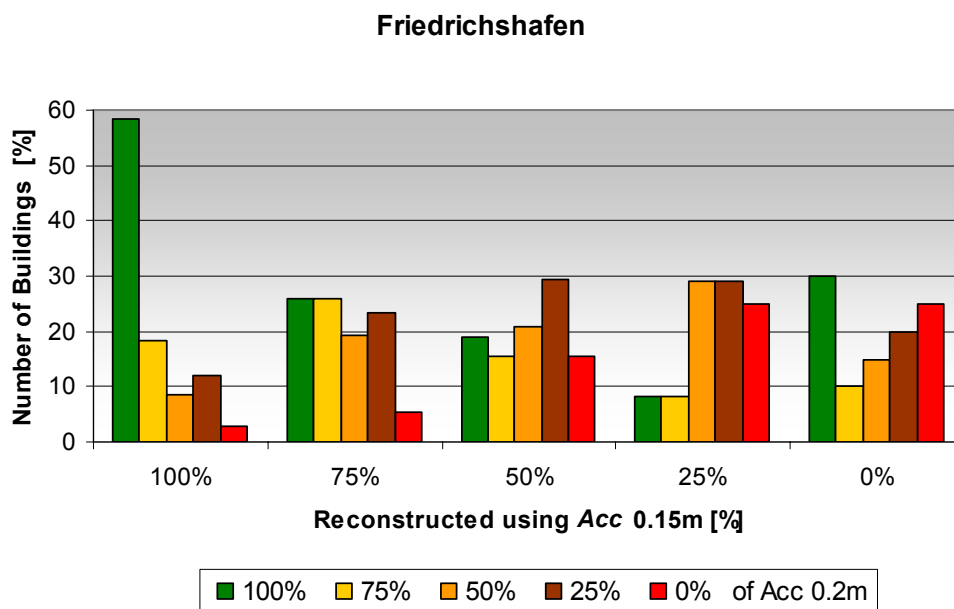


Figure 5-21: Statistics for reconstruction result; The bars of each part (100, 75, ...) show the percentage of “completely” (100%), “mostly” (75%), “partially” (50%) and not useful (25%, 0%) reconstructed building models when using *Acc* 0.2m, which were “completely” (100), ... reconstructed using *Acc* 0.15m

Figure 5-20 compares the percentage of reconstructed building models in the five different categories also used in the previous section. Increasing the parameter *Acc* in size obviously worsens the result. In Figure 5-21 the reconstruction results of using *Acc* 0.15m are compared to those of using *Acc* 0.2m. Table 5-7 provides the numbers of these statistics. It was of interest to find out how many buildings were reconstructed completely using *Acc* 0.2m and using *Acc* 0.15m, for instance. The bars of each part in Figure 5-21 represent the percentage of reconstructed building models in the categories, such as “complete” (100%) or “mostly” (75%) reconstructed, using *Acc* 0.2m. The parts represent the categories of the reconstruction results when using *Acc* 0.15m. One hundred and forty two buildings were completely reconstructed using *Acc* 0.15m. Approximately 58% of these buildings were

reconstructed completely using *Acc* 0.2m as well (see Table 5-7) and 18% were mostly reconstructed using *Acc* 0.2m.

Acc 0.2m \ Acc 0.15m	Complete (100%)	Mostly (75%)	Partially (50%)	Not useful (25%)	Not useful (0%)	Number
Complete (100%)	58%	18%	8%	12%	3%	142
Mostly (75%)	26%	26%	19%	23%	5%	73
Partially (50%)	19%	16%	21%	29%	16%	58
Not useful (25%)	8%	8%	29%	29%	25%	24
Not useful (0%)	30%	10%	15%	20%	25%	20
Number	121	58	48	62	28	

Table 5-7: Numerical statistics on reconstruction result as also illustrated in Figure 5-21

Interpreting the chart a small amount of buildings (30% of 20 buildings) were not reconstructed at all using *Acc* 0.15m, which were reconstructed completely using *Acc* 0.2m. By analysing the reconstructed models themselves, there was no specific apparent reason that would explain the different amount of reconstructed features. Only the number of completely reconstructed hipped roofs and complexes was to some extent higher when using *Acc* 0.2m, but about 10% lower for gable roofs.

## 5.2 Accuracy Verification of Reconstructed Building Models

In addition to the correctness of the reconstructed building models their geometric accuracy is of high interest for practical use and will be discussed in this section. First, the relative accuracy of reconstructed building models is discussed. This includes the comparison of results from different flight strips as well as the fit of the models in the ALS data. Since aerial imagery is the classical information source of deriving 3D building models, the reconstructed roof information will be compared to photogrammetrically derived information in the subsequent section. This is followed by section 5.2.3, which aims at determining the absolute accuracy of reconstructed roofs by comparison to terrestrial measurements.

### 5.2.1 The Fit of Reconstructed Building Models into the LiDAR Data

In order to verify the interpolated roof planes, the standard deviation of the perpendicular distances of laser scanner points of each plane was calculated for a randomly chosen selection of buildings in each data set. Each selection comprised approximately 15 objects including small buildings as well as large storehouses. The main statistical results, summarised in Figure 5-22, are considered good. In general, no remarkable difference between the results of the data sets is evident. The mean perpendicular distance of the points belonging to one roof face compared with the interpolated plane was approximately 6-8cm. The standard deviation of the distances of all points to their plane was

approximately 5-6cm. An asymmetrical distribution of collected triangles on a surface may cause a plane to incorrectly fit the entire surface.

The statistics of the Dresden and Freiberg data set have the most striking appearance (Figure 5-22). The distance value 0.07m and its standard deviation 0.068m are approximately the same and are therefore considered insignificant. The maximum distance value 0.3m of the Dresden data set is also noteworthy, as this originates from a group of triangles, which rather represent an undulating surface than a plane.

In general, no difference in accuracy can be made out for the data sets “Brienz”, “Freiberg” and “Friedrichshafen”. The reason is the parameter *Acc*, which acts by fitting ALS collected points onto a plane, which has the parameters of a cluster. *Acc* was set the 0.15m for “Freiberg” and “Linköping”, but 0.1m for the other data sets. The influence of the parameter *Acc* onto the reconstruction process was discussed in section 3.5.10.

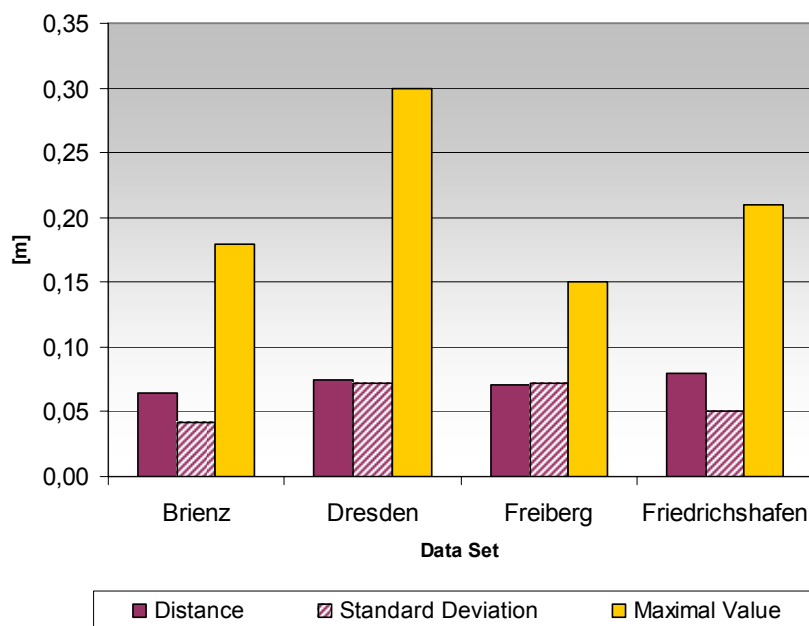


Figure 5-22: Mean perpendicular distance, standard deviation and maximum of the perpendicular distances of points to interpolated planes

Based on the assumption that roof faces, which form a gable roof, have opposite orientations, the relative difference in orientation of such roof faces was determined for all data sets except Linköping. Throughout the chosen examples, opposite roof faces have a difference in orientation of approximately 180 degree  $\pm 2$ degree. This also exemplifies the quality of the generated building models, though it is not known whether the roof faces have exact opposite orientations or not.

Since the data set Brienz was provided with strip information and these strips have an overlap of at least 50%, each building may be covered by three strips. Each of the strips was processed and the reconstructed building models were compared to each other regarding their relative size. The mean difference of 20 analysed buildings is 0.78m  $\pm 0.4$ m in width and 1.09m  $\pm 0.55$ m in length. Both values represent the inner accuracy in terms of reproducibility of the laser scanner data. Interesting is the discrepancy of 0.3m between the mean differences of width and length. As the buildings have different orientations to the

laser scanner strips, the ALS data itself should have only little influence in this. It is more likely that this discrepancy is due to the adjustment of gable ends in the reconstruction algorithm. Another conclusion cannot be drawn with the available information.

### 5.2.2 Comparison with Photogrammetric Measurements

The traditional data used for building model reconstruction are aerial imagery. As photogrammetric measured building models were available for the data set Brienz, the automatically generated building models were compared to manually, in aerial imagery measured building models. Because of the base-height ratio, aerial imagery has a high planimetric precision, which is approximately 0.2m for the “Brienz” data, and a lower accuracy in height with approximately 0.5m. Contrary to this, the planimetric precision of the ALS data of the data set Brienz is approximately 0.5m and the accuracy in height is approximately 0.2cm. Accordingly, the potential in accuracies of both data sets are complements to each other. From that point of view it is beneficial to compare the results derived from the ALS data with photogrammetric measurements.

Within the data set “Brienz” photogrammetric measurements of 50 roofs, originally selected and measured by the Swiss Federal Office of Topography, were available. Forty-four out of the 50 buildings (88%) were reconstructed completely using the ALS data. Table 5-8 shows the average differences of the reconstructed (ALS) and the measured (aerial imagery) corner coordinates. Additional, relative measures such as length, width and roof heights were also compared as these are less sensitive to systematic errors, since they are locally correlated. Therefore, such relative measures form a better indicator for the performance of the technique than absolute ones. From analysis of these values (Table 5-8), it can be concluded that the photogrammetric measurements and the reconstructed information match each other well.

	Difference $\pm$ Variation
RMSE of corner coordinates	1.1m $\pm$ 0.4m
Difference in height of ridge points	-0.4m $\pm$ 0.3m
Difference of relative measures	Length 0.5m $\pm$ 0.6m
	Width 0.1m $\pm$ 0.7m

Table 5-8: Mean differences of reconstructed and photogrammetrically measured corner coordinates

It was found that the accuracy potential in position and height of photogrammetric measurements performed by an operator was the opposite to that of ALS data. The planimetric accuracy of aerial imagery measurements was usually superior to the accuracy in height, depending on the base-height ratio. It is obvious by comparing the reconstructed and measured building models (Figure 5-23) that the photogrammetric measurements differ from the ALS point cloud.

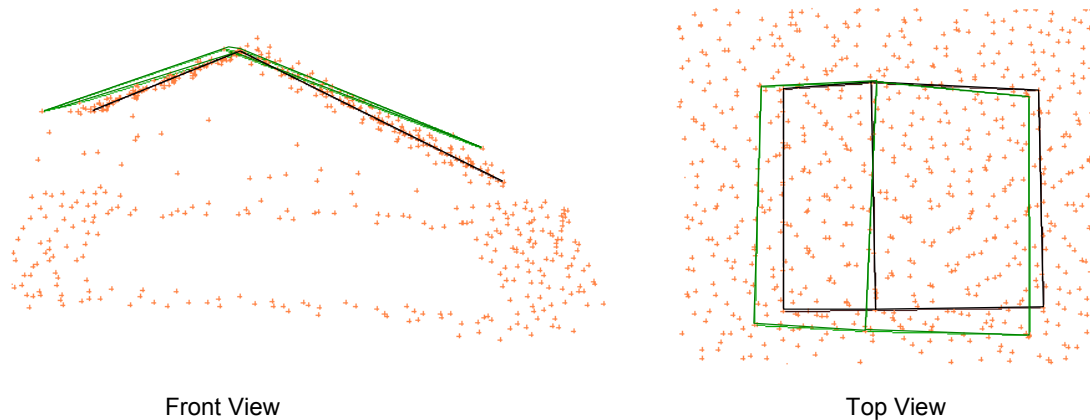


Figure 5-23: Comparison of photogrammetrically measured (green) and reconstructed (black) roof information with underlaid ALS point cloud, Left: top view, Right: front view

Analysing the 44 examples, 4 main systematic differences between both data sources were found:

- The photogrammetric measurements are frequently above or under the ALS point cloud. With maximum distances of 1m.
- Some ridges were found to have systematic horizontal shifts or different azimuths
- The roof inclination of the photogrammetric data did not correspond to the inclination visible in the ALS point clouds.
- The automatically reconstructed building outline was generally of smaller extent when compared to the photogrammetric outline

The first three systematic effects were not correlated to the automatic building reconstruction. The shift and tilting of the roofs may be due to systematic errors of the LiDAR flights, such as GPS/INS sub-optimality and insufficient strip adjustment. With respect to the differences of the roof inclinations, the accuracy in height of the ALS data was higher than the accuracy in height of photogrammetric measurements. A more comprehensive analysis of these factors can be found in [Hofmann2004a] and [Hofmann2004b].

Reconsidering the potential of aerial imagery and the information available with LiDAR data, a fusion of both data sources such as shown in [Rottensteiner2004] appears to be very rational. Under the presumption that both data sources are georeferenced correctly, the high planimetric accuracy of aerial imagery and the high accuracy in height of LiDAR data may be combined.

### 5.2.3 Comparison with Terrestrial Measurements

High accuracy terrestrial measurements of five roofs were available in the Dresden data set. Statistically, this number is not meaningful; however, it provides an idea of the accuracy that can be expected. The completely reconstructed buildings were evaluated by comparing the end points of the eaves and the ridge with the terrestrial measured data. As the ridge was generated by intersecting interpolated planes, the achieved position accuracy must be

analysed separately from that of the gable end points. The ridge points achieved a positional RMS-error of 0.8m and the corner coordinates of the roofs outline were found to have an RMS of 1.2m. Accuracy of the corner coordinates was found to be a function of point density (1m). The accuracy in height was considered as very good with an RMS of less than 0.1m. In terms of the eaves, the height accuracy depends on the roof inclination and position accuracy, and was considered as very good with an RMS of 0.3m. Table 5-9 provides an overview of the accuracies of the reconstructed building models:

	Mean Values	Standard Deviation
Gable Ends [m]		
x, y	1.21	0.29
z	0.28	0.16
Ridge [m]		
x, y	0.83	0.78
z	0.06	0.03
Length [m]	0.14	1.30
Width [m]	-0.37	0.79
Inclination [°]	0.14	1.23
Orientation [°]	0.19	0.57

Table 5-9: Statistics on the accuracies of the reconstructed building models

In Figure 5-19 a comparison between the data derived from the terrestrial measurements and those of the reconstruction procedure is made. Here it can be seen that the ridge of both information is similar. The accuracy of the roof inclination and the roof orientation (Table 5-9) confirm this. Principally, the extensions of the reconstructed building models are smaller than the extensions of the terrestrial data. This may be due to the loss of exact breakline data on interpolation of the ALS data into a 1m grid.

Although, the data set “Dresden” was only available as interpolated ALS data its regularity suited the comparison of derived building models to terrestrial data. The results described above are understood as absolute accuracies of reconstructed building models for this particular point spacing. It is assumed that the planimetric accuracy of building models derived from higher resolution data would improve with the resolution. Unfortunately, ground truth data was not available for data sets with higher point spacing.

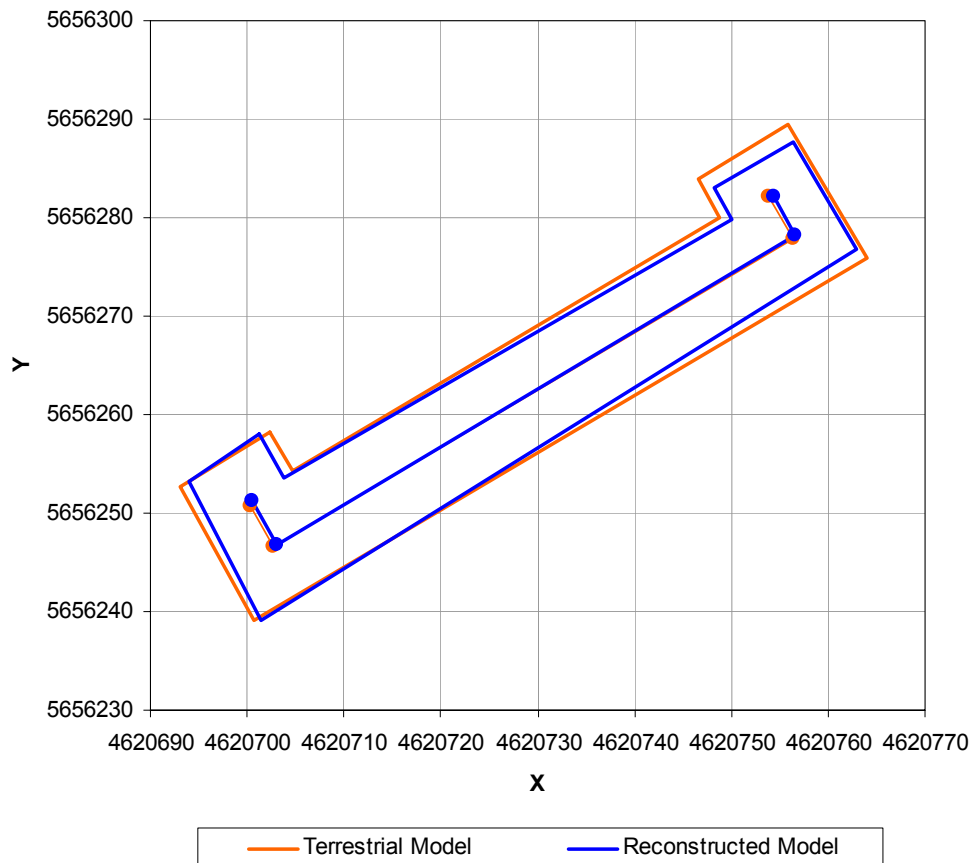


Figure 5-24: Visualisation of terrestrial measurements and reconstructed information

### 5.3 Automatic Labelling of Correct Results

As was discussed in section 1, a system which creates 3D building models should also be capable of analysing its' results. Assessment should divide the results into three “traffic light” categories – Green, Amber and Red. This automatic labelling is important as it saves on time-consuming task of checking each of the created VRML-Models.

With reference to this study, the main problem was that the 3D building model structure was unknown, thus it is not known if the analysed roof structure has a gable or a hipped roof. Therefore the system has to check for unknown parameters. In [Hofmann2003] an approach was suggested, which analysed the parameter space subsequently and drew conclusions about the roof type. In this study [Hofmann2003] approximately 70% of the gable roofs, 35% of building complexes and 0% of hipped roofs were classified correctly in the parameter space. Consequently, this information was considered unreliable if used to check reconstruction results. Relative measures, such as the fit of a plane into its surrounding points or a logical assessment of intersected sides, must still be used. However, statistical information has been used throughout the whole reconstruction process as a decision means for the acceptance or rejection of the hypotheses. The reconstructed model successfully passed all statistical parameter tests therefore no subsequent information available could be employed in a final internal quality check.

Nonetheless, the two suggested approaches were implemented into the reconstruction algorithm. Firstly, the variance (*var*), which is the mean quadratic perpendicular distances of all points of a roof plane, was calculated using Eq. 5-1.

$$\text{var} = \frac{1}{n} \sum_n (ax_i + by_i + cz_i - d)^2 \quad \text{Eq. 5-1}$$

where:

n .. number of points

a, b, c, d .. plane parameters

$X_i$  .. coordinates of point i

To avoid ALS points belonging to a dormer being processed with a roof face, dormers were processed first and their points then excluded from further analyses. Secondly, all planes were checked to determine if they were intersected by another plane. The correct building model was considered more likely if all planes were associated with each other. If only one plane existed then a pent roof was assumed. Both measures were used to decide if the building model was correct (green flag), partially correct (yellow flag) or incorrect (red flag).

The first measure, distance, was tested with the Brienztal data set. This consisted of simple building structures and precise individual ALS points. In 13% of the buildings this measure placed the correct flag on a point cloud. 4% of the results were omission errors and 83% commission errors. The reason for these poor results was that outliers were also included in the variance. For example, where a roof had a number of features, such as windows, the variance would yield a high value, although the interpolated roof plane fit the actual roof points well. The main reason for omission errors was that smaller planes do not cover the whole roof face; however points within their area fit the plane very well. In addition, it was unknown if the detected roof's face was completely represented.

The second measure, which tests if all planes were associated with each other, worked in single clearly defined cases such as gable roofs or hipped roofs. To function properly it also required that there were no erroneously interpreted planes within the point cloud. Once more, missing planes were not detected. Thus a hipped roof, which was reconstructed as gable roof, was considered a commission error. In order to distinguish between a "yellow flag" and a "red flag" the number of unassociated planes could only be counted, as it was not known how many planes could intersect a plane. If ground plan information is available, models could be collected, which define probable roof face constellations. However, this also limits analysis to known situations and would therefore be an impossible task to complete.

Considering the lack of available information it was not possible to create a tool which derives the desired information from the reconstructed building model.

## 5.4 Applicability of the Overall Process

This section summarises practical aspects of the developed building model reconstruction scheme. Besides explanation of steering parameters the computation time is also analysed. From section 5.1.2 it is known that correct results of the method strongly depend on the accuracy parameter *Acc* and the parameter *meanPtdist* (see section 3.5.10 and 5.1.2). The user may influence the reconstruction procedure with the following parameters:

*MergeDist* is the distance two planes must have to be called neighbours. This parameter should be set as  $1.8 * \textit{meanPtdist}$ .

*MergeAcc* is the maximal perpendicular distance two regions must have to be merged in the algorithm, which collects ALS points using clusters. This number should be  $1.5 * \textit{Acc}$ .

*MinSlope* is the minimal slope a roof face must have to be reconstructed. This number should be greater than 3.

*Wallheight* is the minimal possible height, which is presumed in order to separate roof patches from other patches.

*Dormerheight* is the minimal height the lower edge of a dormer has to its roof face. A value of 0.5m is recommended.

*ROV* is the roof orientation variation. It is the maximal angle two planes with opposite orientations are allowed to vary from 180 degree in order to be intersected. This angle was set to 15 degree in this study.

*MinNr* is the minimal number of parameter points a cube has to have to be identified as part of a cluster. For all data sets this number was set to 5 in this study.

Apart from *MergeAcc*, these parameters were not altered whilst processing the five test data sets. *MergeAcc* was varied between 1.2 and 1.5 times *Acc*. With such a defined set of parameters the computational approach is easy to manage.

The computation times, which were taken for the processing of the data sets Brienz, Dresden, Freiberg and Friedrichshafen are plotted in Figure 5-25. All four data sets were computed using the same processor (Athlon 700MHz, 500MB RAM). The Linköping data set was processed with a faster processor (Intel Xeon 2.3GHz, 1GB RAM) machine. Hence, the computation time could not be compared with the other computation times.

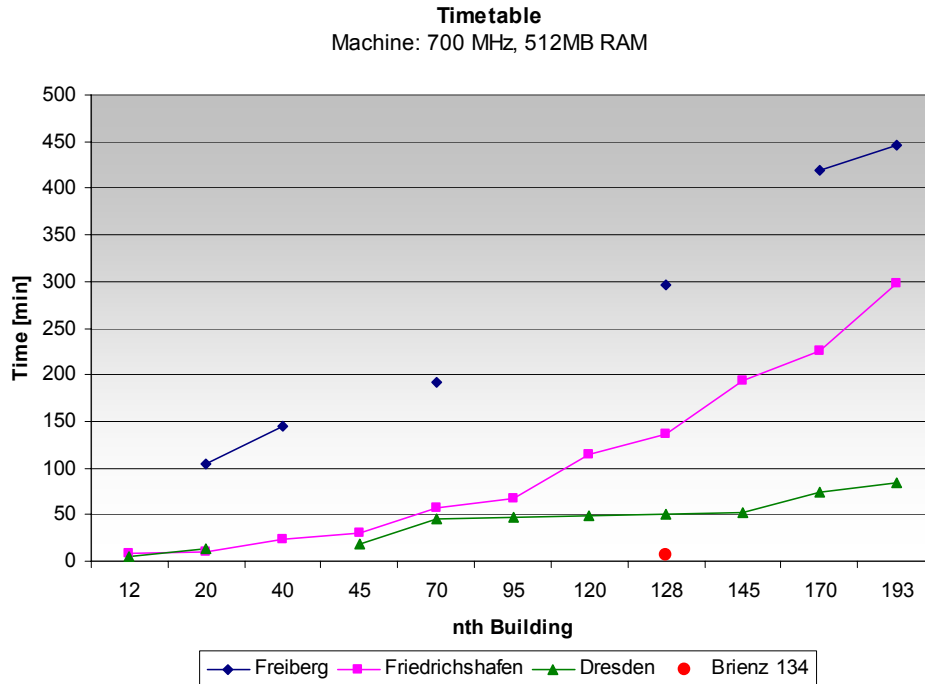


Figure 5-25: Computation times taken for four data sets

The average time taken for a building of average size is summarised in Table 5-10. The number of ALS points processed for each building, together with the number of patches that were intersected, was compared to determine the computation time. The influence of the number of points per point cloud was found to be linear and the influence of the number of patches was found to be quadratic in nature. The number of patches was defined by the building and also the precision of individual laser scanner points.

Data set	Freiberg	Friedrichshafen	Dresden	Brienz
Average computation time	2.31 min	1.62 min	0.34 min	0.05 min
number of points per file	4400 pts	2910 pts	835 pts	592 pts

Table 5-10: Average time taken to compute one average size building within the data sets

As the data set Brienz mainly consisted of gable roofs, the computation time could be compared to the time taken by an operator who generated a 3D building model manually. In general, an operator would measure one gable roof in 30 seconds in a semi-automatic program [PhDHaala]. A gable roof is measured by a trained operator within approximately three minutes using a digital photogrammetric workstation [J.-D. Guisolan]. This time does not include the time taken for the orientation of the stereo pair. Thus, the defined algorithm could process at least 10 times more gable roofs than an operator.

Any step of the building reconstruction algorithm (sections 3.5.1 to 3.5.9), could be switched off if desired. Therefore, if a preference exists to model buildings without adjusted gable ends, this is possible. Thus, the 3D building models may be optically be enhanced.

## 6 Summary, Conclusions and Outlook

### 6.1 Summary and Conclusions

The goal of this research was to create a scheme, which generates 3D building models automatically from ALS data only. The 3D building models may be used for planning purposes or visualisations of any kinds. The developed reconstruction scheme utilises a TIN-structure calculated into single point clouds. These point clouds were extracted from a larger set of ALS data using a segmentation approach. The idea was that triangles on a planar surface, such as a roof face, have similar orientations and positions in space. In order to analyse these triangles, a cluster analysis algorithm was developed. It is employed in parameter space and collects those triangles, which are on roof faces. Cluster analysis applied in parameter space is capable to separating triangles of individual roof faces instantaneously. Via the collected triangles the ALS points on individual roof faces may be grouped. In each collected point group a plane is interpolated. Using the elaborated grouping algorithm, the roof topology between single planes is established automatically as well. This topology is used to intersect the individual planes to a 3D building model. The 3D building models are visualised using VRML (see Figure 6-1).

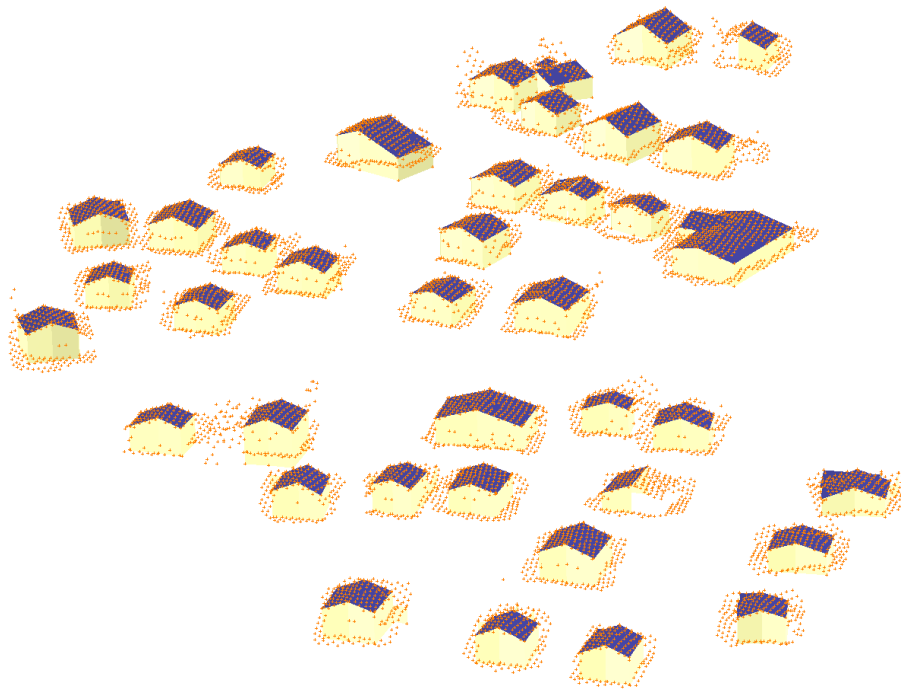


Figure 6-1: Example of a visualisation of a virtual village consisting of reconstructed 3D building models

At the beginning, five criteria were defined, which should be fulfilled or included in a 3D building reconstruction scheme. The first criterion, the robustness, aimed at the performance of the scheme by means of reconstructing as many buildings as possible. It also asked for a tool indicating the degree of completeness of the results. Interpreting the given figures of section 5.1.2, which analysis the results, it can be concluded that the scheme is evidently robust. Up to approximately 64% of the buildings of a data set may be reconstructed completely. The amount of completely reconstructed building models

depends on the ALS point pattern, available strip information, the data quality and the building itself. As the reconstruction method is a plane-based method, a roof structure, which is not composed of planes, is therefore not reconstructed. Concerning the indicator, it was concluded: If only ALS data is provided, there is little information left, which can be used by an indicator pointing out incomplete results. This tool may be established, if further information on the reconstructed building is given.

The second criterion, the flexibility, was demonstrated by testing the reconstruction scheme on different data sets. It was shown in section 5.1.2 that the scheme can be applied to LiDAR data of different densities and with different point patterns, though the scheme produces better results with homogeneously distributed ALS points.

The third criterion, the resolution, referred to the feature detail, which should be achieved by the reconstruction scheme. The required level of detail was defined to be equivalent to that of large-scale maps. Completely reconstructed building models meet this requirement: The main roof faces are reconstructed. If the user desires to increase this level of detail, he or she may allow dormers to be reconstructed as well.

The fourth criterion, the precision of the 3D building models was satisfied as the results of section 5.2 have shown. The reconstructed 3D building models can be compared with building models traditionally measured in aerial imagery. Comparing reconstructed building models with terrestrial measurements indicated a high accuracy in height and a reasonable planimetric accuracy in correlation with the ALS point density (half the mean point spacing).

The fifth criterion, the computation time, was analysed in section 5.4. It was concluded that the computation time taken for the data sets Brienz, Dresden and Friedrichshafen is acceptable. Since the actual reconstruction algorithms were not optimised concerning their running time and the machine used only has 700MHz, further reductions are possible.

The whole building reconstruction process was designed to run automatically starting with the point cloud. In the beginning, the user may decide to include or exclude certain functions, which enforce compulsory conditions on the building model. Along these lines, the reconstruction scheme accomplished the required tasks.

### **6.2 Future Work**

Future work may be, if time given, comprehensive. Those tasks, which are of highest interest have been summarised and grouped into three categories in the following. The first category refers to building detection alone. The second category contains suggestions on cluster analysis and its pre-requirements. Further ideas to the building reconstruction scheme are recapitulated in the third category.

Building detection has only been involved superficially in this research. There still has to be developed a system or a scheme, which detects automatically buildings in airborne laser scanner data. Further work could explore the potential accessible by the use of segmentation algorithms applied at raw laser scanner point information. The delineation and the classification of building objects are two tasks, which still require extensive research.

At the beginning of this study, it was decided to use the applied 3D parameter space. The given suggestion on the 2D parameter space, which is extended after applying a cluster analysis and which is independent of the plane's distance to the origin, may be explored and analysed. Referring to the applied cluster analysis in this study, a 3D mesh calculated into the parameter points would be the preferred solution to a 3D grid. Presently available source code of 3D mesh generators is described in [Meshes]. However, methods of programs, which supply source code, are reported to create 3D meshes insufficiently well or inconsistent. Thus, there definitely is potential for research in this area.

For the scheme of the 3D building model reconstruction following ideas may be realised: The roof plane bounding box algorithm may be extended that it is capable of outlining flat roof faces. This could be accomplished using Douglas-Peucker algorithm. The grouping algorithm may be extended in a way that it uses ground plan information, if available, in order to aid the grouping strategy in ambiguous situations. In general, it is encouraged to make research aiming to amend the grouping scheme or testing further grouping processes. Ground plan information would also provide auxiliary information for an indicator pointing out the completeness of the results. Additional regulations may be forced onto the building model. Roof faces of a gable roof may be forced into symmetry, or ridges may be set horizontally. Also, all gutters of a building may be levelled along the outline of the building, which may be given as additional information. Presently, a patch is limited to a 4-vertices polygon. The related data handling may be extended to be able to process polygons with n-vertices. Finally, the entire source code has to be optimised and placed into a user-friendly environment.

In general, the geometry information of the ALS data may be completed by a fusion with colour or positional information provided by aerial imagery or GIS. Similar work is successful done in [Rottensteiner2004].

## 7 References

### 7.1 Articles

- [Ackermann1999] F. Ackermann, "Airborne laser scanning - present status and future expectations" *ISPRS Journal of Photogrammetry and Remote Sensing*, 54 (1999) 64-67, 1999
- [Alharty2002] A. Alharty, J. Bethel, "Heuristic filtering and 3D feature extraction from lidar data" *IAPRS International Archives of Photogrammetry and Remote Sensing and Spatial Information Sciences Vol.34, Part 3A*, pp.23-28, 2002
- [Alharty2004] A. Alharty, J. Bethel, "Detailed building reconstruction from airborne laser scanner data using a moving surface method" *IAPRS International Archives of Photogrammetry and Remote Sensing Vol.34, Part 3 B3*, pp.213-219, 2004
- [Anderson2002] H.-E. Andersen, S. E. Reutebuch, G.F. Schreuder, "Bayesian Object Recognition for the Analysis of Complex Forest Scenes in Airborne Laser Scanner Data" *IAPRS International Archives of Photogrammetry and Remote Sensing and Spatial Information Sciences Vol.34, Part 3A*, pp. 35-42, 2002.
- [Axelsson1999] P. Axelsson, "Processing of laser scanner data – algorithms and applications" *ISPRS Journal of Photogrammetry & Remote Sensing* 54 (1999) 138-147, 1999
- [Baillard1999] C. Baillard, C. Schmid, A. Zisserman, A. Fitzgibbon, "Automatic Line Matching and 3D Reconstruction of Buildings from Multiple Views" *IAPRS International Archives of Photogrammetry and Remote Sensing and Spatial Information Sciences Vol.32, Part 3-2W5* pp. 69-80, 1999
- [Baltsavias1999a] E.P. Baltsavias, "Airborne laser scanning: basic relations and formulas" *ISPRS Journal of Photogrammetry & Remote Sensing* 54 (1999) 199-214, 1999
- [Baltsavias1999b] E.P. Baltsavias, "Airborne laser scanning: existing firms and other resources" *ISPRS Journal of Photogrammetry & Remote Sensing* 54 (1999) 164-198, 1999
- [Brenner2000] C. Brenner, "Towards fully automatic generation of city models" *IAPRS International Archives of Photogrammetry and Remote Sensing and Spatial Information Sciences Vol.34, Part 3A*, pp.169-174, 2000
- [Brunn1998] A. Brunn, L. Lang, E. Gülch, W. Förstner, "A Hybrid concept for 3D Building Acquisition" *ISPRS Journal for Photogrammetry & Remote Sensing*, Vol.53, No.2, pp.119-129, April 1998
- [Elaksher2002] A.F. Elaksher, J.S. Bethel, "Reconstructing 3D buildings from LIDAR data" *IAPRS International Archives of Photogrammetry and Remote Sensing and Spatial Information Sciences Vol.34, Part 3A*, pp.102-106, 2002
- [Flood1997] M. Flood, B. Gutelius, "Commercial Implication of Topographic Terrain Mapping Using Scanning Airborne Laser Radar" *PR&RS Photogrammetric Engineering and Remote Sensing*, Vol. 63 (1997) pp. 327ff
- [Förstner1999] W. Förstner, "3D-City Models: Automatic and Semiautomatic Acquisition Methods" *Photogrammetrische Woche*, Stuttgart, September 1999
- [Forlani2003] G. Forlani, C. Nardinocchi, M. Scaioni, P. Zingaretti, "Building reconstruction and visualization from LiDAR data" *IAPRS International Archives of Photogrammetry and Remote Sensing and Spatial Information Sciences Vol.34, Part 5/W12*, pp. 151-156, 2003

- [Gerke2001] M. Gerke, C. Heipke, B.-M. Straub, "Building Extraction From Aerial Imagery Using a Generic Scene Model and Invariant Geometric Moments" Proceedings of the IEEE/ISPRS joint Workshop on Remote Sensing and Data Fusion over Urban Areas, November 8-9th 2001, University of Pavia, Rome (Italy), ISBN 0-7803-7059-7, pp. 85-89
- [Gorte2002] B. Gorte, "Segmentation of TIN-structured surface models" Joined Conference on Geospatial Theory, Processing and Applications Ottawa, Canada, 2002
- [Haala1997] N. Haala, K.-H. Anders, "Acquisition of 3D urban models by analysis of aerial images, digital surface models and existing 2D building information" SPIE Conference on Integrating Photogrammetric Techniques with Scene Analysis and Machine Vision III, pp.212-222, 1997
- [Heuel2000] S. Heuel, F. Lang, W. Förstner, "Topological and Geometrical Reasoning in 3D Grouping for Reconstructing Polyhedral Surfaces" IAPRS International Archives of Photogrammetry and Remote Sensing and Spatial Information Sciences Vol.34, Part 3A, pp.169-174, Proceedings of the 19th ISPRS Congress, Amsterdam, 16-23 July, 2000
- [Hofmann2002] A.D. Hofmann, H.-G. Maas, and A. Streilein, "Knowledge-Based Building Detection Based on Laser Scanner Data and Topographic Map Information" IAPRS International Archives of Photogrammetry and Remote Sensing and Spatial Information Sciences Vol.34, Part 3A, pp.169-174, 2002
- [Hofmann2003a] A.D. Hofmann, H.-G. Maas, and A. Streilein, "Derivation of roof types by cluster analysis in parameter spaces of airborne laserscanner point clouds" ISPRS Commission III WG3, Workshop, 3-D reconstruction from airborne laserscanner and InSAR data, " IAPRS International Archives of Photogrammetry and Remote Sensing and Spatial Information Sciences Vol.34, Part 3/W13, pp.112-117, 2003
- [Hofmann2003b] A.D. Hofmann, "Untersuchungen im 1D- und 2D-Parameterraum von Punktwolken aus Flugzeuglaserscannerdaten" Tagungsband der 23. Wissenschaftlich-Technische Jahrestagung der DGPF, Band 12, pp. 73-80, 2003
- [Hofmann2004a] A.D. Hofmann, "Analysis of TIN-structure parameter spaces in airborne laser scanner data for 3-d building model generation" IAPRS International Archives of Photogrammetry and Remote Sensing Vol.34, Part 3 B3, pp.302-307, 2004
- [Hofmann2004b] Hofmann, A.D., Schwalbe, E. "Evaluation automatisch rekonstruierter Gebäudemodelle aus Flugzeuglaserscannerdaten" Tagungsband der 24. Wissenschaftlich-Technische Jahrestagung der DGPF, Band 13, pp. 51-58, 2004
- [Kraus1997] K. Kraus, N. Pfeiffer, "A new method for surface reconstruction from laser scanner data" IAPRS International Archives of Photogrammetry and Remote Sensing, Vol. 32, Part 3-2W3, Haifa, Israel, pp. 80-86.
- [Kraus1999] K. Kraus, W. Rieger, "Processing of laserscanner data for wooded areas" Photogrammetric Week '99 (D. Fritsch and R. Spiller, editors), Wichmann, Heidelberg, Germany, pp. 221-231, 1999
- [Leberl2001] F.W. Leberl, R. Bolter, "Building reconstruction from synthetic aperture radar images and interferometry" 3rd International Workshop on Automatic extraction of man-made objects from aerial and space images, Ascona, 2001
- [Lemmens1997] M. J.P.M. Lemmens, H. Deijkers, P. A.M. Looman, "Building detection by fusing airborne laser-altimeter DEM's and 2D digital maps" IAPRS International Archives of Photogrammetry and Remote Sensing Vol.32, Part 3-4W2, 1997
- [Maas1999a] H.-G. Maas, "Fast determination of parametric house models from dense airborne laserscanner data" ISPRS Workshop on Mobile Mapping Technology, Bangkok, Thailand, April 21-23, 1999

- [Maas1999b] H.-G. Maas, and G. Vosselman, "Two algorithms for extracting building models from raw laser altimetry data" *ISPRS Journal of Photogrammetry & Remote Sensing* 54 (1999) 153-163, 1999
- [Maas2002] H.-G. Maas, "Methods for measuring height and planimetry discrepancies in airborne laserscanner data" *PE&RS Photogrammetric Engineering and Remote Sensing*, Vol. 68, No. 9, pp. 933-940, 2002
- [Nardinocchi2001] C.Nardinocchi, G. Forlani, "Building Detection and Roof Extraction in Laser Scanning Data" 3rd International Workshop on Automatic extraction of man-made objects from aerial and space images, Ascona, pp. 319-328, 2001
- [Pyysalo2002] U. Pyysalo, H. Hyypäe, "Reconstructing Tree Crowns from Laser Scanner Data for Feature Extraction" *IAPRS International Archives of Photogrammetry and Remote Sensing and Spatial Information Sciences* Vol.34, Part 3B, pp. 218-222, 2002
- [Rottensteiner2002a] F. Rottensteiner, Ch. Briese, "A new method for building extraction in urban areas from high-resolution lidar data" *IAPRS International Archives of Photogrammetry and Remote Sensing and Spatial Information Sciences* Vol.34, Part 3A, pp.295-301, 2002
- [Rottensteiner2002b] F. Rottensteiner, J. Jansa, "Automatic extraction of buildings from lidar data and aerial images" *IAPRS International Archives of Photogrammetry and Remote Sensing and Spatial Information Sciences* Vol.34, Part 4, pp.569-574, 2002
- [Rottensteiner2004] F. Rottensteiner, J. Trinder, S. Clode, K. Kubik, "Fusing airborne laser scanner data and aerial imagery for the automatic extraction of buildings in densely built-up areas" *IAPRS International Archives of Photogrammetry and Remote Sensing* Vol.34, Part 3 B3, pp.512-518, 2004
- [Schwalbe2004] E. Schwalbe, "3D building model generation from airborne laserscanner data by straight line detection in specific orthogonal projections" *IAPRS International Archives of Photogrammetry and Remote Sensing and Spatial Information Sciences* Vol.34, Part 3 B3, pp.249-254, 2004
- [Sithole2003] G. Sithole, G. Vosselman, "Comparison of filtering algorithm" *IAPRS International Archives of Photogrammetry and Remote Sensing and Spatial Information Sciences* Vol.34, Part 3 W13, pp.71-78, 2003
- [Shewchuk1996] J.R. Shewchuk, "Triangle: Engineering a 2D Quality Mesh Generator and Delaunay Triangulator" *First Workshop on Applied Computational Geometry* (Philadelphia, Pennsylvania), pages 124-133, ACM, 1996
- [Stilla1999] U. Stilla, K. Jurkiewicz, "Automatic reconstruction of roofs from maps and elevation data" *IAPRS International Archives of Photogrammetry and Remote Sensing* Vol.32, Part 7-4-3 W6, Valadolid, Spain, June 3-4, 1999
- [Stilla2002] U. Stilla, U. Sörgel, U. Thönnessen, "Geometric constraints for building reconstruction from InSAR data of urban areas" *Symposium on Geospatial Theory, Processing and Applications*, Ottawa, 2002
- [Suveg2002] I. Suveg, G. Vosselman, "Automatic 3D reconstruction of buildings from aerial images" *SPIE Photonics West, Electronic Imaging*, Vol. 4661, pp. 56-69, 2002
- [Vosselman1999] G. Vosselman, "Building Reconstruction Using planar Faces in Very High Density Height Data " *ISPRS Conference. "Automatic Extraction of GIS Objects from Digital Imagery*, Munich 8-9-1999, Vol 32/3-2W5, ISBN 0256- 1840, pp. 87-92.
- [Vosselmann2001] G. Vosselman, S. Dijkman, "3D building model reconstruction from point clouds and ground plans", *IAPRS International Archives of Photogrammetry and Remote Sensing* Vol.34, Part 3-W4, pp.37-43, 2001

- [Wehr1999] A. Wehr, U. Lohr, "Airborne laser scanning – an introduction and overview" ISPRS Journal of Photogrammetry & Remote Sensing 54 (1999) 68-82, 1999
- [Weidner1995] U. Weidner, W. Förster, "Towards automatic building extraction from high resolution digital elevation models" ISPRS Journal of Photogrammetry & Remote Sensing 50 (1995), 38-49, 1995

## 7.2 Monographies

- [Anderberg73] M.R. Anderberg, "Cluster Analysis for Applications" Academic Press Inc., New York, 1973
- [Bartelme00] N. Bartelme, "Geoinformatik – Modelle, Strukturen, Funktionen" Springer Verlag, 3. Aufl., 2000
- [Engeln-Müllges96] G. Engeln-Müllges, F. Reutter, "Numerik-Algorithmen" VDI Verlag, 7. Aufl., 1996
- [Kaufman90] L. Kaufman, P.J. Rousseeuw, "Finding Groups in Data – An Introduction to Cluster Analysis" Wiley series in probability and mathematical statistics, John Wiley & Sons, Inc. 1990
- [Kraus00] K. Kraus, "Photogrammetrie, Band 3, Topographische Informationssysteme" Dümmler Verlag, 2000
- [Lehmann97] T. Lehmann, W. Oberschelp, E. Pelikan, R. Repges, "Bildverarbeitung für die Medizin" Springer Verlag, 1997
- [Luhmann00] T. Luhmann, "Nahbereichsphotogrammetrie: Grundlagen, Methoden und Anwendungen" Thomas Luhmann – Heidelberg: Wichmann, 2000
- [Nagel94] M. Nagel, K.-D. Wernecke, W. Fleische, "Computergestützte Datenanalyse" Verlag Technik GmbH Berlin München, 1994

## 7.3 Web Pages

- |              |   |              |
|--------------|---|--------------|
| [CyberCity]  | <a href="http://www.cybercity.tv/">http://www.cybercity.tv/</a>   | (26.11.2004) |
| [Definiens]  | <a href="http://www.definiens-imaging.com">http://www.definiens-imaging.com</a>   | (27.10.2004) |
| [Mathworld]  | <a href="http://mathworld.wolfram.com/Eigenvalue.html">http://mathworld.wolfram.com/Eigenvalue.html</a>                                   | (23.04.2004) |
| [Meshes]     | <a href="http://www.andrew.cmu.edu/user/sowen/software/tetrahedra.html">http://www.andrew.cmu.edu/user/sowen/software/tetrahedra.html</a> | (20.12.2004) |
| [Milan]      | <a href="http://www.milan-flug.de">http://www.milan-flug.de</a>   | (30.08.2004) |
| [Inpho]      | <a href="http://www.inpho.de/">http://www.inpho.de/</a>   | (26.11.2004) |
| [Optech]     | <a href="http://www.optech.on.ca">http://www.optech.on.ca</a>   | (30.08.2004) |
| [TerraSolid] | <a href="http://www.terrasolid.fi">http://www.terrasolid.fi</a>   | (26.11.2004) |
| [TopoSys]    | <a href="http://www.toposys.de">http://www.toposys.de</a>   | (30.08.2004) |
| [TopEye]     | <a href="http://www.topeye.com">http://www.topeye.com</a>   | (15.10.2004) |

## 7.4 Thesis

- [DASchwalbe] E. Schwalbe, “Gebäudemodellierung in reduzierten Parameterräumen von airborne Laserscannerdaten” unpublished diploma thesis, Technische Universität Dresden, Institut für Photogrammetrie und Fernerkundung, 2003  
<http://www.tu-dresden.de/fghgipf/lehre/diplomarbeiten/schwalbe/schwalbe.htm>
- [DASilbermann] D. Silbermann, “Untersuchung zur Genauigkeitsbestimmung von Flugzeug-laserscannerdaten”, unpublished diploma thesis, Technische Universität Dresden, Institut für Photogrammetrie und Fernerkundung, 2004  
<http://www.tu-dresden.de/fghgipf/lehre/diplomarbeiten/silbermann/Untersuchungen.htm>
- [DAWach] J. Wach, “Gebäudedetektierung und -extraktion aus airborne Laserscannerdaten ” unpublished diploma thesis, Technische Universität Dresden, Institut für Photogrammetrie und Fernerkundung, 2004
- [PhDHaala] N. Haala, “Gebäuderekonstruktion durch Kombination von Bild- und Höhendaten”, Universität Stuttgart, Fakultät für Bauingenieur- und Vermessungswesen, 1996  
<http://www.ifp.uni-stuttgart.de/publications/dissertationen/diss.html> (24.11.2004)
- [PhDNiederöst] M. Niederöst “Detection and Reconstruction of Buildings for Automatic Map Update”, ETH Zürich, Institute of Photogrammetry and Remote Sensing, 2003  
„[http://www.photogrammetry.ethz.ch/general/persons/markus\\_pub/publications.html](http://www.photogrammetry.ethz.ch/general/persons/markus_pub/publications.html) (16.11.2004)
- [PhDSüveg] I. Süveg “Reconstruction of 3D Building Models from Aerial Imagery and Maps”, NCG Netherlands Geodetic Commission, Publications on Geodesy 53, 2003
- [SAMeierhold] N. Meierhold, “Untersuchungen zu Filteroperationen in TIN-Strukturen”, unpublished project work (Studienarbeit), Technische Universität Dresden, Institut für Photogrammetrie und Fernerkundung, 2004

## 7.5 Persons

- [J.-D. Guisolan] Jean-Daniel Guisolan, Swiss Federal Office of Topography, Seftigenstrasse 264, CH - 3084 Wabern, Email: [jean-daniel.guisolan@swisstopo.ch](mailto:jean-daniel.guisolan@swisstopo.ch)

---

## Illustration Index

Figure 1-1: Principle of airborne laser scanning (Modified from illustration in Flood, 1997).....	10
Figure 1-2: Classes of building models [Brenner2000] .....	11
Figure 1-3: Roof types.....	12
Figure 1-4: Special cases of roof types.....	12
Figure 1-5: Features of a roof.....	13
Figure 2-1: Segmentation result (blue polygons) of LiDAR data using eCognition with underlaid aerial imagery and map information (red polygons).....	16
Figure 2-2: Classification result (yellow areas) of “building-polygons” with underlaid aerial imagery and map information (red polygons).....	17
Figure 3-1: Methodised diagram of approaches to (semi-)automatic building extraction.....	19
Figure 3-2: Parameter definition of a building primitive [Maas1999a] .....	20
Figure 3-3: Segmentation results as seen in [Rottensteiner2002a] for plane interpolation.....	21
Figure 3-4: Segmentation result of [Gorte2002] .....	21
Figure 3-5: Illustration of the building reconstruction technique from [Schwalbe2004].....	22
Figure 3-6: Point cloud of a building with a Delauney-triangle-mesh structure.....	23
Figure 3-7: 2.5D TIN-structure and definition of the triangle parameters $\varphi$ for slope, $\omega$ for orientation and $d$ for the perpendicular distance of the triangle’s plane to the origin O.....	24
Figure 3-8: Example of a building’s 3D parameter space.....	25
Figure 3-9: Demonstration of parameter variation $\delta$ caused by the error $a$ in the laser scanner data in relation to a given point spacing.....	26
Figure 3-10: Relation between variation in slope and the inclination of a triangle.....	26
Figure 3-11: Variation in triangle slope $\varphi$ in relation to point density and as a function of slope for a laser scanner data accuracy in height of $\pm 0.07\text{m}$ .....	27
Figure 3-12: Demonstration of the triangle’s variation in Orientation.....	27
Figure 3-13 Variation in triangle orientation $\omega$ in relation to point density and as a function of slope for a laser scanner data accuracy of $\pm 0.07\text{m}$ .....	28
Figure 3-14: Relation between variation in parameter $d$ to distance from the centre point $P_M$ of the triangle to origin O .....	29
Figure 3-15: Variation in Distance $d$ in relation to point density and as a function of slope for an example of a laser scanner data accuracy of $\pm 0.07\text{m}$ .....	29
Figure 3-16: Possible assignments of a data point to a cluster.....	31

---

Figure 3-17: Example of a parameter space.....	31
Figure 3-18: Flow chart of clustering process.....	33
Figure 3-19: 3D grid box visualization in parameter space .....	34
Figure 3-20: Coarse clustering procedure .....	35
Figure 3-21: Association of parameter points of clusters and triangles between laser scanner points.....	37
Figure 3-22: Possible constellations of roof faces a) coplanar roof faces, b) roof faces with opposite orientations ( $\pm 180$ degrees), c) planes intersected with walls, d), e) and f) planes of couples with side neighbours, which may belong to a couple themselves.....	44
Figure 3-23: a) Group of planes, b) Group of planes with underlaid TIN-structure.....	44
Figure 3-24: Basic combinations of planes and couples .....	45
Figure 3-25: Examples of successfully reconstructed buildings with sideways-connected roof faces.....	46
Figure 3-26: Types of possible sideway intersection .....	46
Figure 3-27: Point cloud and picture of the Tillich-Bau of the Dresden University of Technology.....	48
Figure 3-28: Flow chart of building model reconstruction .....	49
Figure 3-29: Example TIN-structure of a building with gable roof and bounding boxes a) front view; b) top view.....	50
Figure 3-30: Flow chart of merge planes process .....	51
Figure 3-31: TIN-structure of a building with a gable roof, view from top.....	52
Figure 3-32: Order for ridge intersection .....	53
Figure 3-33: Adjustment of gable ends (Testhouse5572) .....	53
Figure 3-34: Visualization of corridors as used to look for points belonging to the roof (bird's eye view) .....	54
Figure 3-35: Example in which an additional patch (right) is created from a roof face (left), which is too large .....	54
Figure 3-36: Example of the disadvantage of adding an additional patch, the constellation of patches becomes more complicated .....	55
Figure 3-37: Data structure of pairs .....	56
Figure 3-38: Part of decision tree of side intersection .....	57
Figure 3-39: Left: group of planes as input in the intersection algorithm, Right: output of the intersection algorithm .....	58
Figure 3-40: Principle of gutter adjustment .....	59
Figure 3-41: Example of a building model without adjusted dormers (left) and with adjusted dormer (right).....	60

---

Figure 3-42: Suggestion of a procedure for deriving the building outline (black: roof face polygons, red: outline) .....	60
Figure 3-43: Top: Group of patches with underlaid ALS point cloud .....	61
Figure 3-44: Intersection result of Figure 3-44 .....	62
Figure 3-45: Intersected building consisting of two couples with similar orientations.....	63
Figure 4-1: Point pattern of the ALTMS laser scanner by Optech.....	64
Figure 4-2: Point pattern of the LMS-Q140i-80 laser scanner by Riegl with indicated flight direction of the “Freiberg” data set.....	65
Figure 4-3: Point pattern of the FALCON laser scanner with swing mode by Toposys.....	65
Figure 4-4: Point pattern of the TopEye MK II mounted on a helicopter .....	66
Figure 4-5: Example of typical buildings of the data set “Brienz” .....	68
Figure 4-6: Examples of typical buildings of the study area Dresden (top) and Freiberg (bottom).....	69
Figure 4-7: Left: Example of an ALS-point cloud of the data set “Friedrichshafen”, Right: Example of the typical building style.....	70
Figure 4-8: Front view of a gambrel roof in old Swedish style.....	71
Figure 4-9: Statistics of roof types to the study areas.....	71
Figure 5-1: Examples of correct reconstructed building models (100%). The left examples originate from the Dresden data set and show interpolated points at the walls.....	74
Figure 5-2: Examples of mostly correct reconstructed building models ( $\geq 75\%$ ).....	75
Figure 5-3: Examples of partially correct reconstructed building models ( $\geq 50\%$ ).....	76
Figure 5-4: Examples of not useful building models Left: $\leq 50\%$ , Right: $\leq 25\%$ .....	76
Figure 5-5: Overall statistics for reconstructed building models of the five data sets .....	77
Figure 5-6: Percentage of reconstructed roof types in the study area Brienz.....	78
Figure 5-7: a) Shaded TIN-structure of a building b) Parameter space of TIN-structure c) building model.....	79
Figure 5-8: Percentage of reconstructed roof types in the study area Dresden .....	80
Figure 5-9: Example of a common hipped roof within the Dresden data set.....	81
Figure 5-10: Example of an excluded building complex in the data set Dresden .....	81
Figure 5-11: Percentage of reconstructed roof types in the study area Freiberg.....	82
Figure 5-12: a) Part of a TIN-structure of the TopoSys data b) Whole parameter space of the TIN-structure .....	83
Figure 5-13: Percentage of reconstructed roof types in the study area Friedrichshafen ....	84
Figure 5-14: Percentage of reconstructed roof types in the study area Linköping.....	84
Figure 5-15: Parameter space of a flat gable roof within the Linköping study area .....	85
Figure 5-16: Statistics for the results of the five study areas scaled to an average city .....	86

---

Figure 5-17: Point cloud from the Linköping data set .....	88
Figure 5-18: Shaded TIN-structure of a hipped roof, which has a pitched dormer and smaller roof features.....	89
Figure 5-19: Shaded TIN-structure of an ALS data set. Left: Acc 0.1m, Right: Acc 0.13m.....	90
Figure 5-20: Reconstruction results when using Acc 0.15 and Acc 0.2 .....	91
Figure 5-21: Statistics for reconstruction result; The bars of each part (100, 75, ..) show the percentage of “completely” (100%), “mostly” (75%), “partially” (50%) and not useful (25%, 0%) reconstructed building models when using <i>Acc</i> 0.2m, which were “completely” (100), ... reconstructed using <i>Acc</i> 0.15m.....	91
Figure 5-22: Mean perpendicular distance, standard deviation and maximum of the perpendicular distances of points to interpolated planes.....	93
Figure 5-23: Comparison of photogrammetrically measured (green) and reconstructed (black) roof information with underlaid ALS point cloud, Left: top view, Right: front view .....	95
Figure 5-24: Visualisation of terrestrial measurements and reconstructed information .....	97
Figure 5-25: Computation times taken for four data sets.....	100
Figure 6-1: Example of a visualisation of a virtual village consisting of reconstructed 3D building models .....	101

---

## Table Index

Table 4-1: Key information of used laser scanner data .....	67
Table 4-2: Statistics to roof types of the data set “Brienz” .....	68
Table 4-3: Statistics to roof types of the data set “Freiberg” and “Dresden” .....	69
Table 4-4: Statistics to roof types of the data set “Friedrichshafen” .....	70
Table 4-5: Statistics to roof types of the data set “Linköping” .....	70
Table 5-1: Numbers of the overall statistics for reconstructed building models of the five data sets .....	77
Table 5-2: Statistics for roof types of the data set “Brienz” .....	78
Table 5-3: Statistics for roof types of the data set “Dresden” .....	80
Table 5-4: Statistics for roof types of the data set “Freiberg” and “Dresden” .....	82
Table 5-5: Statistics for roof types of the data set “Friedrichshafen” .....	84
Table 5-6: Statistics for roof types of the data set “Linköping” .....	85
Table 5-7: Numerical statistics on reconstruction result as also illustrated in Figure 5-21 .....	92
Table 5-8: Mean differences of reconstructed and photogrammetrically measured corner coordinates .....	94
Table 5-9: Statistics on the accuracies of the reconstructed building models .....	96
Table 5-10: Average time taken to compute one average size building within the data sets .....	100

## Acknowledgments

My first thanks go to Prof. Hans-Gerd Maas, my 1<sup>st</sup> supervisor, who supported me constantly during my work. Along these lines, I am glad Prof. Siegfried Fuchs of the Artificial Intelligence Institute of the Dresden University of Technology and Prof. Karl Kraus from the Institute of Photogrammetry and Remote Sensing, Vienna University of Technology accepted the request to act as my 2<sup>nd</sup> and 3<sup>rd</sup> supervisors.

Over the past four years, I have had the pleasure to work in the Photogrammetry and Remote Sensing group. My colleagues (this includes the secretary) in the group have been very enjoyable, helpful and supportive in scientific as well as real life issues.

I also appreciate the time spent by my friends and colleagues of the Dublin Institute of Technology for proof reading the manuscript. Their names are:

Avril Behan, Audrey Martin and Dorothy Stewart.

I am especially grateful to Avril Behan, who spent hours elucidating English grammar rules and facts to me.

Since this research required a number of different data sets, I am glad to acknowledge the following companies and institutes, which kindly provided the named data sets for this study.

Dam Authority of Saxony (LTV Sachsen)	data set “Dresden”
FOI Swedish Defence Research Agency	data set “Linköping”
Milan Flug GmbH, Schwarze Pumpe	data set “Freiberg”
TopoSys Topographische Systemdaten GmbH, Biberach	data set “Friedrichshafen”
Swiss Federal Office of Topography	data set “Brienz”

Finally, my deepest gratitude goes to my mother.